FUNCTIONALIZED MEMBRANES FOR PROTEIN PURIFICATION AND
PROTEOLYSIS PRIOR TO MASS SPECTROMETRY ANALYSIS

By

Wenjing Ning

A DISSERTATION

Submitted to
Michigan State University
in partial fulfillment of the requirements
for the degree of

Chemistry—Doctor of Philosophy

2016

ABSTRACT

FUNCTIONALIZED MEMBRANES FOR PROTEIN PURIFICATION AND PROTEOLYSIS PRIOR TO MASS SPECTROMETRY ANALYSIS

By

Wenjing Ning

Protein isolation and digestion are often vital steps in studies of protein structures, interactions and post-translational modifications. Porous membranes present an attractive platform for rapid proteolysis and protein purification because convective flow through pores quickly transports proteins or reagents to functional sites. This dissertation demonstrates functionalization of porous membranes with metal-chelating polyelectrolytes, peptide ligands, and enzymes, to create methods for fast protein purification, affinity tag removal and protein digestion. Additionally, attachment of functionalized membranes to pipette tips enables especially rapid and convenient protein digestion or isolation.

Development of high-capacity affinity membranes for protein isolation requires membrane pores coated with thin films that bind multilayers of proteins. To prepare membranes that selectively capture polyhistidine-tagged (His-tagged) proteins, this work explores layer-by-layer adsorption of polyelectrolytes containing chelating groups that form Ni^{2+} complexes. Sequential adsorption of protonated poly(allylamine) (PAH) and carboxymethylated branched polyethyleneimine (CMPEI) leads to membranes that bind Ni^{2+} and capture ~60 mg of His-tagged ubiquitin per mL of membrane. Both binding capacity and metal-ion leaching are similar to values seen with high-binding commercial beads, but membranes should facilitate protein isolation in minutes.

After purification, fusion tag removal is often an essential step prior to protein

characterization. Removal of small ubiquitin-like modifier (SUMO) tags in SUMO-protease-containing membranes served as a proof-of-concept demonstration for in-membrane tag removal. The time required for tag removal is similar with dissolved and immobilized His-tagged SUMO protease, but the membrane is reusable, and immobilized proteases retain much of their activity after three uses.

Membranes are also convenient substrates for trypsin immobilization and subsequent proteolysis. Passage of protein solutions through 100-μm thick trypsin-modified membranes enables reaction residence times as short as milliseconds to limit digestion and provide large peptides for mass spectrometry (MS) analysis. Large peptides can both enhance protein sequence coverage and help identify flexible regions in a protein. With either cytochrome c or apomyoglobin, in-membrane trypsinolysis cleaves the protein after lysine residues in highly flexible regions to generate two large peptides that cover the entire protein sequence.

Further combining membrane techniques with pipette tips yields a convenient platform for rapid protein purification and digestion. Pushing a protein-containing solution through a trypsin-modified membrane at the end of a pipette tip digests proteins in <30 s, and enables tryptic digestion without alkylation of cysteine residues. Similarly, when membranes contain Ni^{2+} complexes, pipetting aqueous His-tagged protein through the membrane and subsequent rinsing and elution yield purified protein in 2 min. These applications demonstrate the potential of functional membranes for rapid proteolysis and protein isolation.

I dedicate this dissertation to my parents, Baojie Ning and Xiuying Zhao, for their endless love and support.

ACKNOWLEDGEMENTS

This dissertation could not have been completed without all the great support that I have received from so many people over the years.

Firstly, I want to express my deepest gratitude for all the guidance and help from my knowledgeable advisor Dr. Merlin Bruening. No matter what kinds of problems I had in my research or daily life, he is always patient and understandable to guide me for solutions. Graduate research can be boring and frustrating sometimes. It is so lucky to have his suggestions and encouragement to survive all the hard times. Besides, I would like to thank Dr. Dana Spence, as my second reader, he was always there when I needed help. Especially, I am grateful for all your recommendations during my job hunting. I also want to thank Dr. James Geiger for giving me great suggestions and introducing Dr. Stacy Hovde to help on my affinity tag removal project. I also want to thank Dr. Min-Hao Guo for helping me develop background in biochemistry through his course.

Besides, I would also like to thank Dr. Jinlan Dong and Dr. Yujing Tan for their guidance and training since I joined the group, Dr. Salinda Wijeratne for his help on polyelectrolyte modification, Dr. Stacy Hovde for providing protein samples, Dr. Li Cui and Dr. Todd Lydic for mass spectrometry analysis. Without them, I can never finish any of my projects successfully and efficiently.

Besides, I want to thank all my lovely group members, who were always willing to help and give their best suggestions. It would have been a lonely lab without you.

Finally, I would like to thank my family. They were always supporting me and encouraging me with their best wishes.

TABLE OF CONTENTS

LIST OF TABLES

LIST OF FIGURES

LIST OF SCHEMES

KEY TO ABBREVIATIONS

MS	Mass spectrometry
His-tagged	Polyhistidine-tagged
His-tag	Polyhistindine-tag
PAH	Poly(allylamine)
CMPEI	Carboxymethylated branched polyethyleneimine
SUMO	Small ubiquitin-like modifier
MBP	Maltose-binding protein
GST	Gglutathione-transferase
HA	Hemagglutinin
c-Myc	c-Myc proto-oncogene
IMAC	Immobilized metal affinity chromatography
EDTA	Ethylenediaminetetraacetic acid disodium salt
LbL	Layer-by-layer
PAA	Poly(acrylic acid)
PEI	Polyethyleneimine
NTA	Nitrilotriacetate
TEV	Tobacco etch virus
HRV 3C	Human rhinovirus 3C protease
pI	Isoelectric point
Gly	Glycine
FT-ICR	Fourier transform ion cyclotron resonance
LC	Liquid Chromatography
LC/MS	Liquid Chromatography/Mass Spectromtery

Omp T	Outer membrane protease T
NMR	Nuclear magnetic resonance
Glu	Glutamic acid
Asp	Aspartic acid
Arg	Arginine
Lys	Lysine
PSS	Poly(sodium 4-styrenesufonate)
PEEK	Polyether ether ketone
PDCMAA	Poly[(*N,N*-dicarboxymethyl) allylamine]
Con A	Conconavalin A
MPA	3-mercaptopropionic acid
FTIR	Fourier transform infrared spectroscopy
PEMs	Polyelectrolyte multiple layers
E. coli	*Escherichia coli*
SDS–PAGE	Sodium dodecyl sulfate–polyacrylamide gel electrophoresis
TOC	Total organic carbon
CM	Carboxymethylated
IDA	Iminodiacetic acid
BSA	Bovine serum albumin
IPTG	Isopropyl-thio-2-D-galactopyranoside
PMSF	Phenylmethylsulfonylfluoride
BAEE	N_α-benzoyl-L-arginine ethyl ester hydrochloride
EDC	*N*-(3-dimethylaminopropyl)-*N'*-ethylcarbodiimide hydrochloride (EDC)
NHS	*N*-hydroxysuccinimide

nESI   Nanoelectrospary ionization

TCEP   Tris(2-carboxyethyl)phosphine

MRM   Multiple reaction monitor

PRM   Parallel reaction monitoring

Chapter 1. Introduction

This dissertation describes the development of functionalized porous membranes for rapid protein purification, affinity tag removal, and proteolysis followed by mass spectrometry analysis. More specifically, I develop membranes that contain (a) adsorbed polyelectrolye-Ni^{2+} complexes for His-tagged protein purification, (b) immobilized His-tagged SUMO proteases for SUMO tag removal, and (c) anchored trypsin for limited proteolysis. Additionally, I attach membranes to pipette tips for rapid protein isolation or digestion. This chapter provides context for the research and first introduces current protein purification techniques and the potential advantages of membrane supports for His-tagged protein separation. Second, the introduction presents current strategies for affinity tag removal after protein purification, and a third section describes limited proteolysis for protein analysis with mass spectrometry analysis as well as bioreactors for this application. Finally, this chapter discusses appropriate platforms for performing in-membrane protein purification and digestion, and briefly outlines the other chapters in the dissertation.

1.1 Protein Purification

Production of recombinant proteins in microbial systems has largely replaced conventional protein culture in animal and plant tissues.[1,2] Overexpression of large quantities of proteins enables both their biochemical characterization and development of enzyme-based commercial processes or therapeutic proteins. Nevertheless, purification of specific recombinant proteins from cell lysates is still a time-consuming endeavor.[3] This section briefly discusses the synthesis of recombinant proteins, common affinity tags for protein expression and purification, and previous functionalized membranes for His-tagged protein purification.

1.1.1 Recombinant proteins

Recombinant proteins result from the expression of recombinant DNA inside living cells.[4] Laboratory methods of genetic recombination (such as molecular cloning) can utilize genetic materials from synthetic, bacterial, human, fungal, or plant DNA to create sequences that are not present in the native cell genome. After insertion of the recombinant DNA, the modified cells will synthesize new proteins based on the recombinant DNA sequence. Such proteins, including human growth hormone and insulin, have a range of pharmaceutical and industrial applications.[5] However, cells continue to produce many other species in addition to the recombinant proteins, so purification of the target proteins is a major challenge.

1.1.1.1 Expression of recombinant proteins with affinity tags

To facilitate recombinant protein purification, researchers insert a piece of tag gene into the recombinant DNA to express an affinity tag at the C terminus or N terminus of the target proteins (Figure 1.1).[4] The affinity tag binds to specific immobilized ligands to facilitate separation from co-expressed proteins. If desired, insertion of a cleavage site between the affinity tag and the target protein can enable enzymatic cleavage of the tag from the protein. Section 1.2 discusses details of tag removal.
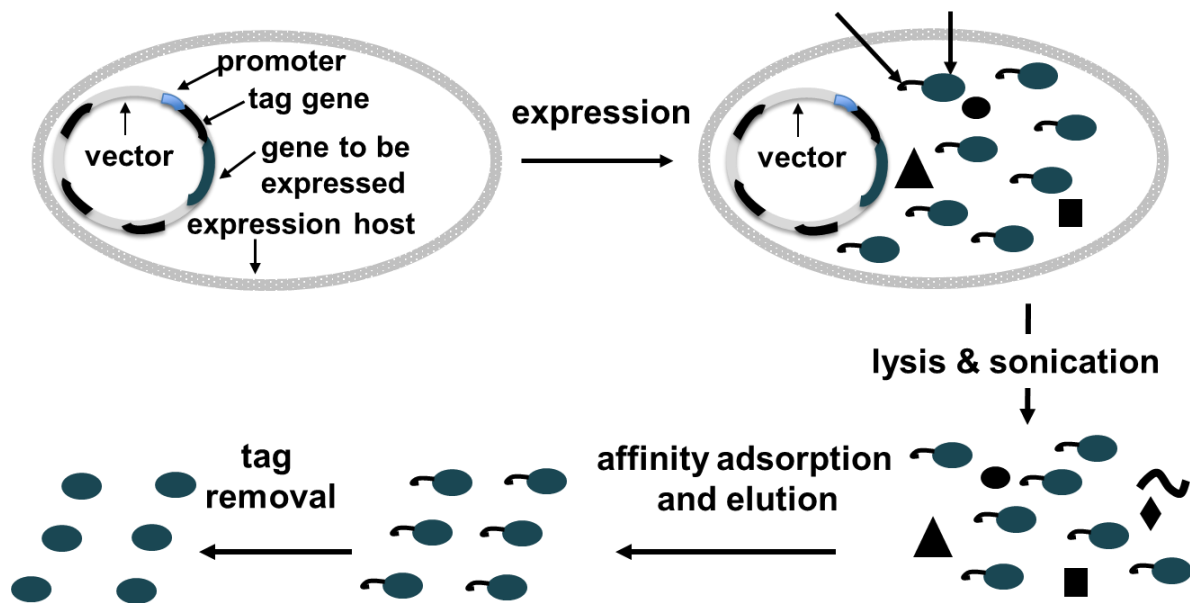
Figure 1.1. Scheme of the synthesis of recombinant proteins with affinity tags, affinity capture and affinity tag removal.

1.1.1.2 Overview of affinity tags for protein purification

Table 1.1 lists common affinity tags for recombinant proteins purification, along with the ligands or matrices that capture these tags. The wide variety of affinity tags includes small polypeptides and proteins, that bind to various substrates such as metal chelates, small molecules, or antibodies.[6-8] In addition to simplifying purification, affinity tags such as maltose-binding protein (MBP) and glutathione-S-transferase (GST) alleviate toxicity and improve expression level or protein solubility.[9-11] Purification of MBP-tagged proteins relies on chromatography with amylose resins, whereas GST-tagged proteins bind to immobilized glutathione, and subsequent elution with glutathione occurs under mild, non-denaturing conditions.[12] However, the large size and immunogenicity of MBP and GST may complicate downstream applications. SUMO fusion tags also enhance protein expression and solubility in prokaryotes and eukaryotes and facilitate subsequent tag removal with a SUMO protease.[13,14] Often a second tag such as polyhistidine serves together with MBP, GST or SUMO to facilitate

purification.

Small peptides such as FLAG, HA (hemagglutinin)-binding peptide, and c-Myc tag (epitope of the human c-Myc proto-oncogene product (EQKLISEEDL)) enable purification through antibody-antigen binding.[7,15-18] In this case, the sequence of an epitope peptide is inserted into the protein of interest and an immobilized anti-epitope antibody binds the tagged proteins through the epitope. Because of the strong binding between antigen and antibody, the elution usually requires harsh conditions such as low pH and detergent. Moreover, the binding capacity is quite low because of the large size of the capture antibody. Antibody immobilization may also sterically hinder binding of the tagged protein. For example, Anti-FLAG affinity gel (Sigma Aldrich) has a binding capacity of > 0.6 mg/mL, Anti-c-Myc agarose (ThermoFisher) has a binding capacity around 3 mg/mL (102 to 144 nmol of protein per mL, proteins size; 26 to 29 kDa), and Anti-HA Magnetic beads (ThermoFisher) have a binding capacity > 100μg/mL (protein size ~ 70 kDa).[19-21]

Table 1.1. Common affinity tags for recombinant protein purification, mAb = monoclonal antibody.

Affinity tag	Size (kDa)	Capture Matrix
Poly-Arg	0.8	Cation-exchange resin
Poly-His	0.84	Metal ion complexes (Ni^{2+}, Co^{2+}, Cu^{2+})
Glutathione S-transferase	26	Glutathione
FLAG	1.01	Anti-FLAG mAb
Streptavidin-binding peptide	4.3	Streptavidin
Strep II	1.06	Strep-Tactin (modified streptavidin)
Maltose-binding protein	42	Amylose
Calmodulin-binding peptide	2.96	Calmodulin
Chitin-binding domain	5.59	Chitin
S	1.75	S-protein of RNase A
HA	1.1	Anti-HA epitope mAb
c-Myc	1.2	Anti-Myc epitope mAb
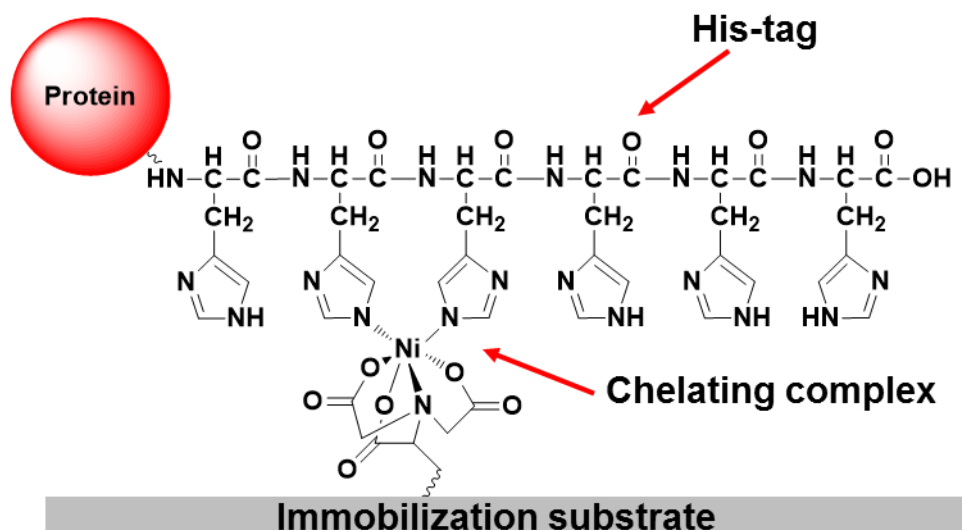
Figure 1.2. Scheme of immobilized metal affinity chromatography for His-tag protein capture.

Among the protein affinity tags, the polyhistidine-tag (His-tag) is the most common because of its small size, electrical neutrality at physiological pH, low toxicity and immunogenicity, and simple isolation.[6] A number of chelated metal ions (Ni^{2+}, Co^{2+}, Cu^{2+}, Zn^{2+}) can serve as affinity ligands for His-tagged protein purification through immobilized metal affinity chromatography (IMAC, Figure 1.2),[22-25] but Ni^{2+} is the most widely used metal ion for His-tag protein purification. The His-tags bind best to IMAC resins in near-neutral buffer, and subsequently readily elute in excess imidazole. Sometimes low pH solutions such as 0.1 M glycine-HCl or buffers containing an excess of strong chelator (e.g., EDTA) can also elute His-tagged protein,[26]

1.2.1 Membrane adsorbers for His-tagged protein purification

Conventional IMAC applies agarose, sepharose or magnetic beads that exhibit binding capacities ranging from 30 to 60 mg of His-tag protein per mL of resin.[27-29] However, porous beads show some limitations for protein purification. In particular, slow diffusion of proteins into bead pores requires long incubation times for on-bead purification, which is especially

6

problematic for proteins that degrade rapidly. Washing and eluting the bound proteins also requires long times and relatively large amounts of buffer. Compared to bead substrates, membrane presents an interesting alternative for rapid protein purification. Flow directly through membrane pores rapidly brings proteins to binding sites, and the low thickness of membranes leads to small pressure drops. However, the membranes suffer from a low surface area, so binding capacities are typically less for membranes than beads.

A number of studies aimed to increase the binding capacities of affinity membranes. Both surface-initiated growth of polymer brushes and layer-by-layer (LbL) polyelectrolyte adsorption can provide highly swollen films that capture multiple layers of proteins, as Figure 1.3 shows.[30-37] Compared to the synthesis of polymer brushes, which is a relatively cumbersome process that frequently requires initiator immobilization and subsequent polymerization under anaerobic conditions, LbL deposition is quite simple. Our group employed LbL adsorption of poly(acrylic acid) (PAA)/(polyethyleneimine) (PEI) films followed by derivatization with aminobutyl nitrilotriacetate (NTA) and Ni^{2+} to form NTA-Ni^{2+} complexes that capture His-tagged proteins.[38] However, derivatization represents more than 95% of the cost of chemicals and materials for creating protein-binding membranes, and most of the aminobutyl NTA does not couple to the membrane. These expensive reagents may make such membranes impractical at large scales. Moreover, in addition to NTA these membranes contain residual -COOH groups of PAA that bind metal ions only weakly, which likely increases metal-ion leaching. Thus, examining whether direct adsorption of relatively inexpensive polyelectrolytes containing chelating groups can effectively modify membranes to

bind metal ions and capture His-tagged protein is potentially important to further decrease the cost for His-tag protein purification. Chapter 2 describes our efforts in this area.

Polymer brushes in a membrane pore   **Polyelectrolyte in a membrane pore**
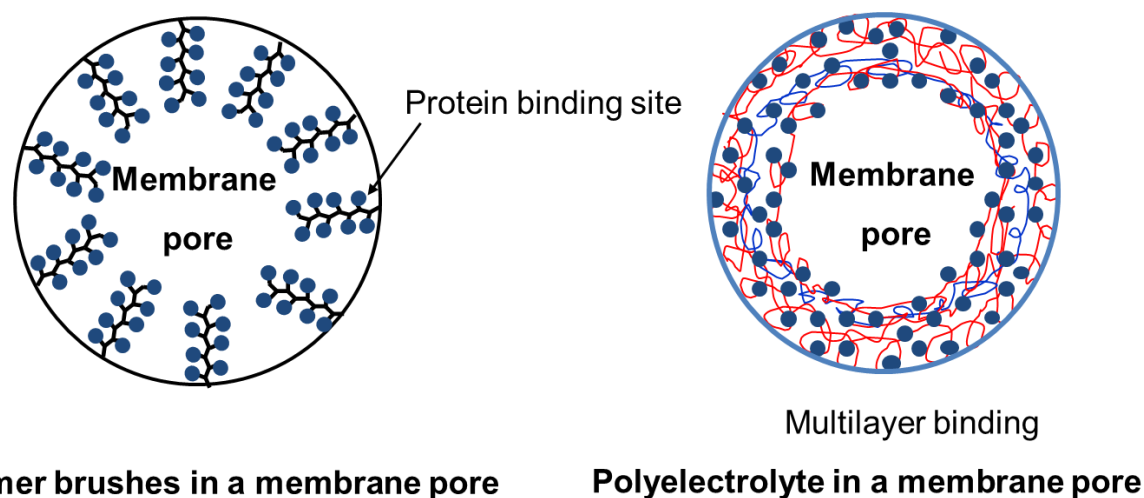
Figure 1.3. Schematic drawing showing modification of membrane pores with polymer brushes or polyelectrolyte multilayers to improve protein-binding capacity.

1.2 Affinity tag removal

Affinity protein purification is typically only one of several steps before the application of recombinant proteins. In addition to further purification steps, tag removal is also necessary because affinity tags may alter the function, bioactivity and structure of recombinant proteins in comparison to the wild-type species. Araú´jo and coworkers reported that the activity of His-tagged chlorocatechol 1,2-dioxygenase was five times lower than the activity of the same protein after thrombin-catalyzed tag cleavage.[39] Bucher et al. found that short affinity tags had profound effects on both the formation of pyrococcus furiosusvmaltodextrin-binding protein crystals and their abilities to diffract X-rays.[13] In the following section, I discuss conventional strategies for affinity tag removal, current research on immobilizing site-specific enzymes for tag removal, and anchoring His-tagged SUMO protease for in-membrane His-tagged SUMO removal.

1.2.1 Methods for His-tag removal

In principle, tag removal can occur through chemical treatment, self-cleavage of inteins, and enzymatic methods.[6,14] For chemical tag removal, a unique methionine residue must reside at the junction between the fusion partner and the protein of interest. The chemical treatment is inexpensive, accessible and easy to scale-up, but it usually leads to protein denaturation due to the harsh chemical treatment with cyanogen bromide. Self-cleavage of inteins requires addition of a thiol such as β-mercaptoethanol or shifts in pH and increases in temperature.[14] The thiol reagent may break disulfide bonds within the protein, which could also cause denaturation and precipitation of proteins. Compared to chemical treatment and self-cleavage of inteins, enzymatic cleavage is attractive because of its high selectivity and mild reaction conditions.

Table 1.2. Common site-specific proteases for tag cleavage and their cleavage sites. TEV = tobacco etch virus. SUMO = small ubiquitin-like modifier. HRV 3C = human Rhinovirus 3C Protease. * denotes the protease cleavage site.

Enzyme	Cleavage site	Origin
Enterokinase	DDDDK*	Recombinant
Thrombin	LVPR*GS	Bovine extraction
TEV protease	EQLYFQ*G	Recombinant
SUMO protease	Conformation of SUMO	Recombinant
Factor Xa	I(E or D)G*R	Bovine extraction
HRV 3C	LEVLFQ*GP	Recombinant

Common proteases for tag removal include enterokinase,[40] factor Xa,[41] human rhinovirus 3C protease (HRV 3C),[40] SUMO protease,[42] tobacco etch virus (TEV) protease,[11,43] and thrombin.[41] Table 1.2 lists the canonical recognition sequences and specific cut sites for each of these proteases. Because these endopeptidases cleave proteins at specific sequences, they are candidates for selective catalysis of tag removal. Exopeptidases can also catalyze the removal of amino acids from the end of a protein but their applications include only the removal of small tags.

Unfortunately, the high cost (and low availability) of endopeptidases limes their application

in large-scale protein manufacturing. Table 1.3 lists the cost and recovery for several endoproteases. However, the current costs are at a minimum $20,000 per g of product. In addition, many of these proteases like thrombin are highly bioactive (non-specific cleavage may happen during the cleavage) and must be separated completely from the target protein.

Table 1.3. Cost and recovery comparison for proteases used for protein tag removal.[14] Costs are based on recommended protocols at laboratory scales and do not take into account protease removal costs; Recovery of substrate protein is based on initial material expressed.

Protease	Cost per g product	% recovery	Protease removal method	Company
Enterokinase	$50100	95	Antibody based	Roche
Thrombin	$39400	85	Chromatography	Sigma
Factor Xa	$22400	95	Chromatography	NEB
TEV	$43300	85	Ni^{2+} column	Invitrogen
SUMO	$560000	85	Chromatography	Invitrogen

1.2.2 Immobilization of site-specific proteases for tag removal

Immobilization of proteases on solid substrates for multiple usages can potentially decrease protease consumption and facilitate protease separation from product. Several studies examined immobilization of site-specific proteases for fusion tag removal. Miladi et al. immobilized the wild-type and S219V mutant Streptag II TEV protease on a streptavidin-

agarose matrix with a retained activity of 83.5% and 81% compared to the free forms.[10] Over

a period of 18 months, they used the wild-type and mutant immobilized proteases for nine batch

reactions with retention of 38% and 51% of their initial activities. Guoqiu Wu *et al.*

immobilized thrombin in a polyacrylamide gel for cleaving recombinant S-thanatin.[9] The

immobilized proteases exhibited greater stability and activity over wider pH and temperature

ranges than free enzyme.

However, similar to resin-based protein purification, slow diffusion into porous beads may

limit the rate of tag removal and require long incubation times for cleavage. In contrast

convective flow through porous membrane supports should eliminate substrate diffusion

limitations[44] and transport the product away from the enzyme active site to minimize additional

cleavage at a second substrate site. Additionally, convective flow allows uniform

immobilization of protease in the membrane,[45] and scale-up of membrane processes through

increasing surface area is relatively simple. Because of the minimal thickness (~100 μm) of

typical polymer membranes, variation of the flow rate through these membranes provides

control over the residence time down to the millisecond level. With short residence times,

proteolysis may occur only at the most accessible and reactive sites to prevent unwanted

additional cleavage within the protein of interest.

1.2.3 Immobilization of SUMO proteases in membranes for tag removal

In this research, I employ SUMO protease in proof of concept studies of the immobilization,

activity, and reusability of tag-removal enzymes in porous membranes. SUMO protease

specifically cleaves the small ubiquitin-related modifier (SUMO) at the C-terminal Gly-Gly

motif by recognizing the SUMO conformation, so non-specific cleavage seldom happens.[12]

The molecular weight of SUMO protease is about 27.5 kDa and the theoretical isoelectric point

(pI) of His-tagged sumo protease is about 7.32 (estimated with ExPASy – Compute pI/Mw

tool). This enzyme cleaves essentially all SUMO fusion proteins, with any amino acid except

proline after the Gly-Gly motif can be cleaved efficiently.

The SUMO often improves the solubility and yield of recombinant proteins, so researchers

employ SUMO fusion constructs to produce proteins with otherwise low solubilities and

expression levels. High purity recombinant preparations of SUMO protease are available, and

usually the protease bears a His-tag for future separation from the protein substrate. However,

continuous production of this enzyme in soluble form is not easily accessible to many

laboratories, and the SUMO protease may precipitate during purification and storage. Thus,

immobilizing SUMO protease to make a reusable enzymatic reactor could decrease the cost of

tag cleavage. Chapter 3 gives details about immobilizing His-tagged SUMO protease in

membranes and subsequent SUMO removal.

1.3 Mass spectrometry analysis of proteins

Characterization of protein structures[46,47] and post-translational modifications[48,49] as well

as protein-drug interactions[50-52] is important for development of new pharmaceutical

compounds and biomarker discovery.[53] Because of its high sensitivity, accuracy and high

throughput, mass spectrometry is the most powerful tool for rapid protein characterization,

including peptide mapping, identification of post-translational modifications and low-

resolution studies of protein structure.[54-56] In the section below, I first discuss different

approaches to mass spectrometric protein analyses including top-down, middle-down and bottom-up strategies. Subsequently I briefly describe limited proteolysis followed by mass spectrometry analysis for protein structure studies and present prior work on immobilized-trypsin bioreactors.

1.3.1 Top-down, bottom-up and middle-down strategies for protein analysis using mass spectrometry

The primary approaches for mass spectrometry studies of proteins include top-down, middle-down and bottom up strategies (Figure 1.4). Top-down mass spectrometry is an emerging approach for protein analysis through directly ionizing and fragmenting intact proteins. It gives the protein molecular weight, and identifies post-translational modifications and different isoforms simultaneously.[57-59] However, this approach usually requires high-resolution mass spectrometers, such as Fourier transform ion cyclotron resonance (FT-ICR) or Orbitrap instruments. Even when coupled with electron capture dissociation or electron transfer dissociation, the fragmentation efficiency is still low, which results in poor sequence coverage for identification of specific sites.

Thus, most mass spectrometry studies still employ enzymes to cut intact proteins into peptides that are more amenable to mass spectrometry analysis. Many different proteases such as trypsin, chymotrypsin, LysC, LysN, AspN, GluC and ArgC can digest enzymes for analysis.[60,61] Depending on the sizes of proteolytic peptides, digestion leads to middle-down or bottom-up strategies for protein analysis. The bottom-up strategy is the most common method.[62] In the most common application of this strategy, proteins undergo complete trypsin digestion in solution followed by separation and analysis with liquid chromatography/mass

spectrometry (LC/MS). Database searching using algorithms such as MASCOT and SEQUEST identifies proteolytic peptides that usually have masses less than 2-3 kDa. Although the bottom-up approach is effective and works with lower amounts of protein than the top-down strategy, it has drawbacks.[63,64] First loss of peptides can occur either in LC separation or mass spectrometry analysis steps. Additionally, this technique is not ideal for identification of proteins isoforms, and it may not generate comprehensive information on post-translational modifications.[59,65]

The middle-down approach is a hybrid of bottom-up and top-down methods. This strategy analyzes larger peptides than bottom-up methods, thus minimizing peptide redundancy between proteins. Additionally, with fewer instrumental requirements than the top-down method, the middle-down strategy also identifies post-translational modifications. Unlike bottom-up techniques that employ trypsin for proteolysis, middle-down digestion usually uses LysC, LysN, AspN, GluC, ArgC to generate larger peptides.[66,67] Other recently developed proteases such as outer membrane protease T (Omp T) can produce especially large peptides (>6.3 kDa on average). Wu and coworkers used this enzyme followed by mass spectrometry-based proteomics to identify 3697 peptides from 1038 proteins. They also differentiated closely related protein isoforms with large Omp T peptides.[68]

Unlike trypsin, which is cheap and specific, the enzymes mentioned above for middle-down methods are either expensive or difficult to express. Thus, middle-down protein analysis with such enzymes can be costly. Controlling and limiting trypsin proteolysis to generate large peptides could serve as an interesting alternative to provide both large and small peptides for middle-down and bottom-up studies.
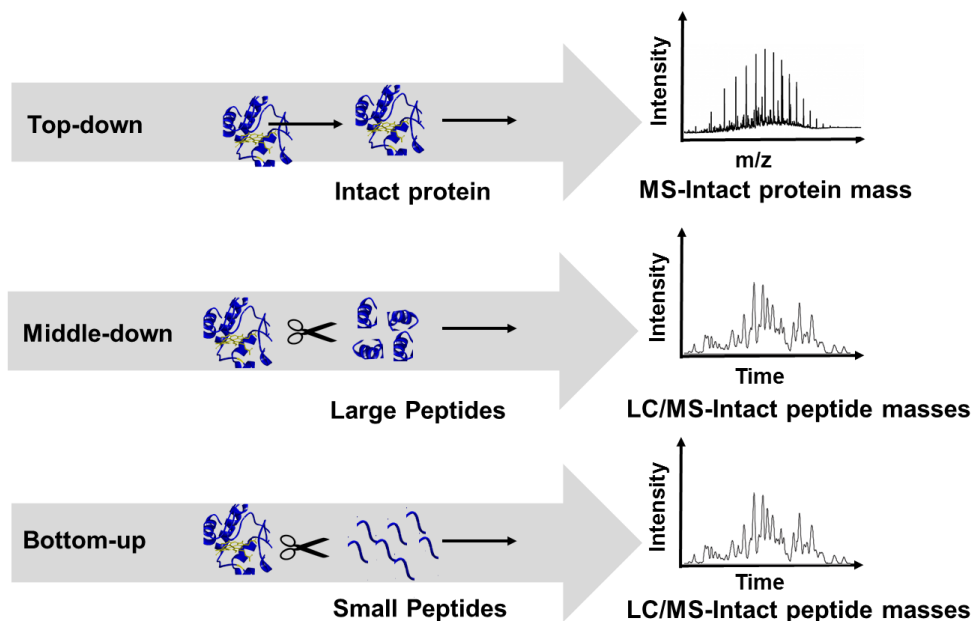
Figure 1.4. Top-down, middle-down and bottom-up approaches for protein studies using mass spectrometry.

1.3.2 Limited proteolysis for protein structure studies

In addition to analysis of peptides for identification of proteins and their post-translational modifications, mass spectrometry can also provide low-resolution information about protein three-dimensional structures. X-ray crystallography, nuclear magnetic resonance (NMR) spectroscopy, electron microscopy and other spectroscopic techniques can successfully interrogate protein structure. However, these methods all have limitations. For example, X-ray crystallography requires protein crystals and provides essentially static images with little information on protein flexibility.[47] NMR studies require a high concentration of pure protein and are difficult for proteins larger than 30 kDa.[47]

Limited proteolysis followed by mass spectrometry can facilitate the identification of disordered protein regions as well as protein conformational changes that take place in the presence of drugs or other proteins. Proteolysis initially occurs in exposed, flexible regions, so

detection of specific proteolytic peptides in partial digests can identify these regions. Moreover, conformational changes alter the sites of initial cleavage and, hence, the peptides that result from digestion. Table 1.4 lists common proteases for limited proteolysis in studies of protein structure.

Table 1.4. Common proteases for limited proteolysis/mass spectrometry analysis of proteins, * denotes the protease cleavage site.

Protease	Cleavage Site
Trypsin	Arg or Lys
Thrombin	LVPR*GS
Subtilisin	Non-specific
Chymotrypsin	Non-specific
Protease K	Non-specific
Papain	Non-specific
Protease V8	Glu
Elastase	Non-specific
Thermolysin	Non-specific
Pepsin	Non-specific

1.3.3 Immobilized-trypsin bioreactors

Although various enzymes can digest proteins for subsequent mass spectrometry analysis, trypsin is the most popular protease because of its high specificity, relatively low cost and high efficiency.[69] Trypsin is a serine protease that cleaves proteins after arginine and lysine residues not followed by proline. Immobilization of trypsin on substrates can restrict autolysis and

increase enzyme density to digest proteins faster than conventional in-solution digestion. A number of research groups immobilized trypsin on substrates such as polymer plates,[70] membranes,[71-73] monoliths,[74] microfluidic channels,[75] and resins[76,77] through covalent linkage or physical adsorption.

Limiting trypsin digestion can provide both high sequence coverage and information on the protein three-dimensional structure. Strategies for effecting limited digestion include short digestion times, low temperatures, and control over pH during protein exposure to a low protease concentration.[78] However, minimizing the level of intact protein while obtaining significant amounts of incompletely digested peptides is often a challenge. Compared to other immobilization substrates such as porous beads and monolith columns, membranes are a particularly attractive platform for immobilizing trypsin for limited proteolysis. Because membranes are only ~100 μm thick, pumping protein solutions through them readily yields residence times from seconds to milliseconds. As Figure 1.5 schematically shows, controlling the flow rate, through trypsin-containing membranes should help control trypsin digestion to generate large peptides at fast flow rates and small peptides at slow flow rates. Control over protein digestion may aid protein primary and three-dimensional structures studies.
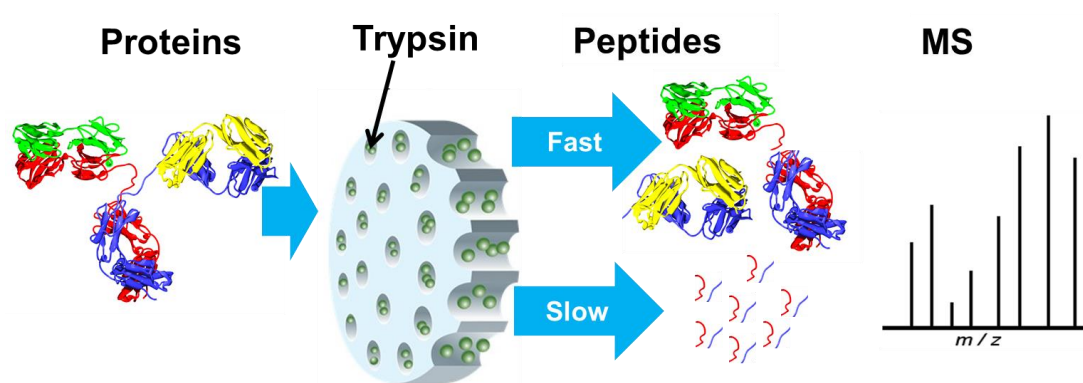
Figure 1.5. Controllable in-membrane trypsin digestion to generate large or small peptides. The cartoon for trypsin immobilized membrane was from Yujing Tan.[71]

1.4 Platforms for in-membrane protein digestion and purification

To perform in-membrane proteolysis, the ideal membrane platform should include: (1) control of residence time; (2) simple operation; and (3) high-throughput. This dissertation examines platforms with the membrane connected to a syringe pump or a pipette tip. The latter will likely provide simpler operation and higher throughput but less control of residence time. For protein purification, selection of the appropriate platform depends on the amount of protein and the solution volume. For isolation of milligrams of protein, I employ a home-made Teflon holder connected to a peristaltic pump, whereas for microgram-scale protein purification, the platforms for protein digestion (membranes connected to syringes or pipette tips) are convenient. In the following section I compare these platforms for protein digestion and purification.

1.4.1 Minimized membrane holder connected to syringe

Fei Xu and other Bruening group members developed a miniaturized membrane holder[72] (Figure 1.6 (a)) that interfaces a membrane with a syringe pump (Figure 1.6 (b)). In the small flangeless fitting system (Upchurch Scientific, A-424) the membrane sits on a frit and is

connected on both sides to tubes fixed in ferrules. The contact between the tubes and the membrane exposes an area of 0.021 cm² to liquid flow, and a syringe pump forces fluid through the membrane. Assuming a porosity of 0.5, the membrane volume exposed to fluid flow is 0.11 µL for a 110 µm thick membrane. The main advantage of this apparatus for in-membrane digestion is the control of residence time.
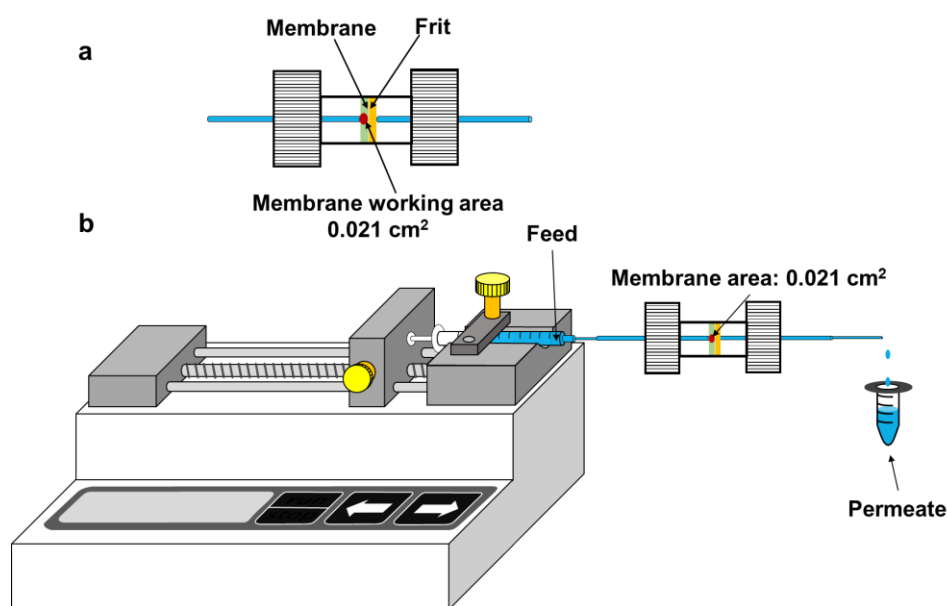
Figure 1.6. (a) Miniaturized membrane holder (flangeless fitting system, Upchurch Scientific, A-424); (b) miniaturized membrane holder connected to a syringe pump for in-membrane digestion. (Zhefei Yang drew the syringe pump cartoon.)

Equation 1.1 describes how to calculate the solution residence time, t_r, in the membrane, where L is membrane thickness (~100 µm); Q is the volumetric flow rate through the membrane; ε is the membrane porosity (~0.5); and A is the membrane surface area (0.02 cm²). For the syringe pump we employ the flow rate ranges from 2 mL/min to 0.01 mL/min, so the residence time can vary from milliseconds to seconds.

$$t_r = \frac{\varepsilon L A}{Q} \tag{1.1}$$

This platform is most appropriate for research requiring fine control of residence time, e.g. limited proteolysis. For protein purification, because the holder exposes a membrane volume of only ~0.22 µL (0.02 cm^2 × 110 µm, including pores and polymer), the membrane will bind only 13 µg of protein (assuming a protein-binding capacity of 60 mg per mL of membrane). Thus this platform is only suitable for purification of micrograms of protein. Additionally, this technique is cumbersome and not for readily adaptable for high-throughput applications.

1.4.2 Home-made Teflon holder connected to a peristaltic pump for membrane modification and protein purification

The most straightforward approach to increase the binding capacity of membrane platforms is to increase the membrane surface area. The membrane holder shown in Figure 1.7 exposes a membrane surface area of 3.14 cm^2, which is 160 times the effective surface area of the syringe pump platform shown in Figure 1.6. Thus, the combination of the larger holder and the peristaltic pump enables purification of milligrams of protein. We also built membrane holders with exposed membrane areas of 0.79 cm^2 for purification of smaller amounts of protein. (These holders are similar to commercial Amicon cells.) In addition to increasing the exposed external membrane surface area, stacking membranes can also increase purification capacity. Guanqing Liu stacked 3 (PSS/PEI)$_{3.5}$-modified membranes to increase lysozyme binding capacity (at 10% breakthrough) almost 3 times compared to a single membrane, showing that stacking increases capacity.[79] However, effective stacking may require small gaskets to physically separate membranes.
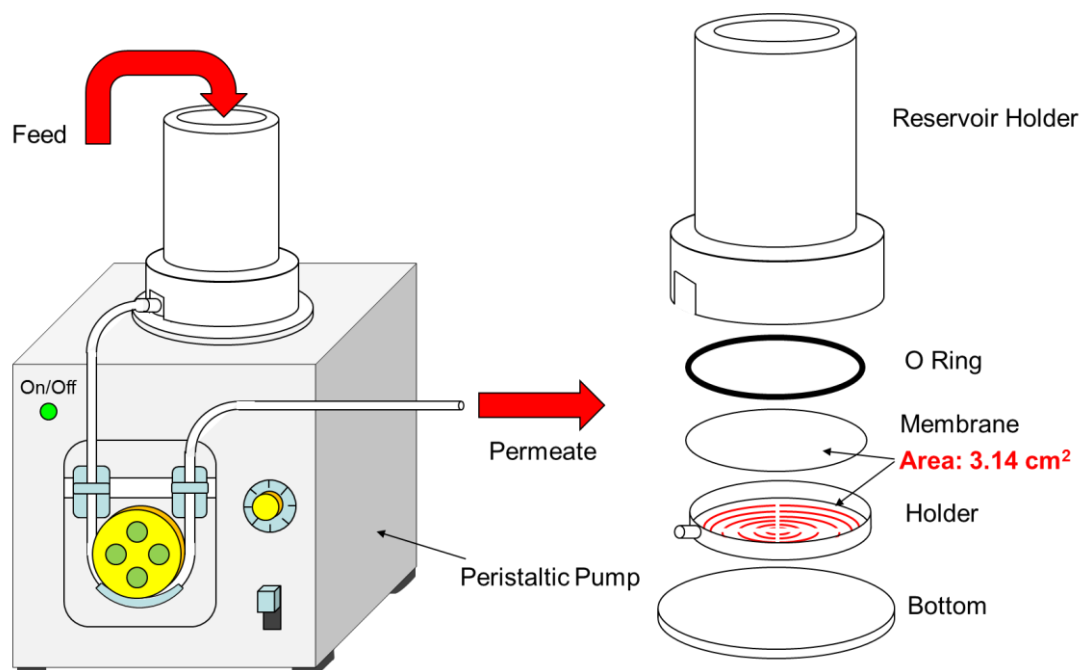
Figure 1.7. Home-made Teflon holder connected to a peristaltic pump for membrane modification and protein purification. (This is a slightly modified version of a figure originally drawn by Zhefei Yang).

The holder depicted in Figure 1.7 has a reservoir of 20 mL and also serves as the apparatus for modifying membranes with polyelectrolytes and trypsin. However, it is not appropriate for modification with small amounts of expensive proteases.   For immobilization of micrograms of enzymes such as His-SUMO protease, we employ the miniature holder with the syringe pump (Figure 1.6).

1.4.3 Pipette tips for in-membrane protein digestion and purification

Membranes attached to the ends of pipette tips are attractive for potential high-throughput applications. Several commercial functionalized pipette tips are available for protein digestion and purification, including Monotip^{TM} (GL Science) and DigestTip^{TM} (ProteoGen Bio) pipette tips containing monoliths or resins for protease immobilization, and PureSpeed Affinity Resin tips (Mettler Toledo) that facilitate purification of His-tagged protein and antibodies.

To attach a membrane to a pipette tip, I developed a membrane holder from the polyether ether ketone (PEEK) Super flangeless ferrule module (IDEX, Catalogue number P-260) illustrated in Figure 1.8. Even though there is some backpressure, pipetting 100 µL of protein solution through the membrane takes only a few seconds. Unlike the minimized membrane holder connected to a syringe pump, this pipette tip platform is promising for high-throughput sample preparation when coupled to robotics. Chapter 5 provides details of using pipette tips to perform in-membrane protein digestion and purification.
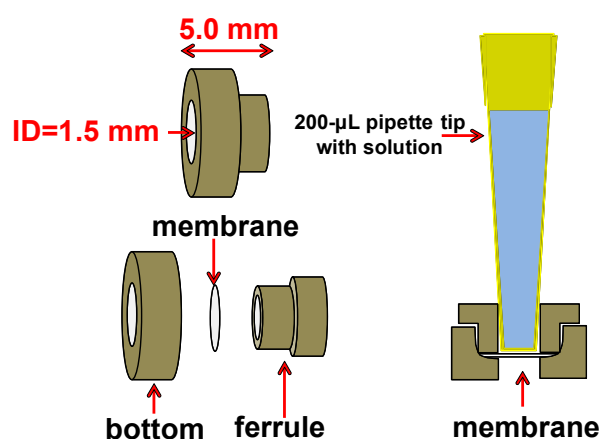
Figure 1.8. Diagram of a miniature membrane holder and attachment of a pipette tip to the holder.[80]

1.5 Outline of this dissertation

In chapter 2, this dissertation describes purification of His-tagged proteins using (PEI/CMPEI)-modified membranes. Layer-by-layer adsorption with the chelating polyelectrolyte and subsequent formation of Ni^{2+} complexes yields membranes that bind up to 60 mg of His-tagged protein per mL. Chapter 3 then discusses immobilization of His-tagged SUMO protease for effective His-SUMO tag removal, and chapter 4 focuses on using trypsin-modified membranes for protein digestion, including limited digestion to identify highly

accessible protein regions. Subsequently, I describe a membrane holder that attaches functionalized membranes to the ends of pipette tips for rapid in-membrane protein purification and digestion (chapter 5). Finally, chapter 6 summarizes my research on developing functionalized membranes for protein purification, affinity tag removal and protein digestion in membranes. Specifically, the next five chapter titles are:

Chapter 2: Immobilization of Carboxymethylated Polyethyleneimine-Metal Ion Complexes in Porous Membranes to Selectively Capture His-tagged Protein

Chapter 3: Enzymatic Membrane Reactor for Affinity Tag Removal

Chapter 4: Controlled Proteolysis in Porous Membrane Reactors Containing Immobilized Trypsin

Chapter 5: Rapid Protein Digestion and Purification with Membranes Attached to Pipette Tips

Chapter 6: Summary and Future work

REFERENCES

REFERENCES

(1) Schein, C. H., Production of Soluble Recombinant Proteins in Bacteria, *Biotechnology* **1989**, *7*, 1141-1147.

(2) Rosano, G. L.; Ceccarelli, E. A., Recombinant Protein Expression in Escherichia coli: Advances and Challenges, *Front Microbiol.* **2014**, *5,* 172.

(3) Saraswat, M.; Musante, L.; Ravidá, A.; Shortt, B.; Byrne, B.; Holthofer, H., Preparative Purification of Recombinant Proteins: Current Status and Future trends, *BioMed. Res. Int.* **2013**, *2013*.

(4) Gräslund, S.; Nordlund, P.; Weigelt, J.; Bray, J.; Gileadi, O.; Knapp, S.; Oppermann, U.; Arrowsmith, C.; Hui, R.; Ming, J., Protein Production and Purification, *Nat. Methods* **2008**, *5*, 135-146.

(5) Johnson, I. S., Human Insulin from Recombinant DNA Technology, *Science* **1983**, *219*, 632-637.

(6) Arnau, J.; Lauritzen, C.; Petersen, G. E.; Pedersen, J., Current Strategies for the Use of Affinity Tags and Tag Removal for the Purification of Recombinant Proteins, *Protein Expr. Purif.* **2006**, *48*, 1-13.

(7) Young, C. L.; Britton, Z. T.; Robinson, A. S., Recombinant Protein Expression and Purification: A Comprehensive Review of Affinity Tags and Microbial Applications, *Biotechnol. J.* **2012**, *7*, 620-634.

(8) Waugh, D. S., Making the Most of Affinity Tags, *Trends Biotechnol.* **2005**, *23*, 316-320.

(9) Wu, G. Q.; Deng, X. P.; Li, X. F.; Wang, X. Y.; Wang, S. L.; Xu, H. M., Application of Immobilized Thrombin for Production of S-Thanatin Expressed in Escherichia Coli, *Appl. Microbiol. Biotechnol.* **2011**, *92*, 85-93.

(10) Miladi, B.; El Marjou, A.; Boeuf, G.; Bouallagui, H.; Dufour, F.; Di Martino, P.; Elm'selmi, A., Oriented Immobilization of the Tobacco Etch Virus Protease for the Cleavage of Fusion Proteins, *J. Biotechnol.* **2012**, *158*, 97-103.

(11) Puhl, A. C.; Giacomini, C.; Irazoqui, G.; Batista-Viera, F.; Villarino, A.; Terenzi, H., Covalent Immobilization of Tobacco-Etch-Virus NIa Protease: A Useful Tool for Cleavage: of the Histidine Tag of Recombinant Proteins, *Biotechnol. Appl. Biochem.* **2009**, *53*, 165-174.

(12) Malakhov, M. P.; Mattern, M. R.; Malakhova, O. A.; Drinker, M.; Weeks, S. D.; Butt,

T. R., SUMO Fusions and SUMO-Specific Protease for Efficient Expression and Purification of Proteins, *J. Struct. Functional Genomics* **2004**, *5*, 75-86.

(13) Bucher, M. H.; Evdokimov, A. G.; Waugh, D. S., Differential Effects of Short affinity Tags on the Crystallization of Pyrococcus Furiosus Maltodextrin-Binding Protein, *Acta Crystallogr. Sect. D. Biol. Crystallogr.* **2002**, *58*, 392-397.

(14) Fong, B. A.; Wu, W.-Y.; Wood, D. W., The Potential Role of Self-Cleaving Purification Tags in Commercial-Scale Processes, *Trends Biotechnol.* **2010**, *28*, 272-279.

(15) Einhauer, A.; Jungbauer, A., The FLAG™ Peptide, A Versatile Fusion Tag for the Purification of Recombinant Proteins, *J. Biochem. Bioph. Methods* **2001**, *49*, 455-465.

(16) Hopp, T. P.; Prickett, K. S.; Price, V. L.; Libby, R. T.; March, C. J.; Cerretti, D. P.; Urdal, D. L.; Conlon, P. J., A Short Polypeptide Marker Sequence Useful for Recombinant Protein Identification and Purification, *Biotechnology* **1988**, *6*, 1204-1210.

(17) Surdej, P.; Jacobs-Lorena, M., Strategy for Epitope Tagging the Protein-Coding Region of Any Gene, *Biotechniques* **1994**, *17*, 560-565.

(18) Evan, G. I.; Lewis, G. K.; Ramsay, G.; Bishop, J. M., Isolation of Monoclonal Antibodies Specific for Human C-Myc Proto-Oncogene Product, *Mol. Cell. Biol.* **1985**, *5*, 3610-3616.

(19) ANTI-FLAG® M1 Agarose Affinity Gel http://www.sigmaaldrich.com/catalog/product/sigma/a4596?lang=en&region=US, 09/01/2016.

(20) Pierce™ Anti-HA Magnetic Beads, https://www.thermofisher.com/order/catalog/product/88836, 09/01/2016.

(21) Pierce™ Anti-c-Myc Magnetic Beads, https://www.thermofisher.com/order/catalog/product/88842, 09/01/2016.

(22) Hengen, P. N., Purification of His-Tag Fusion Proteins from Escherichia Coli, *Trends Biochem. Sci.* **1995**, *20*, 285-286.

(23) Franken, K. L.; Hiemstra, H. S.; van Meijgaarden, K. E.; Subronto, Y.; Den Hartigh, J.; Ottenhoff, T. H.; Drijfhout, J. W., Purification of His-Tagged Proteins by Immobilized Chelate Affinity Chromatography: the Benefits from the Use of Organic Solvent, *Protein Expr. Purif.* **2000**, *18*, 95-99.

(24) Magnusdottir, A.; Johansson, I.; Dahlgren, L.-G.; Nordlund, P.; Berglund, H., Enabling IMAC Purification of Low Abundance Recombinant Proteins from E. coli Lysates, *Nat. Methods* **2009**, *6*, 477-478.

(25) Schmitt, J.; Hess, H.; Stunnenberg, H. G., Affinity Purification of Histidine-Tagged Proteins, *Mol. Biol. Rep.* **1993**, *18*, 223-230.

(26) His-tagged Proteins – Production and Purification, https://www.thermofisher.com/us/en/home/life-science/protein-biology/protein-biology-learning-center/protein-biology-resource-library/pierce-protein-methods/his-tagged-proteins-production-purification.html, 09/01/2016.

(27) His-Tagged Recombinant Protein Purification-His60 Ni Resin, http://www.clontech.com/US/Products/Protein_Expression_and_Purification/His-Tagged_Protein_Purification/Nickel_Resin_Batch_FPLC, 09/01/2016.

(28) Ni-NTA Agarose, https://www.qiagen.com/us/shop/sample-technologies/protein/ni-nta-agarose/#technicalspecification, 09/01/2016.

(29) HisPur™ Cobalt Superflow Agarose, https://www.thermofisher.com/order/catalog/product/25228, 09/01/2016.

(30) Sun, L.; Dai, J. H.; Baker, G. L.; Bruening, M. L., High-Capacity, Protein-Binding Membranes Based on Polymer Brushes Grown in Porous Substrates, *Chem. Mat.* **2006**, *18*, 4033-4039.

(31) Bhut, B. V.; Conrad, K. A.; Husson, S. M., Preparation of High-Performance Membrane Adsorbers by Surface-Initiated AGET ATRP in the Presence of Dissolved Oxygen and Low Catalyst Concentration, *J. Membr. Sci.* **2012**, *390*, 43-47.

(32) Bhut, B. V.; Conrad, K. A.; Husson, S. M., Preparation of High-Performance Membrane Adsorbers by Surface-Initiated AGET ATRP in the Presence of Dissolved Oxygen and Low Catalyst Concentration, *J. Membr. Sci.* **2012**, *390*, 43-47.

(33) Yang, Q.; Ulbricht, M., Cylindrical Membrane Pores with Well-Defined Grafted Linear and Comblike Glycopolymer Layers for Lectin Binding, *Macromolecules* **2011**, *44*, 1303-1310.

(34) Kawakita, H.; Masunaga, H.; Nomura, K.; Uezu, K.; Akiba, I.; Tsuneda, S., Adsorption of Bovine Serum Albumin to A Polymer Brush Prepared by Atom-Transfer Radical Polymerization in A Porous Inorganic Membrane, *J. Porous Mat.* **2007**, *14*, 387-391.

(35) Honjo, T.; Hoe, K.; Tabayashi, S.; Tanaka, T.; Shimada, J.; Goto, M.; Matsuyama, H.; Maruyama, T., Preparation of Affinity Membranes Using Thermally Induced Phase Separation for One-Step Purification of Recombinant Proteins, *Anal. Biochem.* **2013**, *434*, 269-274.

(36) Bhut, B. V.; Wickramasinghe, S. R.; Husson, S. M., Preparation of High-Capacity, Weak Anion-Exchange Membranes for Protein Separations Using Surface-Initiated Atom

Transfer Radical Polymerization, *J. Membr. Sci.* **2008**, *325*, 176-183.

(37) Ulbricht, M.; Yang, H., Porous Polypropylene Membranes with Different Carboxyl Polymer Brush Layers for Reversible Protein Binding via Surface-Initiated Graft Copolymerization, *Chem. Mat.* **2005**, *17*, 2622-2631.

(38) Bhattacharjee, S.; Dong, J. L.; Ma, Y. D.; Hovde, S.; Geiger, J. H.; Baker, G. L.; Bruening, M. L., Formation of High-Capacity Protein-Adsorbing Membranes through Simple Adsorption of Poly(acrylic acid)-Containing Films at Low pH, *Langmuir* **2012**, *28*, 6885-6892.

(39) Araujo, A.; Oliva, G.; Henrique-Silva, F.; Garratt, R.; Cáceres, O.; Beltramini, L., Influence of the Histidine Tail on the Structure and Activity of Recombinant Chlorocatechol 1, 2-Dioxygenase, *Biochem. Biophys. Res. Commun.* **2000**, *272*, 480-484.

(40) Waugh, D. S., An Overview of Enzymatic Reagents for the Removal of Affinity Tags, *Protein Expr. Purif.* **2011**, *80*, 283-293.

(41) Jenny, R. J.; Mann, K. G.; Lundblad, R. L., A Critical Review of the Methods for Cleavage of Fusion Proteins with Thrombin and Factor Xa, *Protein Expr. Purif.* **2003**, *31*, 1-11.

(42) Butt, T. R.; Edavettal, S. C.; Hall, J. P.; Mattern, M. R., SUMO Fusion Technology for Difficult-to-Express Proteins, *Protein Expr. Purif.* **2005**, *43*, 1-9. (43)Tropea, J. E.; Cherry, S.; Waugh, D. S., Expression and purification of soluble His 6-tagged TEV protease, *High Throughput Protein Expression and Purification: Methods and Protocols* **2009**, 297-307.

(44) Bhut, B. V.; Christensen, K. A.; Husson, S. M., Membrane Chromatography: Protein Purification from E. Coli Lysate Using Newly Designed and Commercial Anion-Exchange Stationary Phases, *J. Chromatogr. A* **2010**, *1217*, 4946-4957.

(45) Smuleac, V.; Butterfield, D.; Bhattacharyya, D., Layer-by-layer-Assembled Microfiltration Membranes for Biomolecule Immobilization and Enzymatic Catalysis, *Langmuir* **2006**, *22*, 10118-10124.

(46) Feng, Y. H.; De Franceschi, G.; Kahraman, A.; Soste, M.; Melnik, A.; Boersema, P. J.; de Laureto, P. P.; Nikolaev, Y.; Oliveira, A. P.; Picotti, P., Global Analysis of Protein Structural Changes in Complex Proteomes, *Nat. Biotechnol.* **2014**, *32*, 1036-1044.

(47) Vandermarliere, E.; Stes, E.; Gevaert, K.; Martens, L., Resolution of Protein Structure by Mass Spectrometry, *Mass Spectrom. Rev.* **2014**.

(48) Morris, M.; Knudsen, G. M.; Maeda, S.; Trinidad, J. C.; Ioanoviciu, A.; Burlingame, A. L.; Mucke, L., Tau Post-Translational Modifications in Wild-Type and Human Amyloid Precursor Protein Transgenic Mice, *Nat. Neurosci.* **2015**, *18*, 1183-1189.

(49) Dotz, V.; Haselberg, R.; Shubhakar, A.; Kozak, R. P.; Falck, D.; Rombouts, Y.; Reusch, D.; Somsen, G. W.; Fernandes, D. L.; Wuhrer, M., Mass Spectrometry for Glycosylation Analysis of Biopharmaceuticals, *TrAC, Trends Anal. Chem.* **2015**, *73*, 1-9.

(50) Zinn, N.; Hopf, C.; Drewes, G.; Bantscheff, M., Mass Spectrometry Approaches to Monitor Protein–Drug Interactions, *Methods* **2012**, *57*, 430-440.

(51) West, G. M.; Tucker, C. L.; Xu, T.; Park, S. K.; Han, X.; Yates, J. R.; Fitzgerald, M. C., Quantitative Proteomics Approach for Identifying Protein–Drug Interactions in Complex Mixtures Using Protein Stability Measurements, *Proc. Natl. Acad. Sci. USA.* **2010**, *107*, 9078-9082.

(52) Allardyce, C. S.; Dyson, P. J.; Coffey, J.; Johnson, N., Determination of Drug Binding Sites to Proteins by Electrospray Ionisation Mass Spectrometry: the Interaction of Cisplatin with Transferrin, *Rapid Commun. Mass Spectrom.* **2002**, *16*, 933-935.

(53) Parker, C. E.; Borchers, C. H., Mass Spectrometry Based Biomarker Discovery, Verification, and Validation–Quality Assurance and Control of Protein Biomarker Assays, *Mol. Oncol.* **2014**, *8*, 840-858.

(54) Tipton, J. D.; Tran, J. C.; Catherman, A. D.; Ahlf, D. R.; Durbin, K. R.; Kelleher, N. L., Analysis of Intact Protein Isoforms by Mass Spectrometry, *J. Biol. Chem.* **2011**, *286*, 25451-25458.

(55) Witze, E. S.; Old, W. M.; Resing, K. A.; Ahn, N. G., Mapping Protein Post-Translational Modifications with Mass Spectrometry, *Nat. Methods* **2007**, *4*, 798-806.

(56) Eyles, S. J.; Kaltashov, I. A., Methods to Study Protein Dynamics and Folding by Mass Spectrometry, *Methods* **2004**, *34*, 88-99.

(57) Zhang, H.; Ge, Y., Comprehensive Analysis of Protein Modifications by Top-Down Mass Spectrometry, *Circ. Cardiovasc. Genet.* **2011**, *4*, 711-711.

(58) Cui, W.; Rohrs, H. W.; Gross, M. L., Top-Down Mass Spectrometry: Recent Developments, Applications and Perspectives, *Analyst* **2011**, *136*, 3854-3864.

(59) Chait, B. T., Mass Spectrometry: Bottom-Up or Top-Down?, *Science* **2006**, *314*, 65-66.

(60) Giansanti, P.; Tsiatsiani, L.; Low, T. Y.; Heck, A. J., Six Alternative Proteases for Mass Spectrometry-Based Proteomics beyond Trypsin, *Nat. Protocols* **2016**, *11*, 993-1006.

(61) Switzar, L.; Giera, M.; Niessen, W. M., Protein Digestion: An Overview of the Available Techniques and Recent Developments, *J. Proteome Res.* **2013**, *12*, 1067-1077.

(62) Kelleher, N. L.; Lin, H. Y.; Valaskovic, G. A.; Aaserud, D. J.; Fridriksson, E. K.; McLafferty, F. W., Top Down Versus Bottom up Protein Characterization by Tandem High-Resolution Mass Spectrometry, *J. Am. Chem. Soc.* **1999**, *121*, 806-812.

(63) Ntai, I.; LeDuc, R. D.; Fellers, R. T.; Erdmann-Gilmore, P.; Davies, S. R.; Rumsey, J.; Early, B. P.; Thomas, P. M.; Li, S.; Compton, P. D., Integrated Bottom-Up and Top-Down Proteomics of Patient-Derived Breast Tumor Xenografts, *Mol. Cell. Proteomics* **2016**, *15*, 45-56.

(64) Gillet, L. C.; Leitner, A.; Aebersold, R., Mass Spectrometry Applied to Bottom-Up Proteomics: Entering the High-Throughput Era for Hypothesis Testing, *Annu. Rev. Anal. Chem.* **2016**, *9,* 449-472.

(65) Chen, B.; Peng, Y.; Valeja, S. G.; Xiu, L.; Alpert, A. J.; Ge, Y., Online Hydrophobic Interaction Chromatography–Mass Spectrometry for Top-Down Proteomics, *Anal. Chem.* **2016**, *88*, 1885-1891.

(66) Garcia, B. A.; Shabanowitz, J.; Hunt, D. F., Characterization of Histones and Their Post-Translational Modifications by Mass Spectrometry, *Curr. Opin. Chem. Biol.* **2007**, *11*, 66-73.

(67) Cannon, J.; Lohnes, K.; Wynne, C.; Wang, Y.; Edwards, N.; Fenselau, C., High-Throughput Middle-Down Analysis Using An Orbitrap, *J. Proteome Res.* **2010**, *9*, 3886-3890.

(68) Wu, C.; Tran, J. C.; Zamdborg, L.; Durbin, K. R.; Li, M.; Ahlf, D. R.; Early, B. P.; Thomas, P. M.; Sweedler, J. V.; Kelleher, N. L., A Protease for 'Middle-Down' Proteomics, *Nat. Methods* **2012**, *9*, 822-824.

(69) Lee, T. D.; Shively, J. E., [19] Enzymatic and Chemical Digestion of Proteins for Mass Spectrometry, *Method Enzymol.* **1990**, *193*, 361-374.

(70) Yamada, K.; Nakasone, T.; Nagano, R.; Hirata, M., Retention and Reusability of Trypsin Activity by Covalent Immobilization Onto Grafted Polyethylene Plates, *J. Appl. Polym. Sci.* **2003**, *89*, 3574-3581.

(71) Tan, Y. J.; Wang, W. H.; Zheng, Y.; Dong, J. L.; Stefano, G.; Brandizzi, F.; Garavito, R. M.; Reid, G. E.; Bruening, M. L., Limited Proteolysis via Millisecond Digestions in Protease-Modified Membranes, *Anal. Chem.* **2012**, *84*, 8357-8363.

(72) Xu, F.; Wang, W. H.; Tan, Y. J.; Bruening, M. L., Facile Trypsin Immobilization in Polymeric Membranes for Rapid, Efficient Protein Digestion, *Anal. Chem.* **2010**, *82*, 10045-10051.

(73) Cooper, J. W.; Chen, J. Z.; Li, Y.; Lee, C. S., Membrane-Based Nanoscale Proteolytic

Reactor Enabling Protein Digestion, Peptide Separation, And Protein Identification Using Mass Spectrometry, *Anal. Chem.* **2003**, *75*, 1067-1074.

(74) Krenkova, J.; Lacher, N. A.; Svec, F., Highly Efficient Enzyme Reactors Containing Trypsin and Endoproteinase LysC Immobilized on Porous Polymer Monolith Coupled to MS Suitable for Analysis of Antibodies, *Anal. Chem.* **2009**, *81*, 2004-2012.

(75) Liuni, P.; Rob, T.; Wilson, D. J., A Microfluidic Reactor for Rapid, Low-Pressure Proteolysis with on-Chip Electrospray Ionization, *Rapid Commun. Mass Spectrom.* **2010**, *24*, 315-320.

(76) Bayramoglu, G.; Celikbicak, O.; Arica, M. Y.; Salih, B., Trypsin Immobilized on Magnetic Beads via Click Chemistry: Fast Proteolysis of Proteins in A Microbioreactor for MALDI-TOF-MS Peptide Analysis, *Ind. Eng. Chem. Res.* **2014**, *53*, 4554-4564.

(77) Hu, Z. Y.; Zhao, L.; Zhang, H. Y.; Zhang, Y.; Wu, R. A.; Zou, H. F., The on-Bead Digestion of Protein Corona on Nanoparticles by Trypsin Immobilized on the Magnetic Nanoparticle, *J. Chromatogr. A* **2014**, *1334*, 55-63.

(78) Fontana, A.; de Laureto, P. P.; Spolaore, B.; Frare, E.; Picotti, P.; Zambonin, M., Probing Protein Structure by Limited Proteolysis, *Acta Biochim. Pol.* **2004**, *51*, 299-321.

(79) Liu, G.; Dotzauer, D. M.; Bruening, M. L., Ion-Exchange Membranes Prepared Using Layer-by-Layer Polyelectrolyte Deposition, *J. Membrane Sci.* **2010**, *354*, 198-205.

(80) Ning, W., and Bruening, M. L., Rapid Protein Digestionb and Purification with Membranes Attached to Pipet Tips, *Anal. Chem.* **2015**, *87* (24), 11984–11989.

Chapter 2. Immobilization of Carboxymethylated Polyethyleneimine-Metal Ion Complexes in Porous Membranes to Selectively Capture His-tagged Protein

Portions of this chapter are reprinted from our published paper in *Applied Materials & Interfaces* (Ning, W., Wijeratne, S., Dong, J., and Bruening, M. L. *Applied Materials & Interfaces* **2015**, *7* (4), 2575–2584.).

2.1 Introduction

In most studies of overexpressed proteins, purification employs engineered affinity tags.[1] Hexahistidine is the most common affinity tag because it is relatively small and enables convenient capture by binding to beads containing Ni^{2+} or Co^{2+} complexes.[2,3] Nevertheless, bead-based separations suffer from slow diffusion of large macromolecules into nanopores,[4-7] which necessitates long separation times that may harm sensitive proteins. Purifications are especially time consuming when capturing proteins from large volumes of dilute solutions. Porous membranes modified with affinity ligands are an attractive alternative purification platform because convection through the membrane pores and short radial diffusion distances provide rapid protein transport to binding sites.[8,9] Moreover, membrane pressure drops are low because of small thicknesses.[10-14] However, membranes have a lower specific surface area than nanoporous beads, which often leads to a low binding capacity.

To increase protein-binding capacities, several groups modified membrane pores with thin polymer films. Both surface-initiated growth of polymer brushes and layer-by-layer (LbL) polyelectrolyte adsorption can provide highly swollen films that capture multiple layers of proteins.[5,15-21] Compared to the synthesis of polymer brushes, which is a relatively cumbersome

process that frequently requires initiator immobilization and subsequent polymerization under anaerobic conditions, LbL deposition is quite simple. Our group employed LbL adsorption of poly(acrylic acid) (PAA)/(polyethyleneimine) (PEI) films followed by derivatization with aminobutyl nitrilotriacetate (NTA) and Ni^{2+} to form NTA-Ni^{2+} complexes that capture His-tagged proteins.[22] However, derivatization represents more than 95% of the cost of chemicals and materials for creating protein-binding membranes, and most of the aminobutyl NTA does not couple to the membrane. These expensive reagents may make such membranes impractical. Moreover, in addition to NTA these membranes contain residual -COOH groups of PAA that bind metal ions only weakly, which leads to metal-ion leaching.

This study examines whether direct adsorption of relatively inexpensive polyelectrolytes containing chelating groups effectively modifies membranes to bind metal ions and capture His-tagged protein (Figure 2.1). Specifically, we adsorb protonated poly(allylamine) (PAH)/ (PDCMAA) or PAH/carboxymethylated branched polyethyleneimine (CMPEI) films in membrane pores in ~40 minutes. Both PDCMAA and CMPEI contain iminodiacetic acid groups that form during reaction of the commercial polymers PAH or branched PEI with sodium chloroacetate (Scheme 2.1).[23] Thus, these polymers are readily accessible synthetically and relatively inexpensive. Previous studies examined LbL adsorption of (PAH/PDCMAA)$_n$ films and showed that they can contain up to 2.5 M of metal ions and facilitate selective metal-ion transport.[24,25] Carboxymethylated linear PEI is commercially available, but we employ branched PEI because it may provide thicker, highly swollen films for protein capture.[26] Importantly, we compare protein binding to PAH/PDCMAA and PAH/CMPEI films to test our hypothesis that ammonium groups in the PEI backbone will increase swelling and enhance

protein capture. Membranes modified with PAH/CMPEI rapidly capture as much as 60 mg of protein per mL of membrane, which is equivalent to the capacities of high-binding commercial beads.[27,28]
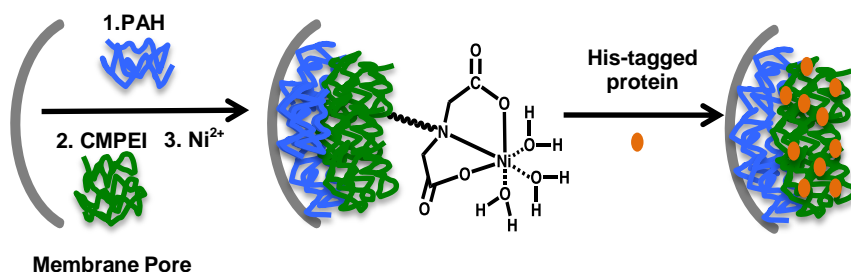
Figure 2.1. Assembly of a (PAH/CMPEI)-Ni^{2+} film in a nylon membrane pore, and capture of multilayers of His-tagged protein.

2.2 Experimental section

2.2.1 Materials

Aqueous solutions containing 0.02 M PAH, 0.01 M CMPEI or 0.01 M PDCMAA were prepared in deionized water (18.2 MΩcm, Milli-Q) or 0.5 M aqueous NaCl, and solution pH values were adjusted by dropwise addition of 0.1 M NaOH or HCl. Polymer concentrations are given with respect to the repeating unit. Au-coated Si wafers (200 nm of sputtered Au on 20 nm of Cr on Si (100) wafers) were cleaned in a UV/O$_3$ chamber for 15 min prior to use. Other materials include hydroxylated nylon (LoProdyne LP, Pall, 1.2 μm pore size, 110 μm thick), Conconavalin A (Con A from *Canavalia ensiformis* (Jack bean), Sigma Aldrich), coomassie protein assay reagent (Thermo Scientific), histidine6-tagged ubiquitin (His-U, human recombinant, Boston Biochem), poly(allylamine hydrochloride) (M_w 120,000−200,000 Da, Alfa Aesar), and poly(sodium 4-styrenesufonate) (PSS, M_w ~ 70 000 Da, Sigma Aldrich). CMPEI synthesis employed a branched poly(ethyleneimine) solution (M_n ~60,000 Da by gel-permeation chromatography, average M_w ~750,000 Da by light scattering, 50 wt. % in H$_2$O,

Sigma Aldrich). Cupric sulfate, nickel sulfate, sodium phosphate, sodium phosphate dibasic, ethylenediaminetetraacetic acid disodium salt (EDTA), sodium chloroacetate (98%), 3-mercaptopropionic acid (MPA, 99%) and imidazole (>99%) were received from Aldrich and used without further purification. Buffers include: binding buffer 1: 20 mM phosphate, pH 6; binding buffer 2: 20 mM phosphate, pH 7.4; washing buffer 1: 20 mM phosphate, 150 mM NaCl, 0.1% Tween 20, pH 7.4; washing buffer 2: 20 mM phosphate, 45 mM imidazole, 150 mM NaCl, pH 7.4; elution buffer: 20 mM phosphate, 500 mM NaCl, 500 mM imidazole, pH 7.4; stripping buffer: 20 mM phosphate, 500 mM NaCl, 50 mM EDTA, pH 7.4. Unless noted otherwise, uncertainties are standard deviations of values derived from three experiments with independent membranes or wafers.

2.2.2 Synthesis and Characterization of PDCMAA and CMPEI

The synthesis of PDCMAA was published previously,[23,25] and synthesis of CMPEI was carried out following the procedure for synthesis of PDCMAA, with slight modifications (Scheme 2.1). (Syntheses were performed by Salinda Wijeratne.) Under a N_2 atmosphere, sodium chloroacetate (20.0 g, 0.25 mol) and 25 mL of water were added to a two-neck round-bottomed flask, and the mixture was stirred at 30 °C for 10 min. This solution was added dropwise with stirring to an aqueous solution (100 mL) containing poly(ethyleneimine) (PEI, 50 wt% solution in water, M_n~6.0 x10^4 Da, 10.0 g, 10.6 mmol, assuming a repeating unit M_W=473 gmol^{-1}) at 50 °C. The reaction mixture was kept at 50 °C for 1 h and then held at 90 °C for 2 h with occasional addition of 30% NaOH to maintain the pH at 10.0. The mixture was stirred at room temperature for 12 h, and then the pH was adjusted to 1 by adding concentrated HCl. The supernatant was decanted, the remaining precipitate was dissolved by addition of

30% NaOH, and the solution was again adjusted to pH 1.0 with concentrated HCl. This process was repeated 3 times, and the precipitate was filtered and dried in vacuo for 12 h. The resulting white carboxymethylated polyethyleneimine (CMPEI, solid, 3.2 g, 63% yield) was characterized by FTIR spectroscopy (KBr) and elemental analysis.
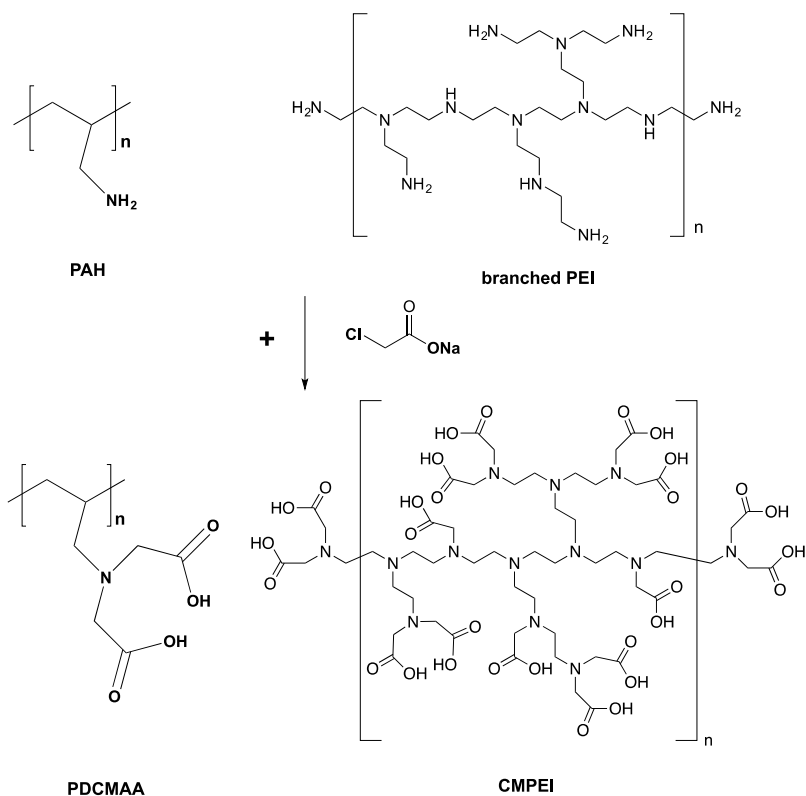
Scheme 2.1. Synthesis of PDCMAA and CMPEI.

To assess the acid-base properties of the new polymer, 30 mL of 1 mg/mL CMPEI (dissolved in 0.025 M NaOH) was titrated with 0.1 M HCl using a pH meter (ORION-420A). The pH meter has a combined glass/reference electrode and was calibrated with pH 4, pH 7, and pH 10 standards. A volumetric pipette was used to add HCl to the CMPEI solution with vigorous stirring.

2.2.3 Adsorption of Polyelectrolyte Multilayers (PEMs)

Au-coated Si substrates (24 mm × 11 mm) were immersed in 5 mM MPA in ethanol for 16 h, rinsed with ethanol, and dried with N_2 to form a monolayer of MPA prior to adsorption of PAH. The MPA-coated substrates were immersed in 0.02 M PAH (adjusted to the desired pH) for 15 min and subsequently rinsed with 10 mL of deionized water and blown dry with N_2. Substrates were then immersed in a 0.01 M CMPEI or PDCMAA solution (adjusted to the desired pH value) for 15 min followed by the same rinsing and drying procedures. Adsorption presumably displaces counterions from the polyelectrolytes and creates electrostatic cross-links between PAH and CMPEI or PDCMAA to stabilize the films despite the high water-solubility of these polymers.[29]   In some cases, the polyelectrolyte solutions also contained 0.5 M NaCl. The process was repeated to form multilayer films.

For some experiments, nylon membranes were first immersed in 0.1 M sodium chloroacetate in 3 M NaOH for 16 h and subsequently washed with deionized water and dried with N_2. The resulting carboxymethylated membrane disks were cleaned for 10 min with UV/O_3 and placed in a homemade Teflon holder (similar to an Amicon cell) that exposed 3.1 cm^2 of external membrane surface area. The UV/O_3 exposure should oxidize contaminants or the surface of the membrane but have minimal effect on the membrane structure.[30] Subsequently, a 5-mL solution containing 0.02 M PAH and 0.5 M NaCl was circulated through the membrane for 15 min at a flow rate of 1 mL/min using a peristaltic pump. A CMPEI or PDCMAA layer was deposited similarly using 0.01 M CMPEI or 0.01 M PDCMAA solutions containing 0.5 M NaCl. After deposition of each polyelectrolyte layer, 20 mL of deionized

water was passed through the membrane at the same flow rate. Nylon membranes without carboxymethylation were modified with PEMs similarly, starting with the UV/O_3 cleaning.

2.2.4 Characterization of Polyelectrolyte Film on Gold Wafers

Spectroscopic ellipsometry (model M-44; J.A. Woollam) was used to determine the thicknesses of PEMs on gold-coated Si wafers, assuming a film refractive index of 1.5. Film thicknesses in aqueous solutions were measured in a home-built cell described previously.[31] In that case, the software determines the refractive index of swollen films. Reflectance FTIR spectra were obtained with a Thermo Nicolet 6700 FTIR spectrometer using a Pike grazing angle (80°) apparatus. A UV/O_3-cleaned Au-coated Si wafer served as a background.

2.2.5 Metal-ion and Protein Binding in $(PAH/CMPEI)_n$- and $(PAH/PDCMAA)_n$-modified wafers and Membranes

Bare carboxymethylated membranes and membranes modified with $(PAH/CMPEI)_n$ and $(PAH/PDCMAA)_n$ films were loaded with Cu^{2+} or Ni^{2+} by circulating 5 mL of 0.1 M $CuSO_4$ or $NiSO_4$ (pH $\approx$ 4 for both) through the membrane for 30 min, followed by passage of 20 mL of water through the membrane. Metal ions were eluted from the membranes with 5 mL of stripping buffer or 2% HNO_3 and subsequently analyzed by atomic absorption spectroscopy.

For protein capture on wafers coated with PEMs, the modified substrates were immersed for 1 h in solutions containing 0.3 mg/mL of Con A in binding buffer 1 or 0.3 mg/mL of His-U in binding buffer 2. Subsequently, using a Pasteur pipet these substrates were rinsed with 10 mL of washing buffer 1 and 10 mL of water for 1 min each and dried with N_2. The amount of protein binding was determined by reflectance FTIR spectroscopy and expressed as the equivalent thickness of spin-coated protein that would give the same absorbance. The

40

equivalent thickness, d, is calculated from the difference in absorbance (ΔA) at 1680 cm^{-1} (amide band I of protein) before and after binding, using the equation d(nm) = ΔA/0.0017.[32] Some of these thicknesses were confirmed using ellipsometry. If the protein density is 1 g/cm^3, each nm of equivalent thickness is equal to 1 mg/m^2 of surface coverage.

Protein breakthrough curves were obtained by passing protein solutions (0.3 mg/mL in binding buffer 1 or binding buffer 2) through the membranes. For Con A binding, these studies employed 3.1 cm^2 of external membrane surface area. His-U binding experiments used a Teflon holder that exposed a membrane area of 0.78 cm^2 (1.0-cm exposed diameter) because of the high cost of this protein. Bradford assays (using calibration with the protein of interest) were employed to quantify the concentrations of proteins in the membrane effluent or eluate.

2.2.6 Protein Separation from a Cell Extract

His-tagged small ubiquitin modifier (His-SUMO) was overexpressed in *Escherichia coli* (*E. coli*) cells. The cells were lysed with sonication in binding buffer 2 and centrifuged. Supernatant was pumped thorough the (PAH/CMPEI)-modified membrane (diameter 2-cm) at room temperature at a flow rate of 1 mL/min. Subsequently the membrane was rinsed with 5 mL of binding buffer 2 and 5 mL of washing buffer 1, and the bound protein was eluted with 2 mL of elution buffer. The purity of the eluted protein was determined by sodium dodecyl sulfate–polyacrylamide gel electrophoresis (SDS–PAGE).

2.2.7 Metal Leaching, Film stability and Film Reusability

To test metal-ion leaching in different buffers, (PAH/PDCMAA)-, (PAH/PDCMAA)$_2$-, (PAH/CMPEI)- and (PAH/CMPEI)$_2$-modified carboxymethylated nylon membranes were loaded with Ni^{2+} using the above procedure (including rinsing with 20 mL of water) and washed

consecutively with 160 bed volumes (5 mL) of binding buffer 2, washing buffer 1, washing buffer 2, elution buffer, stripping buffer, and 2% HNO_3. As a comparison, a GE Healthcare HiTrap^{TM} IMAC FF column (1 mL) was washed with 160 bed volumes (160 mL) of the same buffers. All the samples were diluted 1:5 with deionized water and analyzed by atomic absorption spectrometry. The GE Healthcare HiTrap^{TM} IMAC FF column was loaded with Ni^{2+} by passing 2 mL of 0.1 M $NiSO_4$ through the syringe column (flow rate of 1 mL/min) followed by 160 mL of deionized water.

To examine film stability under purification conditions, we soaked (PAH/CMPEI)$_2$-modified gold wafers in 5 mL of binding buffer 2 for 20 hours. Film thickness values and reflectance FTIR spectra were obtained before and after immersion in the buffer for different times. Total organic carbon (TOC, O.I. Analytical, Model 1010) analysis was used to quantify polyelectrolyte leaching from modified membranes during passage of binding buffer 2 through the membrane. CMPEI solutions with concentrations from 0 to 10 ppm were used for calibration, and the effluent was diluted 1:39 with deionized water before analysis. To study reusability, multiple cycles of charging with Cu^{2+}, binding of Con A, rinsing, and elution were performed with a (PAH/CMPEI)-modified membrane (deposited at pH 2 with 0.5 M NaCl). Protein binding was calculated from the average of capacities determined from the breakthrough curve and the eluate analysis.

2.3 Results and discussion

2.3.1 Characterization of carboxymethylated polyethyleneimine (CMPEI)

Comparison of the IR spectra (Figure 2.2) of acidified branched PEI and branched CMPEI shows the disappearance of bands that correspond to N-H deformation vibrations of PEI (1584 cm^{-1} and 1454 cm^{-1}) and the appearance of stretches from carboxyl groups. The absorption at

1733 cm^{-1} arises from the C=O stretching in the HN$^+$-CH$_2$COOH group, and the band at 1655 cm^{-1} is due to the asymmetric stretching in the HN$^+$-CH$_2$COO$^-$ group. This confirms the presence of the iminodiacetic moiety in CMPEI.
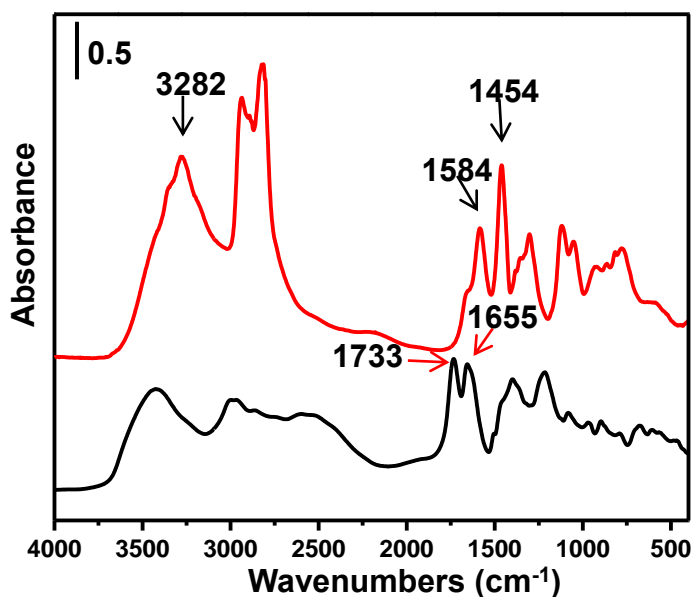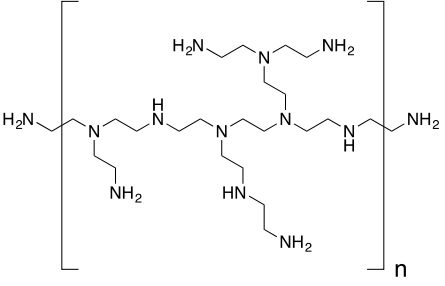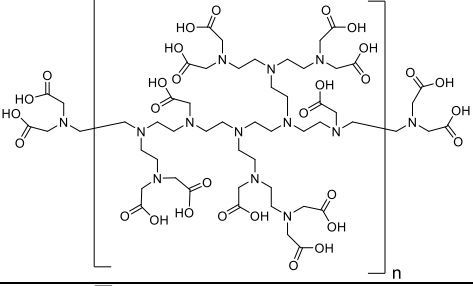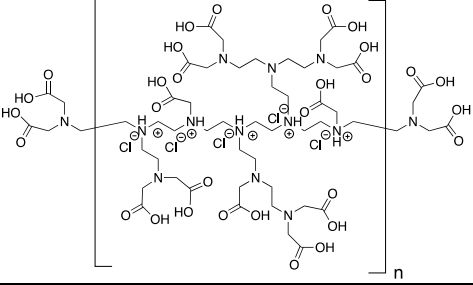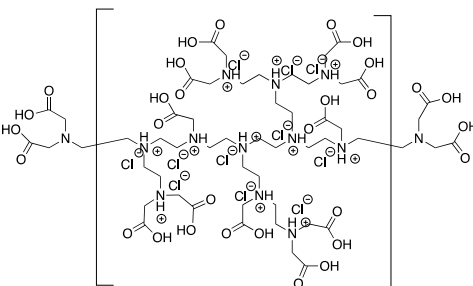
Figure 2.2. KBr FTIR spectra of branched PEI (red) and CMPEI (black). Both polymers were acidified prior to obtaining the spectra.

We also performed elemental analysis to evaluate the synthesis of CMPEI. Table 2.1 provides possible structures for PEI and CMPEI along with elemental compositions. In its fully deprotonated state, the PEI starting material has the following percent composition: C, 55.78; H, 11.70; N, 32.52. Double carboxymethylation of each primary amine plus single carboxymethylation of each secondary amine leads to entry 2 (Table 2.1) with a percent composition of C, 47.52; H, 6.98; N, 13.85; O, 31.65.   However, these values differ significantly from the CMPEI experimental elemental analysis data: C, 40.26; H, 6.65; N, 11.93.   This difference likely stems from formation of hydrochloride salts. Without

43

accounting for chloride, all other atom percentages will be artificially high. Formation of HCl salts only along the polymer backbone (addition of 5 Cl$^-$) gives an elemental composition: C, 40.83; H, 6.39; Cl, 13.69; N, 11.90; O, 27.19 (Table 2.1, entry 3). This is reasonably close to the experimental values. Formation of HCl salts at all amine sites (Table 2.1, entry 4) leads to atomic percentages that are significantly lower than the experimental values. Unfortunately, we cannot specify the protonation state of CMPEI because of the low –COOH pKa values, and –COO$^-$ groups, rather than Cl$^-$, probably provide charge compensation for some of the ammonium groups. Thus, 5 Cl$^-$ ions per repeating unit, as shown in entry 3 of Table 2.1, is possible. Most important, in entries 2-4 the carbon to nitrogen ratio, which does not depend on the number of Cl$^-$ ions or the presence of residual water, is 3.43 close to the experimental value of 3.37. This confirms addition of acetate groups to the polymer in approximately the amount shown in entry 2. (The theoretical C to N ratio in the PEI starting material is only 1.72.)

Table 2.1. Possible elemental compositions of PEI and CMPEI with different numbers of HCl salts.

		Chemical Formula	Molecular Weight	Elemental Analysis
1	Poly(ethylenimine)	$C_{22}H_{55}N_{11}$	473.8	C, 55.78; H, 11.70; N, 32.52
2		$C_{44}H_{77}N_{11}O_{22}$	1112.1	C, 47.52; H, 6.98; N, 13.85; O, 31.65
3		$C_{44}H_{82}Cl_5N_{11}O_{22}$	1294.5	C, 40.83; H, 6.39; Cl, 13.69; N, 11.90; O, 27.19
4		$C_{44}H_{88}Cl_{11}N_{11}O_{22}$	1513.2	C, 34.93; H, 5.86; Cl, 25.77; N, 10.18; O, 23.26

2.3.2 LbL Adsorption of Films Containing CMPEI

CMPEI contains both weakly basic (amine) and weakly acidic (carboxylic acid) groups and thus can potentially form salt bridges with both cations and anions on a surface. Figure 2.3a shows an acid titration of CMPEI. The number of protonated equivalents in CMPEI (Figure 2.3b) was calculated using the following equations:

H⁺(added from titrant) =H⁺(free in solution) + H⁺(added to CMPEI) + OH⁻(neutralized)

(1)

$$Number\ of\ equivalents = \frac{moles\ of\ H^+\ added\ to\ CMPEI}{\frac{mass\ of\ CMPEI}{1112\frac{g}{CMPEI\ unit}}*11\frac{amine\ groups}{CMPEI\ unit}} \qquad (2)$$

In equation (2), 1112 is the molecular mass of the CMPEI repeat unit in Table 2.1, entry 2, and there are 11 amine groups in the CMPEI repeat unit. This calculation may underestimate the number of equivalent by ~15% if there are 5 chloride ions in the solid polymer. However, the trend in the figure should hold.

Figure 2.3 suggests nearly complete protonation of amine groups at pH values below 7, whereas protonation of the carboxylate groups begins below pH 4, which is similar to the titration of PDCMAA.[25] This is reasonably consistent with the pKa values for iminodiacetic acid, which are 9.4, 2.6, and 1.8.[33,34] The ratio of carboxylic acid groups to amines is around 1:1 in CMPEI but 2:1 in iminodiacetic acid and PDCMAA (see Scheme 2.1).
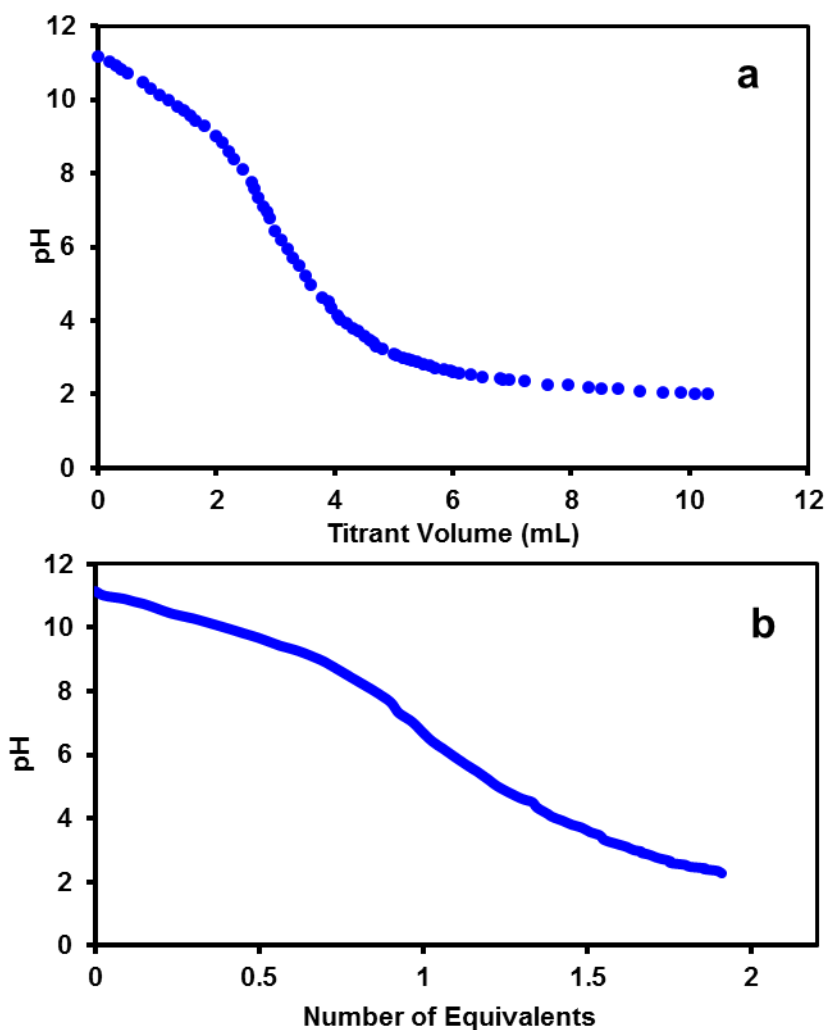
Figure 2.3. (a) Titration curve for 1 mg/mL of CMPEI in 0.025 M NaOH (30 mL). The titrant contained 0.1 M HCl; (b) Number of Equivalents (the number of protons added to CMPEI divided by the number of CMPEI amine groups) as a function of pH.

Based on the polymer titration and a 1:1 ratio of amine to carboxylic acid groups, one might suppose that CMPEI would serve as a polyanion in films formed at basic pH and as a polycation in films formed at acidic pH. However, Hoffman and Tieke reported that linear CMPEI, which also has a 1:1 ratio of amine to carboxylic acid groups, forms multilayer films with protonated poly(vinyl amine) at adsorption pH values ranging from 2 to 8.[35] Thus, even at pH 2, linear CMPEI likely serves as a polyanion in LbL deposition. With branched CMPEI,

adsorption of (polycation/CMPEI)$_n$ coatings also occurs at low pH. Figure 2.4 shows the ellipsometric thicknesses of (PAH/CMPEI)$_n$ films deposited at pH 3.   In the absence of salt in adsorption solutions (red circles), after deposition of the initial bilayer, which is ~1 nm thick, adsorption of each subsequent bilayer adds ~5 nm of thickness. Addition of 0.5 M NaCl to adsorption solutions increases the thicknesses of layers 2- to 4-fold.   At low pH, CMPEI has a net positive charge, so electrostatic repulsion between its positive ammonium groups should make the polymer chains partially extend. Addition of salt increases thickness by screening charges in the polymer to create loops and tails and by increasing surface roughness.[36,37]
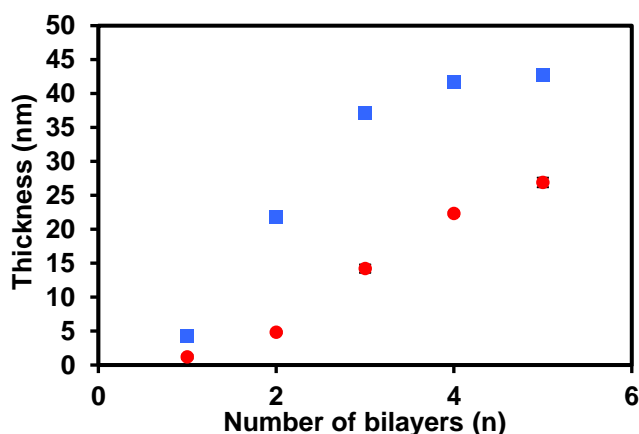
Figure 2.4. Ellipsometric thicknesses of (PAH/CMPEI)$_n$ films as a function of the number of adsorbed bilayers, n. Films were deposited from pH 3 solutions containing 0.5 M NaCl (blue squares) or no added salt (red circles). The substrates were Au-coated Si wafers modified with a monolayer of MPA, and error bars are typically smaller than the symbols.

During adsorption, carboxylate groups on CMPEI most likely bind to ammonium groups of PAH. Reflectance FTIR spectroscopy confirms that most of the carboxylate groups in these films are deprotonated (Figure 2.5). Formation of PAH/CMPEI complexes leads to less protonation of the –COOH groups of CMPEI than in solution and perhaps less protonation of ammonium groups. XPS data (Figure 2.6) show no chloride within CMPEI-capped films,

which suggests that few of the amine groups in CMPEI are protonated and compensated by Cl⁻ ions. The formation of films by adsorption of CMPEI and PAH, which both possess a net positive charge in neutral and acidic solutions, likely occurs due to polarization-induced attraction.[38-40] Electric fields created by positively charged PAH may induce rearrangement of the CMPEI chains to enhance electrostatic interactions between the carboxylates of CMPEI and ammonium groups of PAH. At pH 3 with 0.5 M NaCl, (PAH/CMPEI) growth reaches a plateau at 4-5 bilayers, perhaps because the net positive charge on both polymers leads to repulsions that overcome polarization-induced attraction in thicker films.
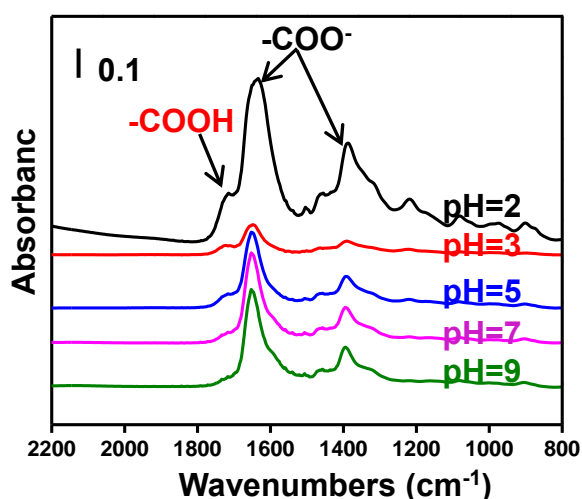
Figure 2.5. Reflectance FTIR spectra (2200-800 cm⁻¹) of (PAH/CMPEI)₅ films deposited at pH 2, 3, 5, 7 or 9 on MPA-modified, Au-coated Si wafers.
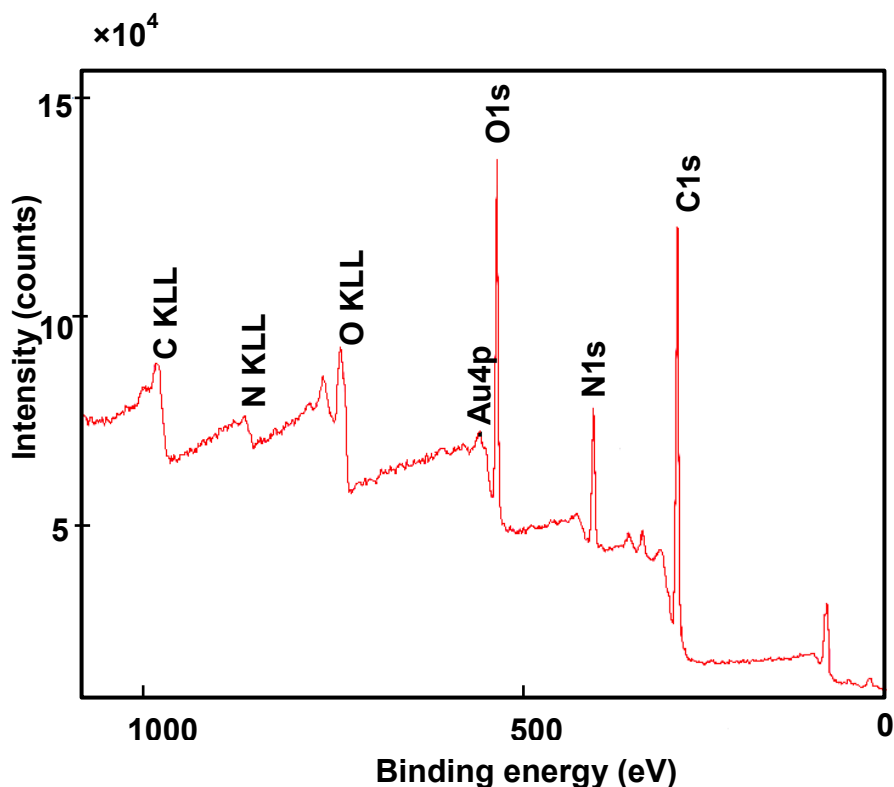
Figure 2.6. XPS spectrum of a (PAH/CMPEI)₅ film adsorbed on a MPA-modified, Au-coated

Si wafer.   Deposition occurred at pH 2 with 0.5 M NaCl in the polyelectrolyte solution, and

the wafer was rinsed extensively with water.

Figure 2.7 shows the thicknesses of (PAH/CMPEI)₅ films as a function of the deposition

pH. Similar to other films with weak-acid polyelectrolytes,[25,41,42] the highest thicknesses occur

with films deposited at the lowest pH.   Films formed at pH 2 are typically about twice as thick

as films adsorbed at pH 3-9.   Due to the relatively low pKa values of the –COOH groups in

CMPEI, thickness only increases at the lowest pH value.   Notably, 4- and 5-bilayer films

deposited at pH 3 are thinner than corresponding films deposited at all other pH values

(compare Figures 2.4 and 2.7).   This may reflect repulsion between CMPEI and PAH at this

pH.   At pH 2, an increased number of protonated –COOH groups may require more CMPEI

to form ion pairs with PAH and overcome decreases in thickness due to repulsion between the two polymers.
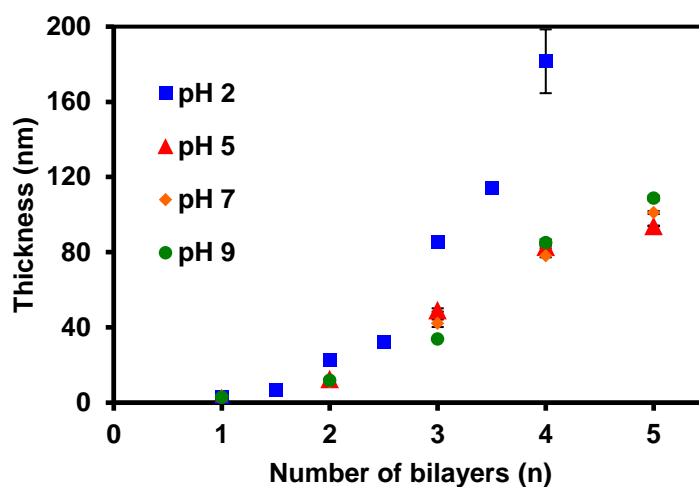
Figure 2.7. Ellipsometric thicknesses of (PAH/CMPEI)$_5$ films as a function of deposition pH. Films were adsorbed from 0.5 M NaCl solutions onto Au-coated Si wafers modified with a monolayer of MPA, and error bars are often smaller than the symbols. (For coatings adsorbed at pH 2, non-integer bilayer numbers indicate films terminated by PAH adsorption.)

For the pH 2 deposition, we also determined the thickness increases due to adsorption of both PAH and CMPEI. As Figure 2.7 shows (blue squares), the thickness increase upon adsorption of CMPEI is more than double that for adsorption of PAH, suggesting that the films contain more CMPEI than PAH, probably because the density of –COO$^-$ groups on CMPEI is lower than the density of protonated amine groups on PAH. After deposition of the fifth (PAH/CMPEI) bilayer at pH 2, the surface is too rough for an accurate thickness determination by ellipsometry.

The reflectance IR spectra of (PAH/CMPEI)$_5$ films deposited at different pH values show that most of the carboxylic groups are deprotonated (Figure 2.5). However, the ratio of the absorbance of the -COO$^-$ stretch (~1650 cm^{-1}) to the absorbance of the acid carbonyl stretch

(1720 cm^{-1}) decreases as the deposition pH decreases, suggesting the films deposited at the lowest pH values contain free -COOH groups. Figure 2.9 shows the reflectance FTIR spectra of films with 1 to 5 (PAH/CMPEI) bilayers for different deposition pH values.
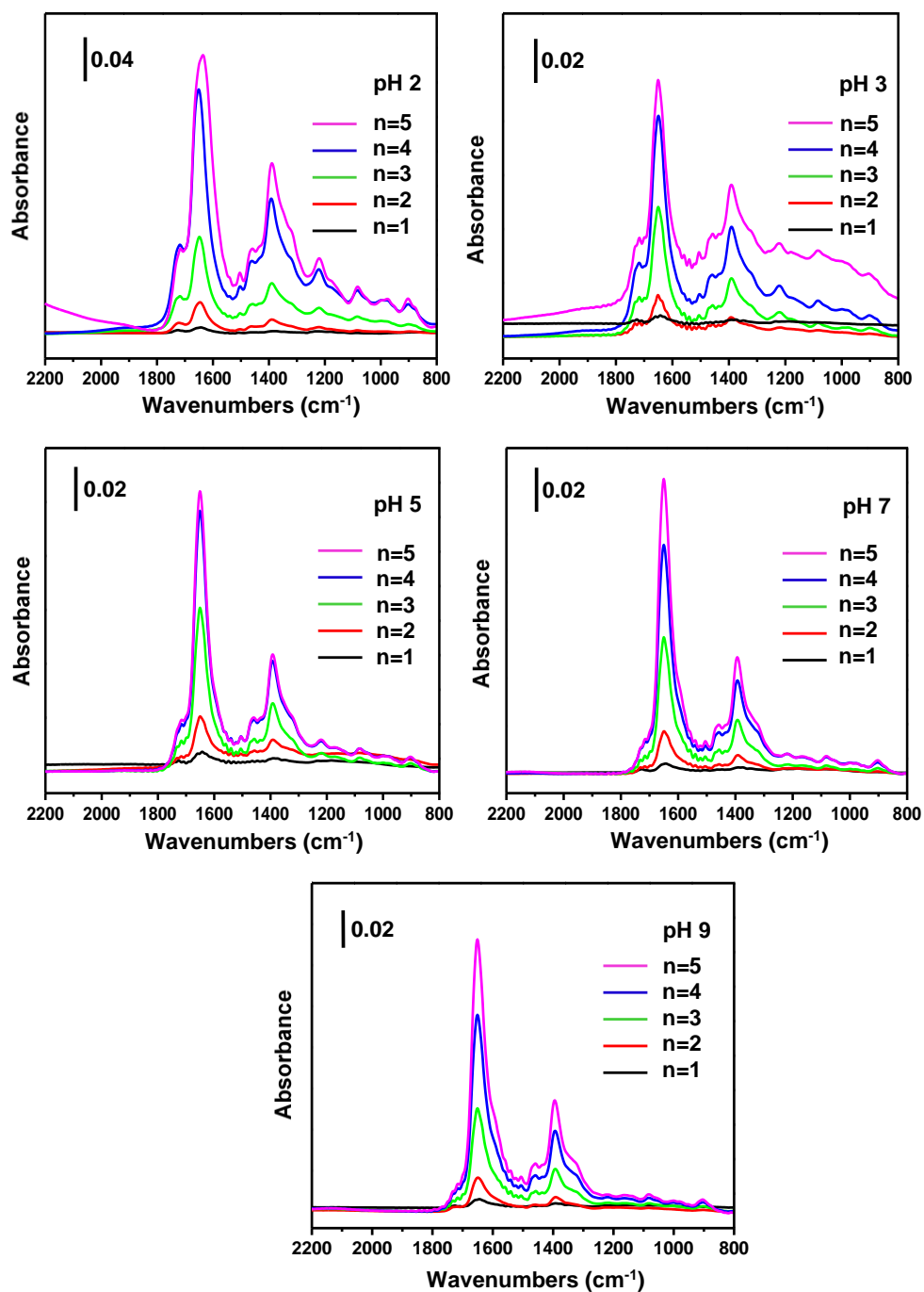
Figure 2.8. Reflectance FTIR spectra (2200-800 cm^{-1}) of (PAH/CMPEI)$_n$ films (n=1 to 5) deposited on MPA-modified, Au-coated　Si wafers at deposition pH values from pH 2 to pH 9.　The deposition pH is listed in the top right of each plot.　Films were deposited with 0.5 M NaCl in the polyelectrolyte solutions.

CMPEI gives very thin films when serving as a polycation in LbL adsorption. (CMPEI/PSS)$_5$ films deposited at pH 3 in 0.5 M salt are only 10±2 nm thick. The positive charges of CMPEI reside mostly in or near the backbone and may be less available for adsorption than -COO$^-$ groups on the side chains. Using a cyclic analogue of linear CMPEI, Hoffman and Tieke also found minimal growth during LbL deposition with PSS over a pH range from 2 to 8.[35]

2.3.3 Film Swelling

This work aims to create thin films that selectively bind proteins in platforms such as porous membranes, and film swelling in aqueous solution is vital to enable extensive protein capture. To examine swelling, we initially performed in situ ellipsometry with (PAH/CMPEI)$_5$ films (deposited at pH 3 with 0.5 M NaCl) immersed in deionized water or binding buffer 2 (pH 7.4). After a 20-minute immersion, film thickness increased 160±30% in deionized water and 680±260% in buffer. Consistent with the approximately 62% and 88% water in the immersed coatings, the film refractive indices decrease from 1.50 to 1.39 and from 1.50 to 1.35 after swelling in water and buffer, respectively. (The refractive index of water at the wavelengths of the spectroscopic ellipsometer is about 1.333.) Deprotonation of carboxylate groups in pH 7.4 buffer likely enhances swelling, which should provide space for binding multilayers of protein in the film. IR spectra confirm the deprotonation after immersing the film in buffer (see Figure 2.9). As a comparison, the swelling of (PAH/PDCMAA)$_5$ films (deposited at pH 3 with 0.5 M NaCl) was 52±16% in deionized water and 220±20% in binding buffer 2. The high swelling of (PAH/CMPEI)$_5$ relative to (PAH/PDCMAA)$_5$ suggests that the ammonium-containing backbone and branched structure of CMPEI facilitate swelling.

((PAH/CMPEI)$_5$ and (PAH/PDCMAA)$_5$ films have similar dry thicknesses of 40 and 60 nm, respectively.)   Note that high swelling may lead to partial polyelectrolyte desorption, which we discuss in section 3.8.
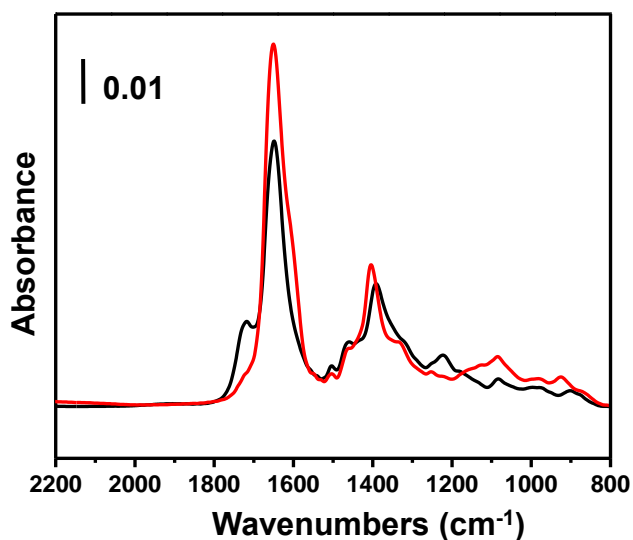
Figure 2.9. Reflectance FTIR spectra (2200-800 cm^{-1}) of a dry (PAH/CMPEI)$_2$ film after adsorption and rinsing with water (black) and after immersion in binding buffer 2 (pH 7.4) followed by rinsing with water (red). The film was initially adsorbed on a MPA-modified, Au-coated Si wafer at pH 3 from solutions containing 0.5 M NaCl.

Modification of porous membranes to bind proteins will most likely involve adsorption of only a few polyelectrolyte bilayers to simplify the process and avoid plugging of pores. Moreover, the films should contain metal-ion complexes for capture of proteins through metal-ion affinity interactions (Figure 2.1).   Thus, we also examined swelling of (PAH/CMPEI)$_2$ and (PAH/PDCMAA)$_2$ films containing Cu^{2+} complexes.   These studies employed binding buffer 1 (pH 6.0) to match subsequent Con A-binding studies, as Con A solutions are not stable at pH 7.4. Figure 2.10 shows that for all film-adsorption pH values (pH 2 to 9), the (PAH/CMPEI)$_2$-Cu^{2+} swelling in pH 6.0 buffer is around 200%. In pH 7.4 buffer the swelling

of a (PAH/CMPEI)$_2$-Cu^{2+} film (deposited at pH 3 with 0.5 M NaCl) is still only 220%.   Thus,

formation of the metal-ion complexes decreases film swelling, probably because Cu^{2+}-

iminodiacetate complexes have no net charge.   When immersed in pH 6.0 buffer, the

(PAH/PDCMAA)$_2$-Cu^{2+} films show average swellings of only 100% for deposition pH vales

of 3, 5, or 7. Although both CMPEI and PDCMAA contain iminodiacetate moieties, the amine

or ammonium groups in the backbone of CMPEI films likely increase swelling compared to

films with PDCMAA, which contains a hydrocarbon backbone.
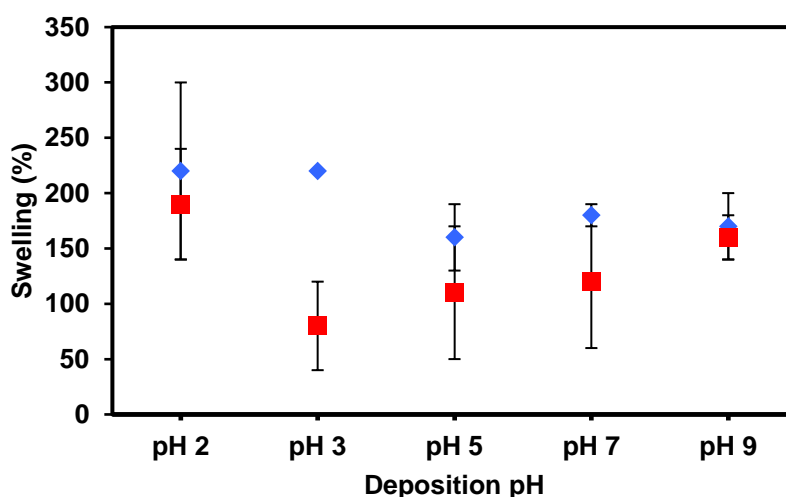
Figure 2.10. Swelling of (PAH/CMPEI)$_2$-Cu^{2+} (blue diamonds) and (PAH/PDCMAA)$_2$-Cu^{2+}

(red squares) films as a function of their deposition pH.   Films were deposited on MPA-

modified, Au-coated Si wafers from polyelectrolyte solutions containing 0.5 M NaCl. All the

swelling tests were performed in binding buffer 1 (pH 6).

2.3.4 Protein Binding to (PAH/CMPEI)$_2$-Cu^{2+} and (PAH/PDCMAA)$_2$-Cu^{2+} Films

Initial studies of protein binding examined capture of Con A in (PAH/CMPEI)$_2$-Cu^{2+} and

(PAH/PDCMAA)$_2$-Cu^{2+} films adsorbed on MPA-modified Au-coated Si wafers. Binding

presumably occurs when histidine groups on the protein coordinate with immobilized Cu^{2+}.

Using reflectance FTIR spectroscopy, we determine the amount of protein binding based on the amide absorbance, which we compare to the absorbance in spin-coated films with different thicknesses.[32] $(PAH/PDCMAA)_2$-Cu^{2+} films have average thicknesses ranging from 7-25 nm, depending on the deposition pH (see Figure 2.11), but these coatings bind the equivalent of <3 nm of protein, or less than a monolayer. (The dimensions of a Con A protomer, M_w=25,500 Da, are $4.2 \times 4.0 \times 3.9$ nm.[43]) Even with an extra bilayer, $(PAH/PDCMAA)_3$-Cu^{2+} films with a thickness of ~60 nm (deposited at pH 2) bind only 8 nm of Con A. Such limited binding will lead to low capacities in membranes modified with these films. In contrast, $(PAH/CMPEI)_2$-Cu^{2+} films adsorbed at pH 2 have an average thickness around 40 nm and capture 18 nm of protein (Figure 2.11). Adsorption of $(PAH/CMPEI)_2$ at deposition pH values from 3-7 leads to thinner films than adsorption at pH 2 and binding of $\leq$5 nm of protein (Figure 2.11). Thus, polyelectrolyte adsorption at low pH to obtain relatively thick CMPEI films and high swelling is likely vital to achieving high binding capacities.
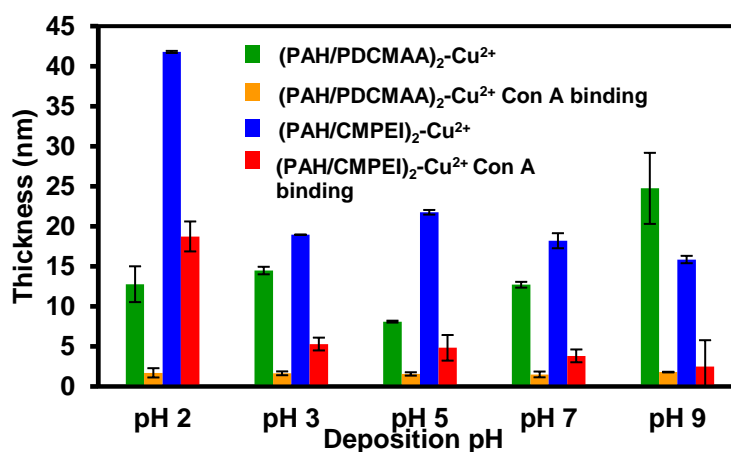
Figure 2.11. Thicknesses of $(PAH/PDCMAA)_2$ and $(PAH/CMPEI)_2$ multilayers after complexation of Cu^{2+}, and the equivalent thicknesses of Con A subsequently adsorbed in these films. PEMs were deposited from polyelectrolyte solutions containing 0.5 M NaCl at various pH values.

2.3.5 Membrane Modification with (PAH/CMPEI)$_n$ and (PAH/PDCMAA)$_n$ Films and Binding of Metal Ions

Adsorption of (PAH/CMPEI)$_n$ and (PAH/PDCMAA)$_n$ films within membrane pores is difficult to quantify. To qualitatively assess the amount of adsorbed polymer we examined Cu^{2+} and Ni^{2+} binding in membranes modified with polyelectrolyte films. As Figure 2.12 shows, an untreated nylon membrane modified with PAH/CMPEI (far left data bars) binds <1 mg of Cu^{2+} per mL of membrane. This implies minimal adsorption of PAH/CMPEI, so we treated the nylon substrates with 0.1 M sodium chloroacetate in 3 M NaOH to increase the number of –COOH groups on pore surfaces and enhance polyelectrolyte adsorption. Unfortunately, in control experiments carboxymethylated (CM) nylon captures 3 mg of Cu^{2+} per mL of membrane. However, adsorption of PAH in the membrane decreases the Cu^{2+} capture to about 2 mg/mL, presumably because PAH forms salt bridges with some COO^- groups to prevent binding. Protonation of the amine groups should prevent them from binding Cu^{2+}. (The pH of the Cu^{2+} loading solution is ~4). Subsequent adsorption of a CMPEI layer leads to capture of 7 mg of Cu^{2+} per mL of membrane, and CM nylon membranes modified with single PAH/CMPEI and PAH/PDCMAA bilayers show similar Cu^{2+} binding. Moreover, (PAH/CMPEI)$_2$- and (PAH/PDCMAA)$_2$-modified CM membranes capture around 12 and 14 mg of Cu^{2+} per mL of membrane, respectively.
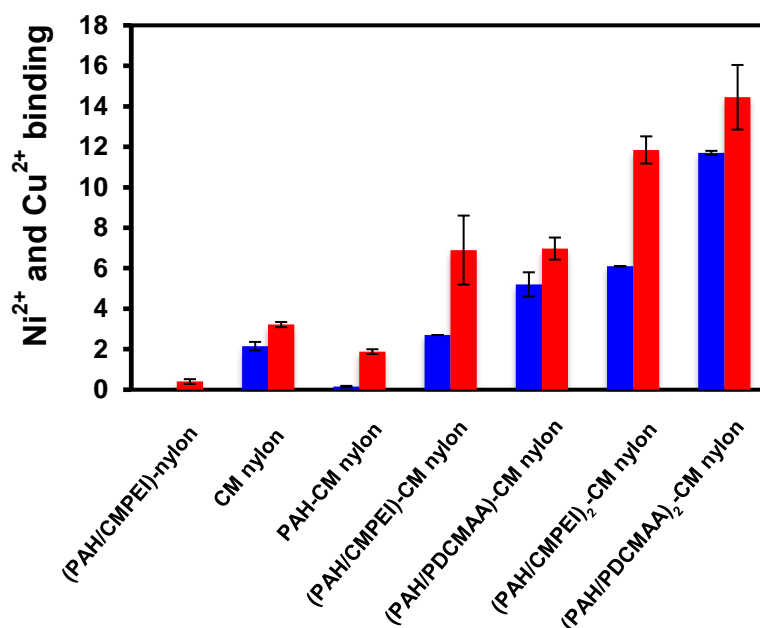
Figure 2.12. Cu^{2+} (red bars) and Ni^{2+} (blue bars) binding capacities in PAH/CMPEI-modified nylon, carboxymethylated (CM) nylon, PAH-modified CM nylon, PAH/CMPEI-modified CM nylon, PAH/PDCMAA-modified CM nylon, (PAH/CMPEI)$_2$-modified CM nylon, and (PAH/PDCMAA)$_2$-modified CM nylon membranes. All polyelectrolytes were adsorbed at pH 2 from solutions containing 0.5 M NaCl. Error bars are the differences between experiments with two different membranes.

Importantly, the PAH/CMPEI-CM nylon membrane binds 16 times the amount of Cu^{2+} captured in an untreated nylon membrane modified with PAH/CMPEI. Figure 2.13 shows SEM images of bare nylon, CM nylon, (PAH/CMPEI)-Cu^{2+} CM nylon and (PAH/CMPEI)$_2$-Cu^{2+} CM nylon. The structures of the nylon membranes show no obvious change after carboxymethylation, so the primary effect of this treatment is the formation of –COOH groups that facilitate adsorption of the initial PAH layer.
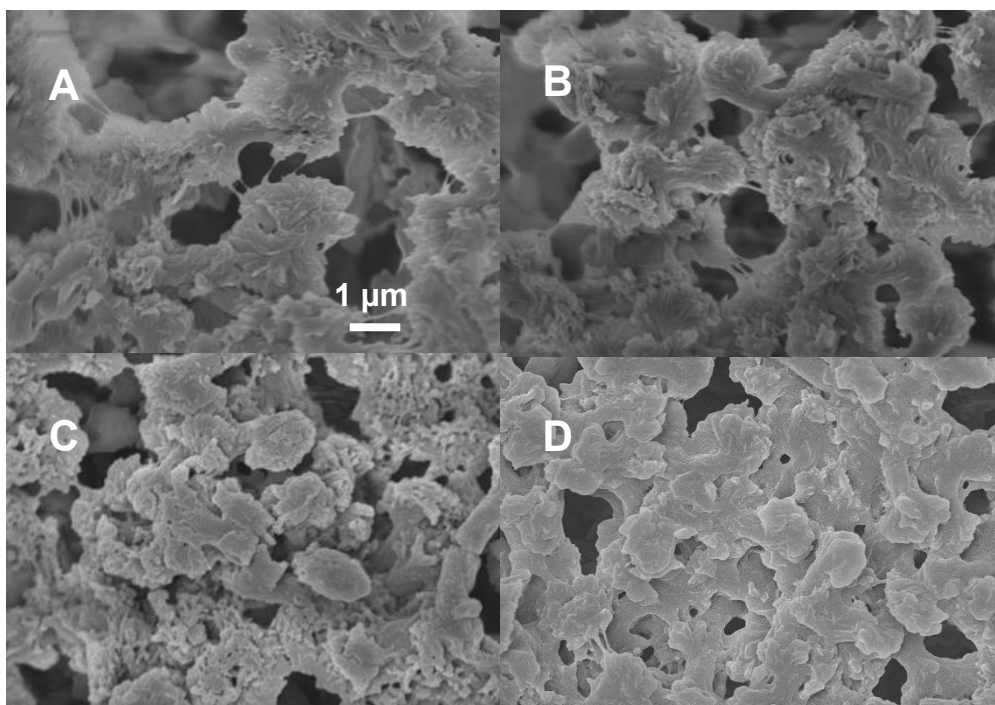
Figure 2.13. SEM images of (A) nylon, (B) carboxymethylated nylon, (C) PAH/CMPEI-Cu^{2+}-modified carboxymethylated nylon and (D) (PAH/CMPEI)$_2$-Cu^{2+}-modified carboxymethylated nylon membranes.   The scale bar is common to all images.

Selective capture of His-tagged proteins typically employs immobilized Ni^{2+} or Co^{2+} complexes, not Cu^{2+}. Histidine binding to Ni^{2+} and Co^{2+} is weaker than to Cu^{2+} and thus requires multiple histidine residues for protein capture, which affords selective sorption of His-tagged species. As Figure 2.12 shows, CM nylon membranes modified with PAH/CMPEI and (PAH/CMPEI)$_2$ films bind 2 mg/mL and 5 mg/mL of Ni^{2+}, respectively.   This is considerably less than the Cu^{2+} binding capacity, perhaps because Ni^{2+} only binds strongly to sites with the full iminodiacetic acid functionality. Amines modified with a single carboxylic acid group (see Scheme 2.1) may not give stable Ni^{2+} complexes. The unmodified CM nylon also shows less Ni^{2+} binding than Cu^{2+} binding, and CM membranes modified with only PAH show minimal Ni^{2+} capture. PDCMAA contains only IDA binding groups, so there is not a large difference between Ni^{2+} and Cu^{2+} binding to membranes with PAH/PDCMAA films. Hence the

membranes modified with PAH/PDCMAA and (PAH/PDCMAA)$_2$ capture more Ni^{2+} than corresponding membranes modified with PAH/CMPEI and (PAH/CMPEI)$_2$. From metal-ion binding, we can estimate the polymer adsorption in a membrane. For (PAH/CMPEI)-modified membranes, the Ni^{2+} (M$_w$=58.7) binding is around 3 mg/mL. Assuming that only complete IDA groups bind Ni^{2+}, 4 metal ions should bind to the CMPEI repeat unit in Scheme 1. Thus, a (PAH/CMPEI)-modified CM membrane will contain 14 mg/mL of CMPEI (repeat unit M$_w$ =1112).

2.3.6 Con A Binding to Membranes Modified with PAH/PDCMAA-Cu^{2+} and PAH/CMPEI-Cu^{2+} Film

Due to the high cost of His-tagged proteins, we first employed Con A binding to Cu^{2+} complexes to evaluate the protein-binding capacities of membranes. Figure 2.14 shows the breakthrough curves for Con A capture in CM nylon membranes modified with PAH/CMPEI-Cu^{2+}(purple circles) and PAH/PDCMAA-Cu^{2+} (green squares) films. Even though both films show similar Cu^{2+} binding (Figure 2.12), the total Con A bound to the membrane with PAH/CMPEI-Cu^{2+} is 59±5 mg/mL, whereas the membrane with PAH/PDCMAA-Cu^{2+} captures just 30±5 mg/mL. Binding capacities determined from Con A elution with 50 mM EDTA are similar to those from the breakthrough curves (55±10 mg/mL and 35±8 mg/mL for PAH/CMPEI-Cu^{2+} and PAH/PDCMAA-Cu^{2+}, respectively). The higher binding capacity with PAH/CMPEI-Cu^{2+} than PAH/PDCMAA-Cu^{2+} is consistent with the trends in Con A binding capacities of PEMs on Au-coated Si wafers (Figure 2.11).
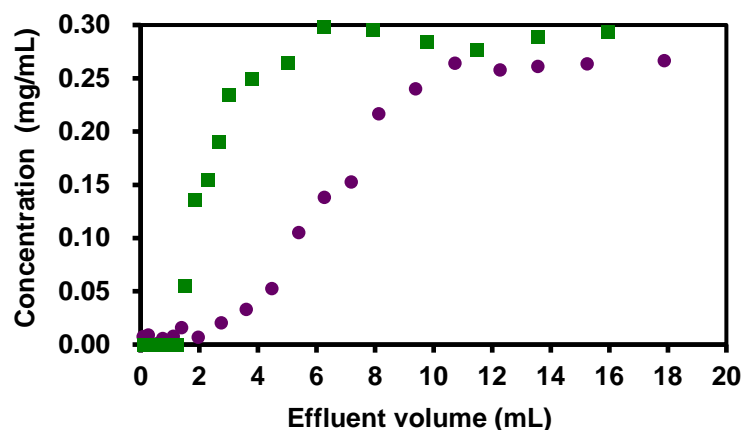
Figure 2.14. Breakthrough curves of Con A capture in CM nylon membranes (2.0-cm diameter) modified with PAH/CMPEI-Cu^{2+} (purple circles) and PAH/PDCMAA-Cu^{2+} (green squares). Both films were deposited at pH 2 with 0.5 M NaCl. The feed Con A concentration was 0.3 mg/mL and the volume flux was 10 cm/h.
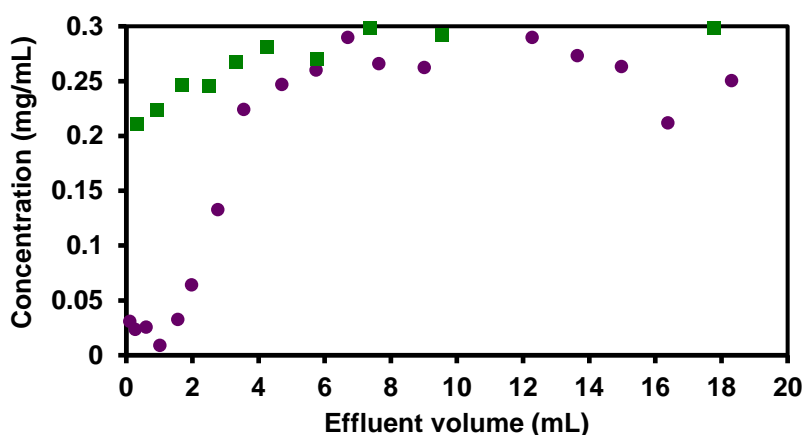
Figure 2.15. Breakthrough curves for Con A capture in (PAH/PDCMAA)$_2$-Cu^{2+}- (green squares) and (PAH/CMPEI)$_2$-Cu^{2+}- (purple circles) modified CM nylon membranes (2.0-cm diameter). The films were deposited at pH 2 with 0.5 M NaCl in the polyelectrolyte solution, the feed Con A concentration was 0.3 mg/mL, and the volume flux was 10 cm/h.

We also tested Con A binding in (PAH/CMPEI)$_2$-Cu^{2+}-modified CM nylon. Based on breakthrough curves (e.g., Figure 2.15), the Con A binding capacity in these membranes is 39±5 mg/mL, or less than in membranes with PAH/CMPEI-Cu^{2+} films. The unexpected

decrease in binding compared to a film with a single bilayer may reflect decreased swelling with more bilayers or limited access to some small pores after coating the spongy membrane structure (see Figure 2.13) with two bilayers. Con A capture in membranes modified with $(PAH/PDCMAA)_2$-Cu^{2+} is also less than in membranes with $(PAH/PDCMAA)$-Cu^{2+} (see Figure 2.15).

2.3.7 Capture of His-tagged Protein Using Membranes Containing PAH/CMPEI-Ni^{2+} Films

Because they showed the highest Con A capture, we determined the binding capacity for His-tagged ubiquitin using CM nylon membranes modified with PAH/CMPEI films. However, in this case we employed the Ni^{2+} complex, which is necessary for selective capture of His-tagged protein.   Based on breakthrough curves (Figure 2.16), the binding capacity is ~60 mg/mL, and protein elution gave a capacity of ~70 mg/mL. This His-U binding is about 2/3 of what we previously obtained using polymer brush- or (PAA/PEI/PAA)-NTA-Ni^{2+}-modified membranes (~90 mg/mL membrane).[22,44] However, this new strategy avoids the challenges of growing polymer brushes or the expensive reaction of PAA/PEI/PAA with aminobutyl NTA. The dynamic binding capacity, i.e. the amount of protein bound when the effluent concentration is 10 % of the loading concentration, is around 30 mg/mL.
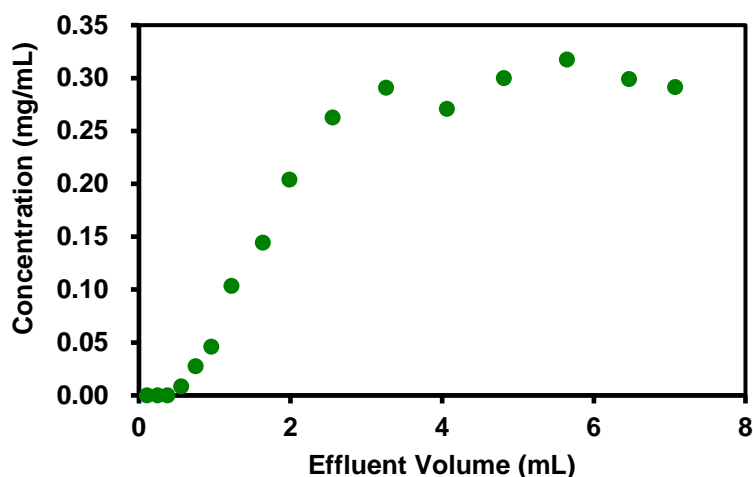
Figure 2.16. Breakthrough curve for His-tagged ubiquitin capture in a (PAH/CMPEI)-modified CM membrane. The flow rate was 10 cm/h, the membrane had a diameter of 1.0-cm, and the feed His-tagged ubiquitin concentration was 0.3 mg/mL. The His-tagged ubiquitin binding capacity was 55 mg/mL for this membrane and 64 mg/mL for a second replicate membrane.

To demonstrate that membranes can isolate His-tagged protein directly from cell extracts, we purified His-tagged SUMO protein that was over-expressed in *E. coli*. Figure 2.17 shows the SDS-PAGE analysis of a cell extract that contained His-tagged SUMO (lane 2), the same cell extract after passing through a (PAH/CMPEI)-modified CM membrane (lane 3), and the eluate (lane 4) from the membrane loaded with the cell extract. Notably, the effluent of the loading solution contains minimal His-tagged SUMO protein, and the only detectable band from the eluate stems from the His-tagged SUMO protein. Thus the membranes selectively capture His-tagged protein.
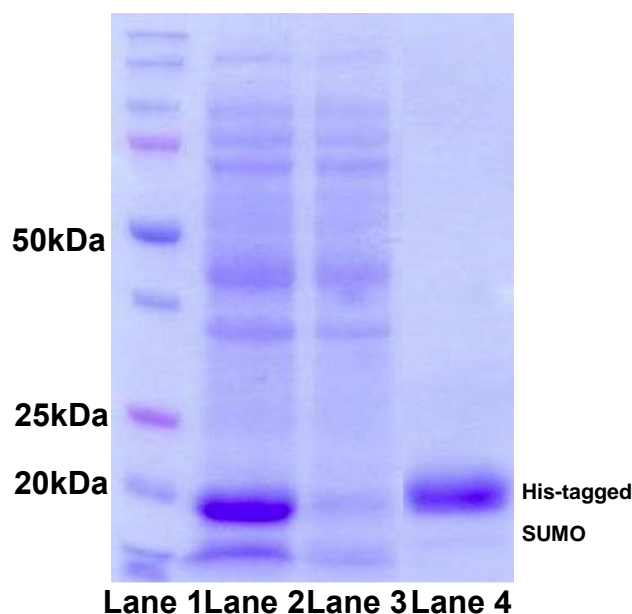
Figure 2.17. SDS-PAGE analysis of purification of overexpressed His-tagged SUMO protein from an *E. coli*. lysate. Lane 1: molecular marker; Lane 2: cell lysate containing His-tagged SUMO protein; Lane 3: the cell lysate after passing through a (PAH/CMPEI)-Ni^{2+}-modified CM membrane; Lane 4: the eluate of the loaded membrane.

2.3.8 Metal-ion Leaching

Low metal-ion leaching is sometimes important to avoid contaminating protein solutions. Thus, we examined leaching from several modified membranes and a common commercial Ni^{2+} column. Membranes modified with one and two bilayers of PAH/CMPEI-Ni^{2+} or PAH/PDCMAA-Ni^{2+} (deposited at pH 2 in 0.5 M NaCl) were washed with 5 mL each (160 bed volumes) of binding buffer 2, washing buffer 1, washing buffer 2, stripping buffer, and 2% HNO$_3$. (We summed the amounts of Ni^{2+} in the stripping buffer and HNO$_3$.) The GE Hitrap^{TM} FF Ni column with a 1-mL bed volume was washed with 160 mL (160 bed volumes) each of binding buffer 2 and washing buffers 1 and 2. Subsequently, the remaining Ni^{2+} was eluted from the column with 15 mL of stripping buffer (elution was complete with EDTA so 2%

HNO$_3$ was not needed). All the solutions were analyzed by atomic absorption spectroscopy.

Table 2.2. Ni^{2+} leaching from a GE Hitrap^{TM} FF Ni column and CM nylon membranes modified with (PAH/PDCMAA), (PAH/PDCMAA)$_2$, (PAH/CMPEI) and (PAH/CMPEI)$_2$ films. The numbers represent the percentage of Ni^{2+} ion lost in each solution. All the substrates were treated with 160 bed volumes (each) of binding buffer 2, washing buffers 1 and 2, elution buffer, and stripping buffer. The experiment was repeated twice for all substrates, and errors are differences between two trials.

	Binding buffer 2	Wash 1	Wash 2	Elution buffer	Stripping buffer and 2% HNO$_3$
GE column (%)	30.7±2.4	7.6±0.8	7.5±0.6	16.9±1.1	37.2±0.5
(PAH/PDCMAA) (%)	14.3±4.0	6.5±0.2	13.6±0.1	14.8±1.8	30.7±2.2
(PAH/PDCMAA)$_2$(%)	6.9±0.9	4.4±0.3	6.2±0.1	31.0±3.6	52.4±4.7
(PAH/CMPEI) (%)	0.7±1.3	2.0±1.4	4.7±1.5	34.7±2.5	57.8±4.0
(PAH/CMPEI)$_2$ (%)	0.7±0.1	0.3±0.6	1.7±0.4	21.8±3.4	75.4±2.4

Table 2.2 shows the leaching from the GE Hitrap^{TM} FF Ni column and different membranes as a percentage of the total Ni^{2+} binding. The (PAH/CMPEI)- and (PAH/CMPEI)$_2$-modified membranes show the least percentage leaching in the binding and washing buffers, and the percentage of leaching in the elution buffer is within a factor of ~2 for all systems, although the GE column shows the lowest leaching in that buffer. The low leaching in the elution buffer for the GE column partly reflects the high leaching in the binding buffer. For all systems, the higher leaching in the elution buffer (0.5 M imidazole) than in the washing buffers stems from the formation of imidazole-Ni^{2+} complexes. Nevertheless, all the membrane substrates had less than 10 ppm Ni^{2+} in the 5 mL of elution buffer except the membrane modified with

(PAH/PDCMAA)$_2$, which had 12.9 ± 1.1 ppm Ni^{2+}. (Note the values in Table 2.2 are percentages of the total Ni^{2+} loaded and not concentrations.) The Ni^{2+} binding capacity of the GE Hitrap^{TM} FF Ni column is 1.6 ± 0.2 mg/mL, and Figure 2.12 shows that the Ni^{2+} binding capacities for all the membranes are higher than that for the Ni column. (For example, the Ni^{2+} binding capacity of the (PAH/CMPEI)-modified membrane is 2.7 mg/mL.) Overall, the metal leaching from all the substrates is similar, which is not surprising given that they likely have related ligands.

2.3.9 Film Stability and Reusability

Adsorption of (PAH/CMPEI)-Ni^{2+} films may prove sufficiently simple and inexpensive to provide disposable, functional membranes. However, membrane reuse is always desirable, and the high swelling of PAH/CMPEI films (as much as 680%, see section 2.2) in buffer may lead to partial polyelectrolyte desorption. We evaluated the stability of CMPEI-containing films both on wafers and in membranes. For (PAH/CMPEI)$_2$ films on Au-coated Si wafers (deposited on a MPA monolayer at pH 2 in 0.5 M NaCl), immersion for 20 h in binding buffer 2 (pH 7.4) led to only a 10% decrease in thickness, most of which occurred in the first 4 h (see Figure 2.18). Absorbances in reflectance IR spectroscopy also decreased about 10%, suggesting that the change in thickness results from a small loss of film and not simply deswelling or a change in conformation.
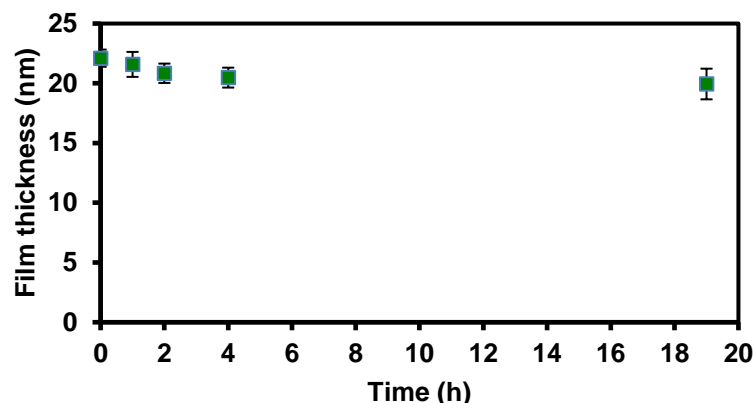
Figure 2.18. Ellipsometric thicknesses of (PAH/CMPEI)$_2$ films on MPA-modified, Au-coated Si wafers after immersion in binding buffer 2 for different times. The film was deposited at pH 2 from solutions containing 0.5 M NaCl. Error bars represent the standard deviations of measurements on at least three different films. Films were rinsed with water prior to determining their thickness.
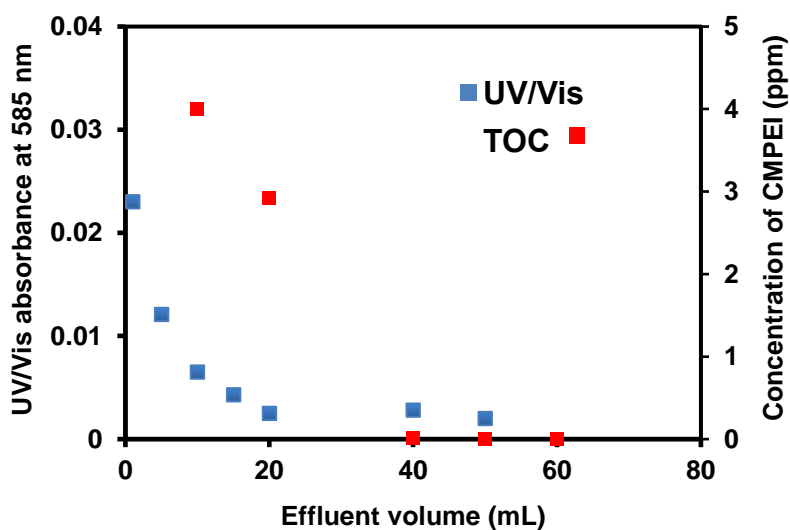
Figure 2.19. UV/Vis absorbance at 595 nm and the concentration of CMPEI in the effluent binding buffer 2 passing through a (PAH/CMPEI)-Ni^{2+}-modified membrane. Thirty μL of effluent was added to 1.5 mL of Bradford assay dye for UV/Vis analysis. The concentration of CMPEI was determined by TOC using CMPEI solutions (0-10 ppm) as standards.

Using TOC analysis, we determined the amount of the polyelectrolyte film lost during passage of binding buffer 2 (pH 7.4) through a membrane. After forming a (PAH/CMPEI) film and rinsing with only water, the first 20 mL of washing buffer passed through the membrane contained around 4 ppm of polymer (we assumed that the leaching was only due to CMPEI and used 1-10 ppm CMPEI solutions as standards). This corresponds to <20% of the total polymer based on our estimate of 14 mg of CMPEI/mL of membrane (the membrane volume in these leaching studies was 0.035 cm^3, diameter 2-cm). Subsequent buffer washes contained <0.005 ppm (TOC detection limit) of polymer. Additionally, we added wash solutions to the Bradford dye and tested the absorbance at 595 nm (Figure 2.19) as in a typical Bradford assay. The first mL of washing solution gave an absorbance of 0.02, which is equivalent to the absorbance given by 0.03 mg/mL of Con A. This absorbance rapidly declines and was only 0.002 after passing 20 mL of washing buffer through the membrane. In a typical protein-binding test, we wash the membranes with 40 mL of binding buffer prior to loading protein. However, some breakthrough curves such as that for (PAH/CMPEI)$_2$-Cu^{2+} (Figure 2.15) show a small and decreasing Bradford assay signal over the first 1-2 mL of protein loading. This may indicate that protein replaces a small amount of polyelectrolyte, i.e. the initial loading solution might contain 5 ppm of polyelectrolyte after passing through the membrane. We did not see this issue in binding of His U. As a further test of membrane stability, we performed 4 cycles of loading and elution of Con A in (PAH/CMPEI)-Cu^{2+}-modified CM membranes. The Con A binding decreased by 40% (from 58 mg/mL to 35 mg/mL) over four cycles of loading, recharging with Cu^{2+}, and elution (Figure 2.20). Thus, reuse is possible, but performance declines with use.
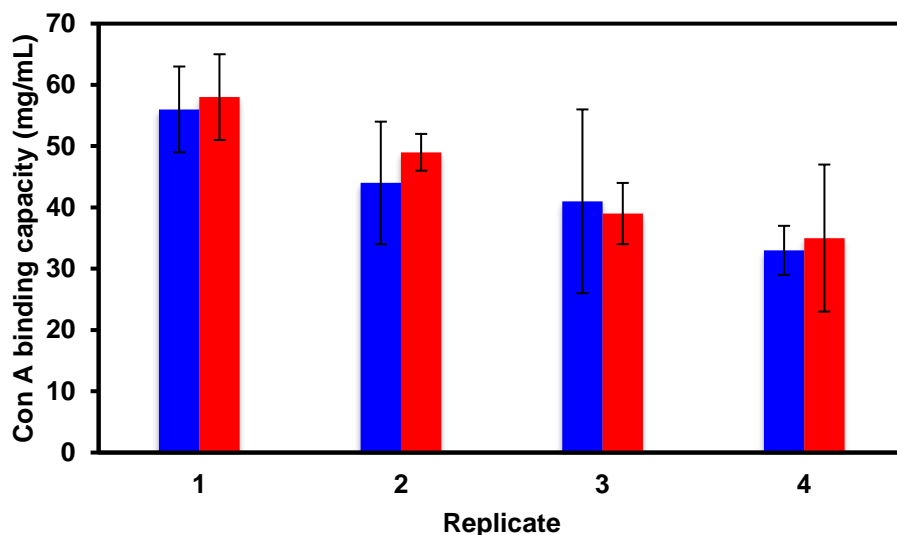
Figure 2.20. Con A binding capacities of (PAH/CMPEI)-Cu^{2+}-modified CM nylon membranes (blue bars and red bars represent two different membranes) in repeated measurements. Con A (0.3 mg/mL in binding buffer 1) was loaded and eluted four times, and membranes were recharged with Cu^{2+} before each capture experiment. The error bars are the differences between Con A binding capacities determined from the breakthrough curve and elution.

2.4 Conclusions

This study presents a facile method, LbL adsorption of functional polyelectrolytes, to modify membranes with metal-ion complexes that selectively capture His-tagged proteins. PAH/CMPEI adsorption yields a membrane with a His-tagged ubiquitin binding capacity of ~60 mg/mL, which is equal to the capacity of high-binding commercial beads. Moreover, these (PAH/CMPEI)-modified membranes show less than 10 ppm of Ni^{2+} in the elution buffer (0.5 M imidazole). Membranes modified with PAH/CMPEI show about twice the protein binding of corresponding membranes modified with PAH/PDCMAA, presumably because of more swelling with PAH/CMPEI. The His-tagged protein-binding capacity of the (PAH/PEI)-Ni^{2+}-modified membranes is 2/3 of that for membranes modified through growth of polymer brushes or LbL adsorption of PAA/PEI/PAA followed by derivatization. However, direct adsorption of

PAH and CMPEI in membranes is much simpler and less expensive than previous membrane modification methods and may lead to inexpensive, disposable membranes for rapid purification of His-tagged protein.

REFERENCES

REFERENCES

(1) Lichty, J. J.; Malecki, J. L.; Agnew, H. D.; Michelson-Horowitz, D. J.; Tan, S., Comparison of Affinity Tags for Protein Purification, *Protein Expr. Purif.* **2005**, *41*, 98-105.

(2) Porath, J., Immobilized Metal-Ion Affinity-Chromatography, *Protein Expr. Purif.* **1992**, *3*, 263-281.

(3) Arnau, J.; Lauritzen, C.; Petersen, G. E.; Pedersen, J., Current Strategies for the Use of Affinity Tags and Tag Removal for the Purification of Recombinant Proteins, *Protein Expr. Purif.* **2006**, *48*, 1-13.

(4) Kawai, T.; Saito, K.; Lee, W., Protein Binding to Polymer Brush, Based on Ion-Exchange, Hydrophobic, and Affinity Interactions, *J. Chromatogr. B* **2003**, *790*, 131-142.

(5) Bhut, B. V.; Husson, S. M., Dramatic Performance Improvement of Weak Anion-Exchange Membranes for Chromatographic Bioseparations, *J. Membr. Sci.* **2009**, *337*, 215-223.

(6) Ghosh, R., Protein Separation Using Membrane Chromatography: Opportunities and Challenges, *J. Chromatogr. A* **2002**, *952*, 13-27.

(7) Datta, S.; Bhattacharyya, D.; Ray, P. D.; Nath, A.; Toborek, M., Effect of Pre-Filtration on Selective Isolation of Tat Protein by Affinity Membrane Separation: Analysis of Flux, Separation Efficiency, And Processing Time, *Sep. Sci. Technol.* **2007**, *42*, 2451-2471.

(8) Wang, J.; Sproul, R. T.; Anderson, L. S.; Husson, S. M., Development of Multimodal Membrane Adsorbers for Antibody Purification Using Atom Transfer Radical Polymerization, *Polymer* **2014**, *55*, 1404-1411.

(9) Yin, D. X.; Ulbricht, M., Antibody-Imprinted Membrane Adsorber via Two-Step Surface Grafting, *Biomacromolecules* **2013**, *14*, 4489-4496.

(10) Thommes, J.; Etzel, M., Alternatives to Chromatographic Separations, *Biotechnol. Prog.* **2007**, *23*, 42-45.

(11) Roper, D. K.; Lightfoot, E. N., Separation of Biomolecules Using Adsorptive Membranes, *J. Chromatogr. A* **1995**, *702*, 3-26.

(12) Thommes, J.; Kula, M. R., Membrane Chromatography - An Integrative Concept in the Downstream Processing of Proteins, *Biotechnol. Prog.* **1995**, *11*, 357-367.

(13) Saxena, A.; Tripathi, B. P.; Kumar, M.; Shahi, V. K., Membrane-Based Techniques

for the Separation and Purification of Proteins: An Overview, *Adv. Colloid Interface Sci.* **2009**, *145*, 1-22.

(14) Zeng, X. F.; Ruckenstein, E., Membrane chromatography: Preparation and Applications to Protein Separation, *Biotechnol. Prog.* **1999**, *15*, 1003-1019.

(15) Sun, L.; Dai, J. H.; Baker, G. L.; Bruening, M. L., High-Capacity, Protein-Binding Membranes Based on Polymer Brushes Grown in Porous Substrates, *Chem. Mat.* **2006**, *18*, 4033-4039.

(16) Bhut, B. V.; Conrad, K. A.; Husson, S. M., Preparation of High-Performance Membrane Adsorbers by Surface-Initiated AGET ATRP in the Presence of Dissolved Oxygen and Low Catalyst Concentration, *J. Membr. Sci.* **2012**, *390*, 43-47.

(17) Yang, Q.; Ulbricht, M., Cylindrical Membrane Pores with Well-Defined Grafted Linear and Comblike Glycopolymer Layers for Lectin Binding, *Macromolecules* **2011**, *44*, 1303-1310.

(18) Kawakita, H.; Masunaga, H.; Nomura, K.; Uezu, K.; Akiba, I.; Tsuneda, S., Adsorption of Bovine Serum Albumin to A Polymer Brush Prepared by Atom-Transfer Radical Polymerization in A Porous Inorganic Membrane, *J. Porous Mat.* **2007**, *14*, 387-391.

(19) Honjo, T.; Hoe, K.; Tabayashi, S.; Tanaka, T.; Shimada, J.; Goto, M.; Matsuyama, H.; Maruyama, T., Preparation of Affinity Membranes Using Thermally Induced Phase Separation for One-Step Purification of Recombinant Proteins, *Anal. Biochem.* **2013**, *434*, 269-274.

(20) Bhut, B. V.; Wickramasinghe, S. R.; Husson, S. M., Preparation of High-Capacity, Weak Anion-Exchange Membranes for Protein Separations Using Surface-Initiated Atom Transfer Radical Polymerization, *J. Membr. Sci.* **2008**, *325*, 176-183.

(21) Ulbricht, M.; Yang, H., Porous polypropylene membranes with different carboxyl polymer brush layers for reversible protein binding via surface-initiated graft copolymerization, *Chem. Mat.* **2005**, *17*, 2622-2631.

(22) Bhattacharjee, S.; Dong, J. L.; Ma, Y. D.; Hovde, S.; Geiger, J. H.; Baker, G. L.; Bruening, M. L., Formation of High-Capacity Protein-Adsorbing Membranes through Simple Adsorption of Poly(acrylic acid)-Containing Films at Low pH, *Langmuir* **2012**, *28*, 6885-6892.

(23) Naka, K.; Tachiyama, Y.; Hagihara, K.; Tanaka, Y.; Yoshimoto, M.; Ohki, A.; Maeda, S., Synthesis and Chelating Properties of Poly (*N*,*N*-dicarboxymethyl)allylamine Derived from Poly(allylamine), *Polym. Bull.* **1995**, *35*, 659-663.

(24) Sheng, C. J.; Wijeratne, S.; Cheng, C.; Baker, G. L.; Bruening, M. L., Facilitated Ion Transport Through Polyelectrolyte Multilayer Films Containing Metal-Binding Ligands, *J.*

Membr. Sci. **2014**, *459*, 169-176.

(25) Wijeratne, S.; Bruening, M. L.; Baker, G. L., Layer-by-Layer Assembly of Thick, Cu2$^+$-Chelating Films, *Langmuir* **2013**, *29*, 12720-12729.

(26) Anzai, J.; Kobayashi, Y.; Nakamura, N.; Nishimura, M.; Hoshi, T., Layer-by-Layer Construction of Multilayer Thin Films Composed of Avidin and Biotin-Labeled Poly(amine)s, *Langmuir* **1999**, *15*, 221-226.

(27) Qiagen, http://www.qiagen.com/us/products/catalog/sample-technologies/protein-sample-technologies/purification-kits-and-resins/ni-nta-agarose#technicalspecification, 08/06/2016.

(28) Clonetech, His60 Nickel Resin Beats Ni-NTA Resin for His-Tag Purification, http://www.clontech.com/US/Support/Applications/Tagged_Protein_Purification/Ni-NTA_Resin_vs_His60, 08/06/2016.

(29) Bucur, C. B.; Sui, Z.; Schlenoff, J. B., Ideal Mixing in Polyelectrolyte Complexes and Multilayers: Entropy Driven Assembly, *J. Am. Chem. Soc.* **2006**, *128*, 13690-13691.

(30) Vig, J. R., Uv Ozone Cleaning Of Surfaces, *J. Vac. Sci. Technol. A* **1985**, *3*, 1027-1034.

(31) Miller, M. D.; Bruening, M. L., Correlation of the Swelling and Permeability of Polyelectrolyte Multilayer Films, *Chem. Mat.* **2005**, *17*, 5375-5381.

(32) Dai, J. H.; Bao, Z. Y.; Sun, L.; Hong, S. U.; Baker, G. L.; Bruening, M. L., High-Capacity Binding of Proteins By Poly(Acrylic Acid) Brushes and Their Derivatives, *Langmuir* **2006**, *22*, 4274-4281.

(33) Nakamoto, K.; Morimoto, Y.; Martell, A. E., Infrared Spectra of Aqueous Solutions .2. Iminodiacetic Acid, N-Hydroxyethyliminodiacetic Acid and Nitrilotriacetic Acid, *J. Am. Chem. Soc.* **1962**, *84*, 2081-&.

(34) Pack, D. W.; Arnold, F. H., Langmuir Monolayer Characterization of Metal Chelating Lipids for Protein Targeting to Membranes, *Chem. Phys. Lipids* **1997**, *86*, 135-152.

(35) Hoffmann, K.; Tieke, B., Layer-by-Layer Assembled Membranes Containing Hexacyclen-Hexaacetic Acid And Polyethyleneimine N-Acetic Acid and Their Ion Selective Permeation Behaviour, *J. Membr. Sci.* **2009**, *341*, 261-267.

(36) McAloney, R. A.; Sinyor, M.; Dudnik, V.; Goh, M. C., Atomic Force Microscopy Studies of Salt Effects on Polyelectrolyte Multilayer Film Morphology, *Langmuir* **2001**, *17*, 6655-6663.

(37) Schlenoff, J. B.; Dubas, S. T., Mechanism of Polyelectrolyte Multilayer Growth: Charge Overcompensation and Distribution, *Macromolecules* **2001**, *34*, 592-598.

(38) Dobrynin, A. V.; Rubinstein, M.; Joanny, J. F., Adsorption of A Polyampholyte Chain on a Charged Surface, *Macromolecules* **1997**, *30*, 4332-4341.

(39) Jeon, J.; Dobrynin, A. V., Monte Carlo Simulations of Polyampholyte-Polyelectrolyte Complexes: Effect of Charge Sequence and Strength of Electrostatic Interactions, *Phys. Rev. E* **2003**, *67*.

(40) Bowman, W. A.; Rubinstein, M.; Tan, J. S., Polyelectrolyte-Gelatin Complexation: Light-Scattering Study, *Macromolecules* **1997**, *30*, 3262-3270.

(41) Fu, J. H.; Ji, J.; Shen, L. Y.; Kueller, A.; Rosenhahn, A.; Shen, J. C.; Grunze, M., pH-Amplified Exponential Growth Multilayers: A Facile Method to Develop Hierarchical Micro- and Nanostructured Surfaces, *Langmuir* **2009**, *25*, 672-675.

(42) Bieker, P.; Schonhoff, M., Linear and Exponential Growth Regimes of Multi layers of Weak Polyelectrolytes in Dependence on pH, *Macromolecules* **2010**, *43*, 5052-5059.

(43) Becker, J. W.; Reeke, G. N.; Wang, J. L.; Cunningham, B. A.; Edelman, G. M., Covalent and 3-Dimensional Structure of Concanavalin-A .3. Structure Of Monomer and Its Interactions with Metals and Saccharides, *J. Biol. Chem.* **1975**, *250*, 1513-1524.

(44) Anuraj, N.; Bhattacharjee, S.; Geiger, J. H.; Baker, G. L.; Bruening, M. L., An All-Aqueous Route to Polymer Brush-Modified Membranes with Remarkable Permeabilites and Protein Capture Rates, *J. Membr. Sci.* **2012**, *389*, 117-125.

Chapter 3. Enzymatic Membrane Reactor for Affinity Tag Removal

3.1 Introduction

Affinity tag removal is a critical step after affinity protein purification and prior to characterization and biopharmaceutical application of recombinant proteins. Due to their high catalytic activity and relatively high specificity, site-specific enzymes including thrombin, SUMO (small ubiquitin-like modifier) protease, and tobacco etch virus (TEV) protease are the most common catalysts for cleaving tags from fusion proteins.[1-4] Cleavage procedures often employ overnight protein incubation in solutions with a low protease to protein ratio, and for some protein applications, tag removal processes also require subsequent separation of the protease and protein. Protease recycling is usually not possible, and tag-removal proteases are expensive, even though enzymes such as TEV protease and SUMO protease can be overexpressed in *E.Coli*.[5,6] Long incubation times, expensive proteases, and the need for protease/protein separations after cleavage limit the applications of conventional enzymatic methods for large-scale applications.

Protease immobilization can potentially provide reusable enzymatic reactors and improve the thermal, pH and storage stability of these enzymes.[6-8] Moreover, an enzymatic reactor with a high immobilized protease density may decrease the time needed for tag cleavage from the target protein, and such reactors do not require subsequent protease removal to prevent non-specific cleavage during protein storage. The most common immobilized enzyme reactors employ beads in either packed or spin columns.[9,10] In contrast this chapter explores tag removal using enzymes immobilized in porous membranes. Compared to bead-based columns, microporous synthetic membranes have minimal thickness and smaller (micron-sized) flow

channels. The small channels minimize diffusion limitations on cleavage reactions to increase rates, and the low membrane thickness enables control of the protein residence time in the membrane through variation of flow rate.[11] With short residence times (from ms to s), proteolysis should occur only at the most accessible and reactive sites in a protein to prevent cleavage at undesired sites. The research described in this chapter aims to immobilize proteases in membrane pores to create enzymatic reactors that remove fusion tags in short residence times. Because of the broad application of SUMO protease, I use this specific enzyme to study the activity, stability, and reusability of protease-functionalized membranes.

3.2 Experimental

3.2.1 Materials

Hydroxylated nylon (LoProdyne LP, Pall, 1.2 μm pore size, 110 μm thick) membranes were used as immobilization substrates. Polyethylenimine (branched, PEI, M_w ~25,000 Da), poly(sodium 4-styrenesulfonate) (PSS, M_w ~ 70,000 Da), poly(acrylic acid) (PAA, M_w ~100,000 Da, 35% aqueous solution, Sigma Aldrich), N-(3-(dimethylamino)-propyl)-N'-ethylcarbodiimide hydrochloride (EDC), N-hydroxysuccinimide, and N_α,N_α-bis(carboxymethyl)-L-lysine hydrate (aminobutyl NTA) were purchased from Sigma Aldrich and used without further purification. Coomassie protein assay reagent and bovine serum albumin (BSA) standards were acquired from Thermo Scientific. The buffers for SDS-PAGE (sodium dodecyl sulfate-polyacrylamide gel electrophoresis) analysis are SDS-PAGE sample loading buffer: pH 6.8, 0.5 M Tris buffer-7.3 mL, SDS-0.95 g, glycerol-1.2 mL, bromophenol blue-0.95 mg (add water to 1L); SDS-PAGE running buffer: glycine-28.8 g, Tris base-6.04 g, SDS-2 g (add water to 2 L); Coomassie stain solution: Coomassie R250-1 g, glacial acetic acid-

100 mL, methanol-400 mL, water-500 mL; Destain I solution: methanol-400 mL, acetic acid-100 mL, water-500 mL; and Destain II solution: methanol-280 mL, glycerol-40 mL, water-3.48 L, acetic acid-200 mL. These buffers were prepared using analytical grade chemicals and deionized water (Milli-Q, 18.2 MΩ cm).

3.2.2 His-tagged SUMO protease and substrate protein His-tagged SUMO branching enzyme

3.2.2.1 Expression and purification of His-tagged SUMO protease

Cell pellets containing SUMO protease and protease substrate proteins were prepared by Dr. Stacy Hovde. The His-tagged SUMO protease sequence was subcloned into the his-modified pet28b vector (Novagen). The plasmid was then transformed into BL21DE3 codon plus (Stratagene) competent cells. Colonies were grown in LB broth with Kanamycin at 37 °C until an O.D. of 0.6 was reached. The growth was induced with 0.75 mM isopropyl-thio-2-D-galactopyranoside (IPTG) for 4 h at 30 °C. The cells were pelleted by centrifugation and resuspended in Tris-sucrose buffer (50 mM Tris-HCl, pH 7.5, 1 mM phenylmethylsulfonylfluoride(PMSF), 10 mM sodium metabisulfite, 2 μg/mL of leupeptin, 10 wt% sucrose, and 5 mM β-mercaptoethanol). The suspension was sonicated and then centrifuged to pellet the debris. The resulting supernatant was diluted 4:1 with 20 mM pH 8 phosphate buffer containing 10 mM imidazole and 300 mM NaCl, and the His-tagged SUMO protease was purified with a Ni^{2+}-NTA (nitrilotriacetic acid) column, eluted with 250 mM midazole and dialyzed against 20 mM pH 8 phosphate buffer overnight at 4 °C. Cell lysate, cell pellet, supernatant and samples from Ni^{2+}-NTA column purification were further mixed with SDS-PAGE sample loading buffer for purity analysis.

3.2.2.2 Expression and purification of His-tagged SUMO branching enzyme

His-tagged SUMO branching enzyme was used as a substrate for His-tagged SUMO protease. This branching enzyme helps to catalyze the conversion of glucose to glycogen by adding branches to the growing glycogen.[12] The theoretical molecular weight of His-tagged SUMO branching enzyme is 96.7 kDa, and after His-tagged SUMO cleavage, the molecular weight should decrease to 84.3 kDa. This mass change is detectable in SDS-PAGE.

To produce His-tagged SUMO branching enzyme, the protein sequence was subcloned into the His-SUMO modified pet28b vector (Novagen). The plasmid was transformed into BL21DE3 codon plus (Stratagene) competent cells. Colonies were grown in LB broth with Kanamycin at 25 °C until an O.D. of 0.6 was reached. The growth was induced with 0.4 mM IPTG for 5 h at 25 °C, and the cells were pelleted by centrifugation. The pellet was resuspended in Tris-sucrose buffer at a pH of 8.0 and sonicated and then centrifuged to pellet the debris. The resulting supernatant was diluted 4:1 with 20 mM pH 8 phosphate buffer containing 10 mM imidazole and 300 mM NaCl, purified with a Ni^{2+}-NTA column, eluted with 250 mM imidazole and dialyzed against 20 mM pH 8 phosphate buffer overnight at 4 °C. Cell lysate, supernatant and samples from Ni^{2+}-NTA column purification were further mixed with SDS-PAGE sample loading buffer for purity analysis.

3.2.2.3 Estimation of His-tagged SUMO protease and His-tagged SUMO branching enzyme concentrations

The concentrations of purified His-tagged SUMO protease and His-tagged SUMO branching enzyme were estimated using a Bradford assay, with calibration based on BSA

standards (0.0 to 1.0 mg/mL). For analyses, 15 μL of every test or standard solution, including the purified His-tagged SUMO protease and His-tagged SUMO branching enzyme, was diluted with 1.5 mL of Coomassie Brilliant Blue G-250 at room temperature. The absorbance was then detected using a Perkin-Elmer UV/vis (model Lambda 25) spectrophotometer at 595 nm.

3.2.3 Immobilization of His-tagged SUMO protease in membranes modified with polyelectrolytes

For enzyme immobilization, we employ hydroxylated nylon membranes as substrates because of their mechanical strength and low nonspecific protein adsorption. To immobilize protease in these membranes, we first deposit a polyelectrolyte film and then adsorb the enzyme electrostatically. Previous studies in our group showed that sequential adsorption of PSS and trypsin or pepsin yields an enzymatic reactor for rapid protein digestion.[11] Additionally, PAA/PEI/PAA films in membranes strongly adsorb lysozyme through electrostatic interactions.[13] Figure 3.1 shows the structures of the polyelectrolytes. The protease conformation and activity may depend on the polyelectrolyte film to which it adsorbs. Thus, in this research I anchored His-tagged SUMO protease in membranes modified with PSS or PAA/PEI/PAA, and compared proteolysis with the two systems.

3.2.3.1 Membrane modification with PAA/PEI/PAA and PSS films

Hydroxylated nylon membrane sheets were cut into 25-mm disks. After cleaning with UV/O$_3$ for 10 min, the disks were placed in a homemade Teflon holder (similar to an Amicon cell) that exposed 3.14 cm^2 of external membrane surface area. To modify the membrane with a PAA/PEI/PAA film, a 20 mL solution containing 0.01 M PAA (pH 3, 0.5 M NaCl) was first

circulated through the membrane for 20 min at a flow rate of 1 mL/min using a peristaltic pump. After passing 20 mL of water through the membrane, 20 mL of 2 mg/mL PEI (pH 3) was circulated through the membrane for 20 min prior to again passing 20 mL of water through the membrane. Finally, 20 mL of 0.01 M PAA (pH 3, 0.5 M NaCl) was again circulated through the membrane followed by rinsing with water to complete the PAA/PEI/PAA film. Modification of a membrane with PSS occurred by circulating 20 mL of a 2 mg/mL PSS solution (pH 4.5, 0.5 M NaCl) through the membrane for 20 min at a flow rate of 1 mL/min, followed by rinsing with 20 mL of distilled water.[9] After modification, membranes were dried with N_2 and stored in a desiccator.

Figure 3.1. Structures of the polyelectrolytes (PEI, PAA and PSS) employed in membrane modification.

3.2.3.2 Immobilization of His-tagged SUMO protease in PSS- and PAA/PEI/PAA-modified membranes

To immobilize SUMO protease in membranes, the polyelectrolyte-modified membranes were punched into pieces with 6-mm diameters and placed in a small flangeless fitting system (flangeless fitting system, Upchurch Scientific, A-424). The small membrane was supported by a frit and connected on both sides to tubes fixed in ferrules. The contact between the tubes

and the membrane exposes an area of 0.021 cm^2 to liquid flow (see Figure 3.2). The membrane holder was further connected to a syringe pump. Assuming a porosity of 0.5, the membrane volume exposed to fluid flow is 0.11 μL (the membrane thickness is 110 μm).　After assembling the membranes in the cell, 100 μL of 20 mM Tris buffer (pH 6.5) followed by 100 μL of 20 mM Tris buffer (pH 6.5) containing 2 μg of His-tagged SUMO protease were passed through the membrane at a flow rate 2 mL/min using the syringe pump. Both the protease loading solution and permeate solution were analyzed by SDS-PAGE with color densitometry. Scheme 3.1 shows the immobilization procedure. In a control experiment, we also performed the enzyme immobilization with an unmodified nylon membrane.
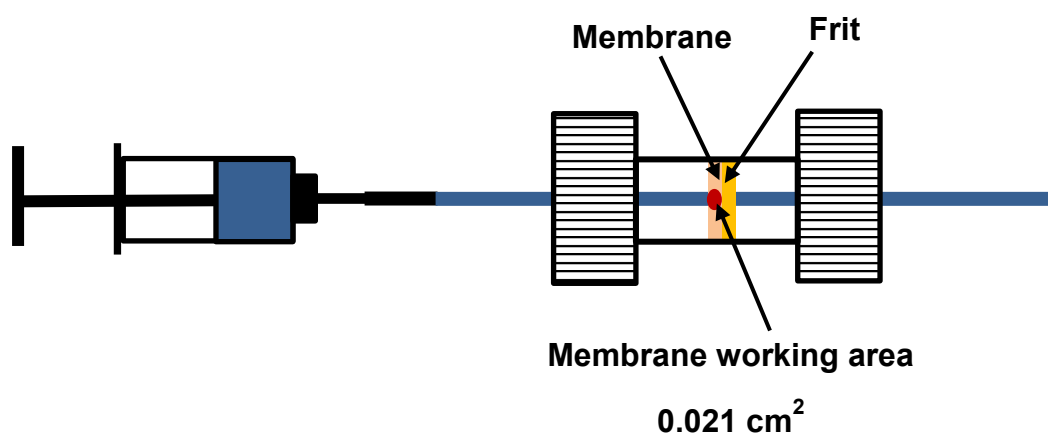
Figure 3.2. Minimized membrane holder for in membrane digestion.
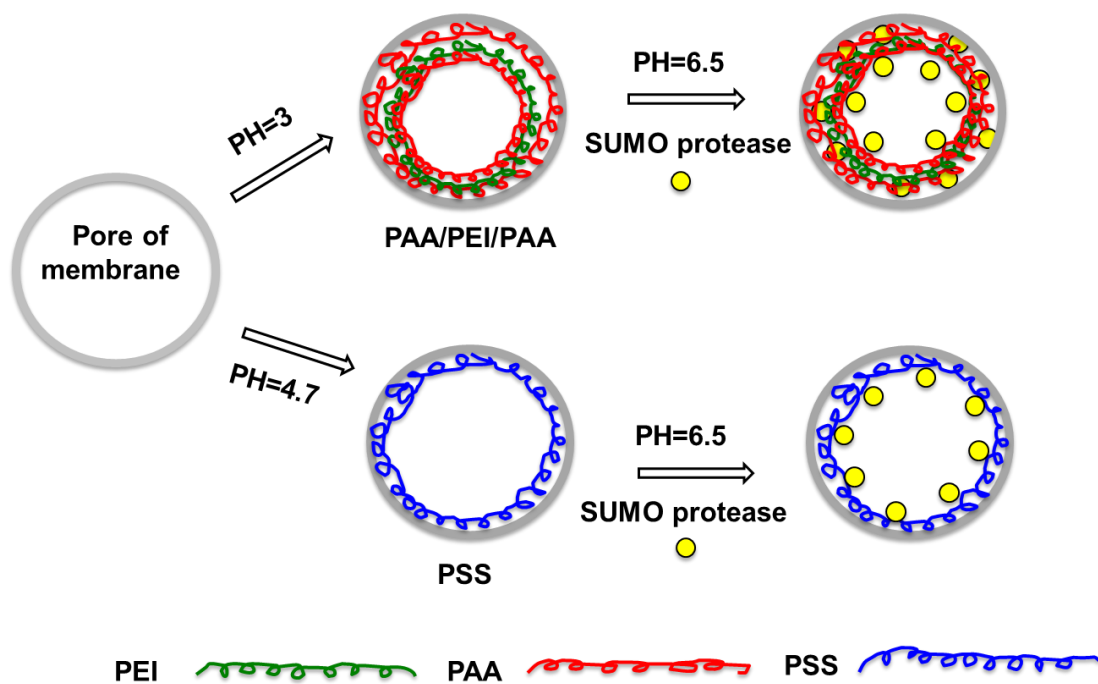
Scheme 3.1. Immobilization of His-tagged SUMO protease in membranes modified with PSS and PAA/PEI/PAA films.

3.2.4 SDS-PAGE densitometry for protein quantitation

After protein separation in SDS-PAGE, color densitometry can provide estimates of protein loading. Because various proteins interact differently with Coomassie dye, the staining intensities for different proteins at identical loadings are often different. Thus, SDS-PAGE generally gives only relative quantitation. However, for a given protein the use of standards with different concentrations can enable absolute quantitation. In this research, I studied the extent of His-tagged SUMO branching enzyme cleavage by analyzing the percentage of intact fusion protein that remains after cleavage for different times.

To test whether the band intensity of His-tagged SUMO branching enzyme in SDS-PAGE is proportional to the loading of this protein, I prepared standard curves of band intensity versus loading on three different SDS-PAGE gels. Different amount of His-tagged SUMO branching

enzyme (15 µL, 12 µL, 9 µL, 6 µL, 3µL, and 2 µL a 0.7 mg/mL solution) were loaded on the lanes of each gel. After electrophoresis, the gel was stained with Coomassie blue scanned with a Scanmarker 3800 instrument and quantitatively analyzing with ImageJ software.[14]

3.2.5 Comparison of the activities of His-tagged SUMO protease immobilized in PSS- and PAA/PEI/PAA-modified membranes

After loading of His-tagged SUMO protease in both PAA/PEI/PAA- and PSS-modified membranes, 120 µL of His-tagged SUMO branching enzyme (1.66 mg/mL, in 20 mM pH 8 phosphate buffer) was pumped though the membranes at a flow rate of 1.44 mL/h (the weight ratio of His-tagged SUMO branching enzyme passed through the membrane to immobilized His-tagged SUMO protease was 100:1). Effluent aliquots from the membrane were mixed with SDS-PAGE loading buffer and analyzed by SDS-PAGE as mentioned above.

3.2.6 Comparison of in-membrane and in-solution His-tagged SUMO protease activity

To compare in-membrane and in-solution tag removal, the protease to substrate weight ratio was 1:100 in both cases. For in-membrane cleavage, 50 µg of His-tagged SUMO protease was first loaded on a large membrane (surface area 3.14 cm^2), followed by circulating 3 mL of 1.66 mg/mL His-tagged SUMO branching enzyme protein solution (20 mM pH 8 phosphate buffer) through the membrane for 5, 15 and 30 min. For the in-solution reaction, ~0.2 mL of of 0.13 mg/mL His-tagged SUMO protease was added to 1.5 mL of a solution containing 1.66 mg/mL of His-tagged SUMO branching enzyme protein solution (20 mM pH 8 phosphate buffer). Sample aliquots were removed after 5 min, 15 min, 30 min, and proteolysis was

stopped by dilution in SDS-PAGE loading buffer. All the samples were mixed with SDS-PAGE loading buffer and analyzed by SDS-PAGE as described above.

3.2.7 Reusability of His-tagged SUMO protease-modified membranes

After 25 μg of His-tagged SUMO protease was immobilized on the large (3.14 cm^2) membrane, ~2.5 mg (1.5 mL, 1.66 mg/mL) of His-tagged SUMO branching enzyme was circulated through the protease-containing membrane continuously at a flow rate of 1 mL/min. After circulating for 5 min, the sample was removed and analyzed by SDS-PAGE gel. The membrane was washed with 1.5 mL of 20 mM pH 8 phosphate buffer prior to subsequent tag removal reactions with the same membrane.

3.3 Results and Discussion

This section first discusses purification and quantitation of His-tagged SUMO protease and its substrate protein, His-tagged SUMO branching enzyme. Then I compare the immobilization of His-tagged SUMO protease on membranes modified with different polyelectrolyte films. Finally, I examine the activity and reusability of immobilized His-tagged SUMO protease and compare in-membrane tag removal to conventional in-solution tag cleavage.

3.3.1 His-tagged SUMO protease and His-tagged SUMO branching enzyme

Figures 3.3 and 3.4 show the SDS-PAGE gels that characterize the production of His-tagged SUMO protease and His-tagged SUMO branching enzyme, and their purification with Ni^{2+}-NTA columns. The lanes of these gels showing eluates from the Ni^{2+}-NTA columns demonstrate high purities of both His-tagged SUMO protease and His-tagged SUMO branching enzyme (see lane C1-D4 in Figure 3.3 and C3-D5 in Figure 3.4). We pooled the

imidazole elution fractions (D1-D4) of His-tagged SUMO protease as well as the corresponding fractions (D1-D5) of His-tagged SUMO branching enzyme. After dialysis, we determined the concentration of His-tagged SUMO protease and His-tagged SUMO branching enzyme using a Braford assay. Figure 3.5 shows the BSA standard curve. The concentration of His-tagged SUMO protease estimated from the BSA calibration curve was 0.13 ± 0.01 mg/mL in about 20 mL of solution. We later adjusted the solution pH to 6.5 with 0.1 M HCl and 0.1 M NaOH prior to electrostatic adsorption in membranes. The estimated concentration of His-tagged SUMO-branching enzyme was 1.66 ± 0.04 mg/ml in about 25 mL of solution.
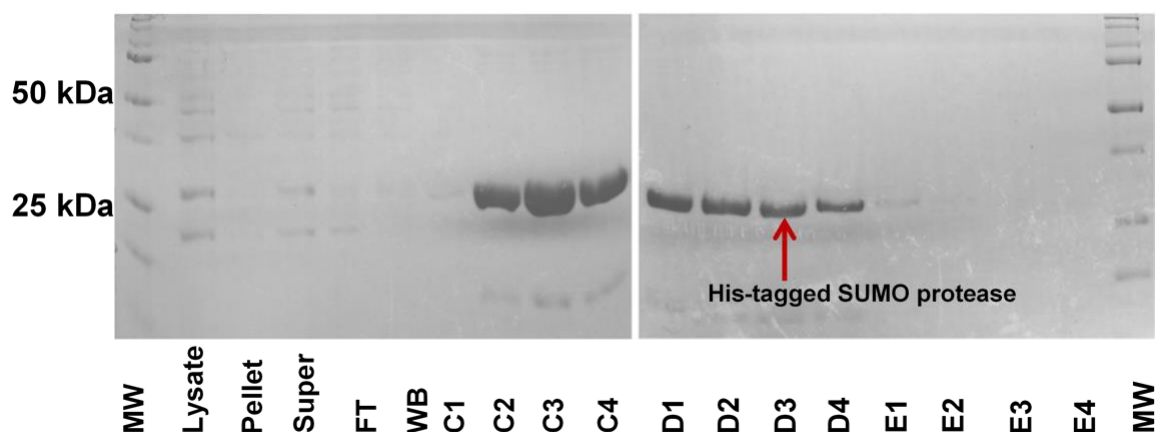
Figure 3.3. SDS-PAGE analysis of the production of His-tagged SUMO protease and purification with a Ni^{2+}-NTA column. From left to right the lanes are: MW- molecular marker; Lysate- cell lysate (including cell pellet and supernatant); Pellet- cell pellet. Super- supernatant of the cell lysate; FT- effluent cell lysate after flowing through the Ni^{2+} column. WB- 20 mM imidazole pH 8 Tris washing buffer used to rinse the Ni^{2+} column; C1-C4- 5 mL aliquots of the 100 mM imidazole Tris buffer (pH=8) used to elute the His-tagged SUMO protease; D1-D4- 5 mL aliquots of the 250 mM imidazole Tris buffer (pH=8) used to elute the His-tagged SUMO protease; E1-E4- 5 mL aliquots of the 400 mM imidazole Tris buffer (pH=8) used to elute the

Figure 3.3 (cont'd) His-tagged SUMO protease.   From MW to WB, 1 µL of solution was loaded on the gel, whereas in C1-E4, 5 µL of solution was loaded on the gel.

Figure 3.4. SDS-PAGE analysis of the production of His-tagged SUMO branching enzyme and purification with a Ni^{2+}-NTA column; MW- molecular marker; FT- effluent cell lysate after flowing through the Ni^{2+} column; WA- 10 mM imidazole pH 8 Tris washing buffer used to rinse the Ni^{2+} column (5 mL); WB- 20 mM imidazole pH 8 Tris washing buffer used to rinse the Ni^{2+} column (5 mL); C1-C4- 5 mL aliquots of the 100 mM imidazole Tris buffer (pH=8) used to elute the His-tagged branching enzyme; D1-D4 - 5 mL aliquots of the 250 mM imidazole Tris buffer (pH=8) used to elute the His-tagged branching enzyme.   From MW to WB, 1 µL of solution was loaded on the gel, whereas in C1-D5, 5 µL of solution was loaded on the gel.
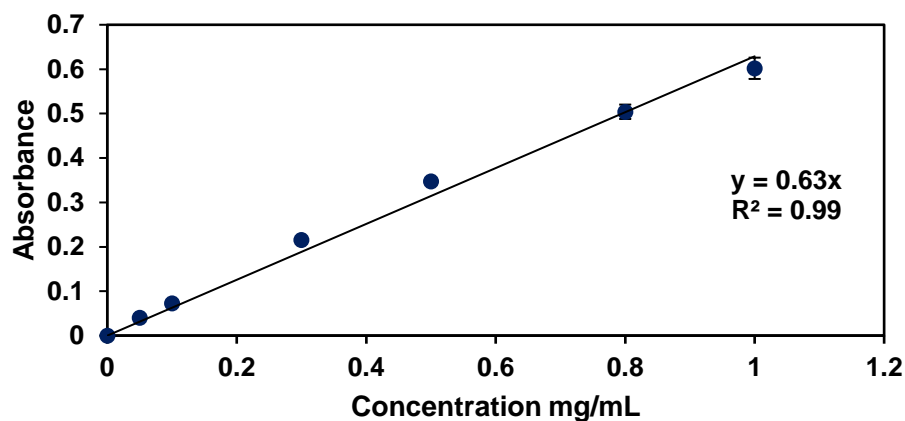
Figure 3.5. Bradford assay calibration curve for BSA.

3.3.2 His-tagged SUMO protease immobilization

Figure 3.6 shows SDS-PAGE analysis of His-tagged SUMO protease solutions before and after passing through bare, PSS-modified, and PAA/PEI/PAA-modified nylon membranes. The His-tagged SUMO protease gives rise to a band at an apparent molecular weight around 26 kDa. The disappearance of band for the permeate solutions suggests nearly complete adsorption of the protease (2 μg) by PSS- and PAA/PEI/PAA-modified nylon membranes, implying a binding capacity of at least 9 mg per mL of membrane. Even for the bare nylon, the intensity of the protease band declines after the solution passes through the membrane, suggesting that the bare nylon membrane shows some non-specific adsorption of His-tagged SUMO protease. However, part of the decrease in the intensity of the protease band may stem from some dead volume in the flow system. Solution in the dead volume may dilute the protease in the effluent.   Note that the polyelectrolyte coatings may decrease non-specific adsorption.[15] Regardless, the polyelectrolyte-modified membranes adsorb more protease than the bare nylon, suggesting electrostatic adsorption of the positively charged protease (the theoretical pI is around 7) to the negative charged polyelectrolyte-modified membrane surfaces.
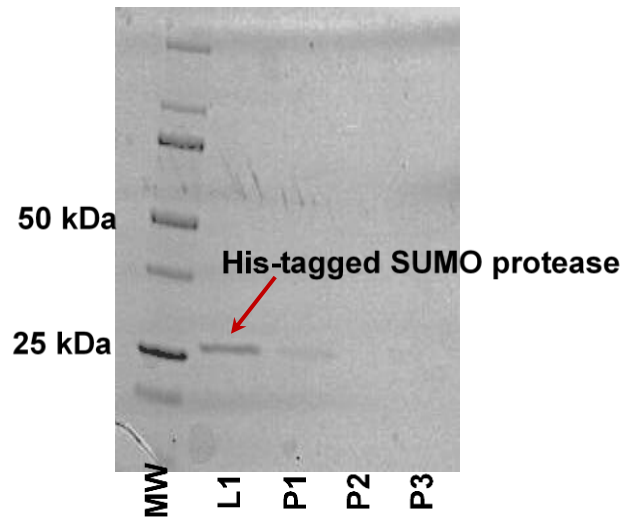
Figure 3.6. SDS-PAGE analysis of the solutions employed for His-tagged SUMO protease immobilization in bare, PSS-modified and PAA/PEI/PAA-modified nylon membranes. From left to right the lanes are: MW-molecular weight marker; L1- the protease loading solution prior to passing through a membrane; P1- the permeate solution after passing through a bare nylon membrane; P2- the permeate solution after passing through a PSS-modified nylon membrane. P3- the permeate solution from a PAA/PEI/PAA modified nylon membrane.

3.3.3 SDS-PAGE densitometry for protein quantitation

Figure 3.7. Image of the part of the SDS-PAGE gel showing the band for His-tagged SUMO branching enzyme. From left to right, the bands correspond to loading of 15 μL, 12 μL, 9 μL, 6 μL, 3μL, 2 μL and 0 μL of a solution containing 0.7 mg/mL of His-tagged SUMO branching enzyme.
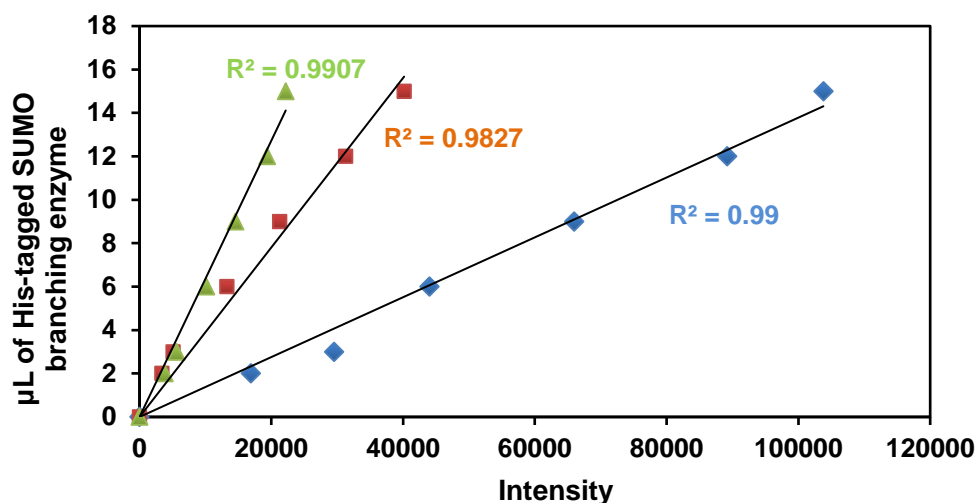
Figure 3.8. Calibration curves showing band intensity in SDS-PAGE versus protein loading of His-tagged SUMO branching enzyme. The figure shows data from three different SDS-PAGE gels (with different extents of staining and destaining). The loading solution contained 0.7 mg/mL of protease, and after scanning of gels, band intensities were determined with ImageJ software.

Because each gel has a different extent of staining and destaining, one cannot compare band intensities on different gels directly. However, the three calibration curves in Figure 3.8 show that the amount of His-tagged SUMO branching enzyme is proportional ($R^2 > 0.98$) to the band intensity on the same gel. This result shows that SDS-PAGE densitometry analysis is feasible to determine the extent of the cleavage reaction by comparing band intensities on the same gel, as described in the next section.

3.3.4 Comparison of His-tagged SUMO protease activity in PSS- and PAA/PEI/PAA-modified membranes

Figure 3.9. SDS-PAGE analysis of His-tagged SUMO branching enzyme proteolysis during passage through bare, PSS-, PAA/PEI/PAA-modified nylon membranes that contained His-tagged SUMO protease.   The residence time in the membrane was ~0.17 s.

Figure 3.9 shows the SDS-PAGE analysis of His-tagged SUMO branching enzyme solutions before and after passing through bare nylon membranes and modified membranes containing adsorbed His-tagged SUMO protease. The bare membrane shows SUMO tag cleavage (appearance of the cleaved branching enzyme band on the gel), probably because of a small amount of non-specific adsorption of His-tagged SUMO protease on the bare nylon. For the PSS-modified nylon membrane, despite increased protease adsorption compared to the bare membrane, the cleavage of the His-tagged SUMO protein is similar to that for the bare membranes. Perhaps a strong, hydrophobic interaction between PSS and the His-tagged SUMO protease induces protease conformational changes to decreases proteolytic activity. The PAA/PEI/PAA-modified nylon membrane shows the largest extent of His-tagged SUMO cleavage, suggesting a more active enzyme conformation in this system. Thus, we selected

PAA/PEI/PAA-modified nylon membranes for protease immobilization in further studies.

3.3.5. In-membrane and in-solution His-tagged SUMO protease activity comparison
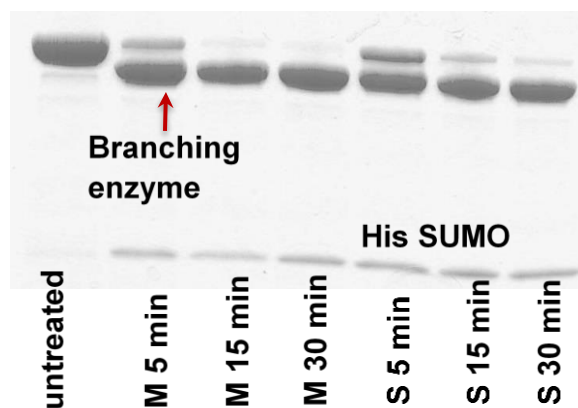
Figure 3.10. SDS-PAGE analysis of in-membrane and in-solution His-tagged SUMO tag cleavage from His-tagged SUMO branching enzyme. The in-membrane digestion (labeled with M on the gel) ocurred during circulation of 1.5 mL of 1.66 mg/mL His-tagged SUMO branching enzyme through the membrane for 5 min, 15 min and 30 min at a rate of 1 mL/min. (The protease to total substrate weight ratio is 1:100). In-solution digestion (labeled with S on the gel) occurred for different times in a solution of 1.66 mg/mL His-tagged SUMO branching enzyme containing a 1:100 protease to substrate weight ratio.   The band labeled untreated is the His-tagged SUMO branching enzyme solution prior to cleavage.

Figure 3.10 shows the SDS-PAGE analysis of in-membrane and in-solution digestion using a 1:100 protease to substrate ratio in both cases. Based on the intensities for the His-tagged SUMO branching enzyme before and after cleavage, the conversion after 5 min of digestion is similar for the in-membrane (0.675) and in-solution (0.619) procedures. However, at long times, the in-membrane appears to show more complete tag removal.

The similar conversion at short times suggests that the protease activities are similar for both the immobilized and dissolved protease. Equation (3.1) gives an expression for the concentration of intact His-tagged SUMO branching enzyme, C, as a function of time for a pseudo first-order reaction, where C_0 is the initial His-tagged SUMO branching enzyme concentration, and k' is the pseudo first-order rate constant defined in equation (3.2), where C_{enz} is the enzyme concentration.

$$C = C_0 exp(k't) \tag{3.1}$$

$$k' = kC_{enz} \tag{3.2}$$

Under the conditions of Figure 3.10, the His-tagged SUMO protease amounts are the same for in-membrane and in-solution digestion. However, for the same amount of enzyme, the local enzyme concentration is higher in the membrane than in solution because concentration is inversely proportional to volume. In contrast, for a given total reaction time, the residence time in the membrane is directly proportional to the membrane volume (divided by the total volume). Thus, the factor $k't$ (where t is total time for in-solution digestion and the residence time for the membrane) will be the same for in-solution and in-membrane cleavage as long as k is the same in both cases and the amount of enzyme and solution volumes are the same. Similar extents of tag cleavage for in-membrane and in-solution reactions suggest that k is similar for dissolved and immobilized enzymes.

3.3.6 Reusability of immobilized His-tagged SUMO protease
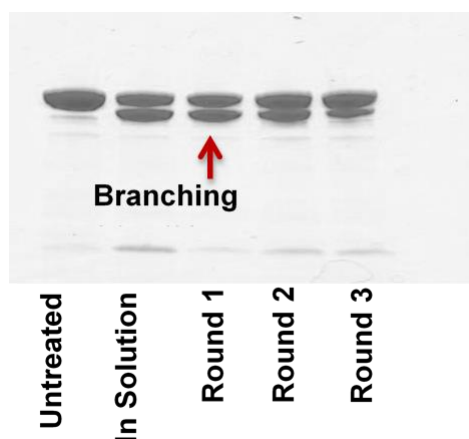
Figure 3.11. SDS-PAGE analysis of His-tagged SUMO branching enzyme after in-solution and in-membrane tag cleavage with repeated use of the same membrane. Cleavage occurred for 5 min in solution or during 5 min of circulation through the membrane, and both in-solution and in-membrane cleavage employed 25 μg of enzyme and 1.5 mL of a solution containing 1.66 mg/mL of His-tagged SUMO branching enzyme. The weight ratio of protease to substrate is 1:100.

To study the reusability of His-tagged SUMO protease modified membrane, I used the same membrane to perform three rounds of tag removal. Each round of tag cleavage included circulation of 1.5 mL of a 1.66 mg/mL (2.5 mg) His-tagged SUMO branching enzyme solution through the membrane, with a 1.5-mL water rinse between rounds. Figure 3.11 shows the SDS-PAGE analysis of the proteins after in-solution and in-membrane tag removal (three circulations through the membrane). Densitometry was tried for estimating the conversion of His-tagged SUMO branching enzyme to branching enzyme, however results calculated from remaining His-tagged SUMO branching enzyme, cleaved His-tagged SUMO and branching enzyme are not consistent. Thus, no quantitative data was generated. But the His-tagged SUMO

protease still works after three times circulation (appearance of branching enzyme band on SDS-PAGE gel). Even though the activity of His-tagged SUMO protease gradually decreases compared to the first round of cleavage, it is still active after 3 usages and should effectively remove the tag with longer circulation times.

3.4 Conclusions

In summary, adsorption of His-tagged SUMO protease to polyelectrolyte-modified nylon membranes successfully immobilizes the enzyme. However, PAA/PEI/PAA-modified nylon membranes show higher protease activity than PSS-modified membranes. The immobilized protease activity in the PAA/PEI/PAA-modified nylon membranes is similar to that in solution, and the use of membranes should avoid the need to separate the cleaved protein from the enzyme. However, further studies should investigate the extent to which the enzyme leaches from the membrane.   Moreover, the membrane is reusable. In a third round of tag cleavage, the immobilized protease retained 79% of its initial activity.

REFERENCES

REFERENCES

(1) Jenny, R. J.; Mann, K. G.; Lundblad, R. L., A Critical Review of the Methods for Cleavage of Fusion Proteins with Thrombin and Factor Xa, *Protein Expr. Purif.* **2003**, *31*, 1-11.

(2) Liu, L.; Spurrier, J.; Butt, T. R.; Strickler, J. E., Enhanced Protein Expression in the Baculovirus/Insect Cell System Using Engineered SUMO Fusions, *Protein Expr. Purif.* **2008**, *62*, 21-28.

(3) Peroutka, R. J.; Elshourbagy, N.; Piech, T.; Butt, T. R., Enhanced Protein Expression in Mammalian Cells Using Engineered SUMO Fusions: Secreted Phospholipase A2, *Protein Sci.* **2008**, *17*, 1586-1595.

(4) Arnau, J.; Lauritzen, C.; Petersen, G. E.; Pedersen, J., Current Strategies for the Use of Affinity Tags and Tag Removal for the Purification of Recombinant Proteins, *Protein Expr. Purif.* **2006**, *48*, 1-13.

(5) Reverter, D.; Lima, C. D., Preparation of SUMO Proteases and Kinetic Analysis Using Endogenous Substrates, *SUMO Protocols* **2009**, 225-239.

(6) Wu, G. Q.; Deng, X. P.; Li, X. F.; Wang, X. Y.; Wang, S. L.; Xu, H. M., Application of immobilized thrombin for production of S-thanatin expressed in Escherichia coli, *Appl. Microbiol. Biotechnol.* **2011**, *92*, 85-93.

(7) Miladi, B.; El Marjou, A.; Boeuf, G.; Bouallagui, H.; Dufour, F.; Di Martino, P.; Elm'selmi, A., Oriented Immobilization of the Tobacco Etch Virus Protease for the Cleavage of Fusion Proteins, *J. Biotechnol.* **2012**, *158*, 97-103.

(8) Puhl, A. C.; Giacomini, C.; Irazoqui, G.; Batista-Viera, F.; Villarino, A.; Terenzi, H., Covalent Immobilization of Tobacco-Etch-Virus Nia Protease: A Useful Tool for Cleavage: of the Histidine Tag of Recombinant Proteins, *Biotech. Appl. Biochem.* **2009**, *53*, 165-174.

(9) Bayramoglu, G.; Celikbicak, O.; Arica, M. Y.; Salih, B., Trypsin Immobilized on Magnetic Beads via Click Chemistry: Fast Proteolysis of Proteins in a Microbioreactor for MALDI-TOF-MS Peptide Analysis, *Ind. Eng. Chem. Res.* **2014**, *53*, 4554-4564.

(10) Yamaguchi, H.; Miyazaki, M., Enzyme-Immobilized Reactors for Rapid and Efficient Sample Preparation in MS-Based Proteomic Studies, *Proteomics* **2013**, *13*, 457-466.

(11) Tan, Y. J.; Wang, W. H.; Zheng, Y.; Dong, J. L.; Stefano, G.; Brandizzi, F.; Garavito, R. M.; Reid, G. E.; Bruening, M. L., Limited Proteolysis via Millisecond Digestions in Protease-Modified Membranes, *Anal. Chem.* **2012**, *84*, 8357-8363.

(12) Abad, M. C.; Binderup, K.; Rios-Steiner, J.; Arni, R. K.; Preiss, J.; Geiger, J. H., The X-ray Crystallographic Structure of Escherichia coli Branching Enzyme, *J. Biol. Chem.* **2002**, *277*, 42164-42170.

(13) Bhattacharjee, S.; Dong, J.; Ma, Y.; Hovde, S.; Geiger, J. H.; Baker, G. L.; Bruening, M. L., Formation of High-Capacity Protein-Adsorbing Membranes through Simple Adsorption of Poly(acrylic acid)-Containing Films at Low pH, *Langmuir* **2012**, *28*, 6885-6892.

(14) Schneider, C. A.; Rasband, W. S.; Eliceiri, K. W., NIH Image to ImageJ: 25 years of image analysis, *Nat methods* **2012**, *9*, 671-675.

(15) Ning, W. J. B., M.L. , Rapid Protein Purification and Digestion with Membrane-Containing Pipette Tips, *Anal. Chem.* **2015**, *87*, 11984-11989.

Chapter 4. Controlled Proteolysis in Porous Membrane Reactors Containing Immobilized Trypsin

This chapter is adapted from our manuscript "Limited Proteolysis in Porous Membrane Reactors Containing Immobilized Trypsin" by Ning, W., Dong, J., and Bruening, M. L.

Proteolysis is often a critical step in protein characterization via mass spectrometry. Compared to complete digestion, limited proteolysis gives rise to larger peptides that often cover a greater portion of the protein's amino acid sequence. This chapter explores controlled, limited proteolysis in porous nylon membranes containing immobilized trypsin. Passage of protein solutions through 100-μm thick membranes enables reaction residence times as short as milliseconds to limit digestion. Additionally, variation of the membrane pore size (5.0, 1.2 or 0.45 μm) and the protease-immobilization method (electrostatic adsorption or covalent anchoring) affords control over the proteolysis rate. Large pores (5.0 μm) and covalent anchoring yield particularly long tryptic peptides and high protein sequence coverages. For example, the sequence coverages of β-casein digested during a 33 ms residence time in membranes containing covalently or electrostatically immobilized trypsin are 100% and 88%, respectively. Limited proteolysis followed by mass spectrometry can also help identify flexible regions in a protein. With both cytochrome c and apomyoglobin, in-membrane trypsinolysis with short residence times cleaves the protein after lysine residues in highly flexible regions to generate two large peptides that cover the entire protein sequence.

4.1 Introduction

Detection of protein sequence variations and post-translational modifications should provide valuable information about human development and diseases such as cancer[1] and

Alzheimer's disease.[2] Mass spectrometry (MS) is the most comprehensive and versatile analytical tool to characterize proteins and their post-translational modifications, and MS techniques continue to evolve and give higher resolution, faster analysis, and higher mass accuracy.[3,4] However, even with recent advances in MS, analysis of intact proteins with molecular weights greater than 50 kDa is challenging.[5-7] As a result, proteolytic digestion to convert proteins to peptides is usually a vital step in sample preparation for MS analysis.[8,9] Conventionally, digestion occurs after mixing a small amount of a proteolytic enzyme with protein solutions. Several proteases including chymotrypsin,[10] trypsin,[11] LysC,[12] and AspN[13] are effective, but trypsin, which catalyzes cleavage at the carboxyl side of Lys or Arg when neither is followed by Pro, is the most popular enzyme due to its high cleavage specificity and low cost.[14]

Several research groups developed reactors containing immobilized trypsin,[15-17] and trypsin-containing columns are commercially available.[18,19] Immobilization of trypsin can improve its stability, extend its working pH range, and allow digestion in low levels of detergent.[20-22] Substrates for trypsin immobilization include polymer plates,[23] membranes,[9,20,24] monoliths,[25] microfluidic channels,[26] and resins,[27,28] and enzyme anchoring can occur via hydrophobic,[24] covalent,[29] or electrostatic interactions.[9,20] Porous membranes present a unique enzyme-immobilization platform for controlling proteolysis because of their small thickness (~100 μm). Even with pressure drops < 0.1 atm,[30] flow through a membrane can yield digestion times ranging from milliseconds to seconds. Previous studies in our group showed that decreasing residence times to milliseconds in pepsin-modified membranes gives missed cleavages sites to create large peptides that provide high sequence coverage for antibody

characterization.[9,31] However, peptic digestion, which occurs around pH 3, suffers from low cleavage specificity and is not as common as tryptic digestion, especially for studies of native protein structures.[32] Thus, this study aims to control tryptic digestion by varying the flow rate through trypsin-containing membranes.

Because trypsin is a more active enzyme than pepsin,[33] simply decreasing residence times to a few milliseconds may not result in highly limited digestion. In this work, we aim to control and limit tryptic digestion in membranes by either increasing membrane pore sizes or covalently immobilizing trypsin. Large pore diameters should lead to decreased digestion due to a relatively low amount of immobilized enzyme and long average times for proteins to diffuse to enzymes on pore walls. In contrast, covalent immobilization will likely decrease the protease activity to give more missed cleavages. This study employs trypsin-containing membrane to controllably digest β-casein and denatured bovine serum albumin. Increased flow rates through the membrane (shorter residence times) lead to both larger tryptic peptides and higher peptide coverage of the protein sequence. Additionally, we show that in some cases limited tryptic digestion can reveal the regions of a protein that are most amenable to enzymatic cleavage.

4.2 Experimental section

4.2.1 Materials

Hydroxylated nylon (LoProdyne® LP, Pall, 1.2 μm pore size, 110 μm thick) and nylon (0.45 μm, Millipore, HNWP02500 or 5.0 μm, Sterlitech, NY5025100) membranes were employed as substrates for trypsin immobilization. Trypsin from bovine pancreas (type I, 12200 units/mg solid), benzamidine hydrochloride, N_α-benzoyl-L-arginine ethyl ester hydrochloride (BAEE), poly(acrylic acid) (PAA, average molecular weight ~100,000 Da, 35%

aqueous solution), poly(sodium 4-styrenesufonate) (PSS, M_w ~ 70,000 Da), *N*-(3-dimethylaminopropyl)-*N'*-ethylcarbodiimide hydrochloride (EDC), *N*-hydroxysuccinimide (NHS), bovine serum albumin (BSA), bovine β-casein, bovine heart cytochrome c, apomyoglobin (protein sequencing grade from horse skeletal muscle, salt-free lyophilized powder), and myoglobin (from horse skeletal muscle 95-100%, salt-free lyophilized powder) were purchased from Sigma-Aldrich.   Buffers were prepared using analytical grade chemicals and deionized (Milli-Q, 18.2 MΩ cm) water.

4.2.2 Trypsin immobilization in membranes

4.2.2.1. Electrostatic immobilization of trypsin

Modification of hydroxylated nylon membranes (2-cm exposed diameter) employed a home-made Teflon holder (similar to an Amicon cell, Model 8010, 10 mL, Millipore) and a peristaltic pump. Nylon membrane with 5.0 μm was hydroxylated prior to further modifications with following procedure: 12 pieces of membranes were incubated in heated solution containing 55 mL of formaldehyde and 1 mL of 85% w/v phosphoric acid for overnight, washed with water and dried with N_2 gas. 0.45 μm was used directly without chemical treatment. After exposing the membrane to UV/O_3 for 10 min, 10 mL of PSS solution (1 mM repeat unit concentration, 0.5 M NaCl, pH 2.3) and 20 mL of deionized water were sequentially passed through the membrane at 1 mL/min. Trypsin solution (0.5 mg/mL, 3 mL, in 2.7 mM HCl) was then circulated through PSS modified membranes for 15 min at a flow rate of ~1 mL/min. After passing 30 mL of 1 mM HCl through the membranes, they were dried with flowing N_2 and stored in refrigerator.

4.2.2.2 Covalent immobilization of trypsin

Hydroxylated nylon membranes (2-cm exposed diameter, 1.2 µm pore size) were exposed to UV/O$_3$ for 10 min and placed in the Teflon holder prior to circulation of 10 mL of 20 mM PAA (pH 3, 0.5 M NaCl, concentration is with respect to the repeating unit) through the membrane for 30 min. Subsequently, 20 mL of deionized water was pumped through the membrane at 1 mL/min. The adsorbed PAA was activated by circulating 10 mL of aqueous 20 mM NHS, 20 mM EDC through the membrane for 2 h followed by passage of 20 mL of water and 20 mL of ethanol through the membrane. Subsequently, 5 mL of 0.4 mg/mL trypsin solution in 20 mM phosphate buffer (pH 7.6) supplemented with 20 mM benzamidine was circulated through the membrane for 2 h to complete the covalent immobilization. These membranes were washed by passing 20 mL of phosphate buffer containing 20 mM benzamidine and 20 mL of 1 mM HCl through the membrane before drying with N$_2$ and storage at 8 °C.

4.2.3 Quantitation of trypsin immobilization and activity

We employed the UV-Vis absorbance (280 nm, PerkinElmer Lambda 25 spectrophotometer) of the trypsin loading solution before and after circulating through the membrane to estimate the amount of trypsin immobilized in membranes. For electrostatically immobilized trypsin, calibration solutions contained trypsin (0-0.5 mg/mL) in 2.7 mM HCl. For covalently immobilized trypsin, calibration solutions contained 20 mM benzamidine, and because NHS absorbs at 280 nm under basic conditions, 2.5 mL of standard or sample solution was mixed with 0.5 mL of 1 M HCl before absorbance measurements.[34]

We determined the proteolytic activity of trypsin both in solution and in membranes using the substrate BAEE. For in-solution studies, 10 µL of 1 mg/mL trypsin in 2.7 mM HCl was

added to 3 mL of 1 mM BAEE in 10 mM NH_4HCO_3 (pH 7.6) buffer and mixed with a pipet for ~ 5 s. The UV absorbance at 253 nm was monitored every 10 s using 1 mM BAEE as a background until the absorbance plateaued. The solution was not stirred during this time, but a separate experiment showed that the extent of reaction after 1, 2, 3, 4, 5, and 6 min was not significantly different with and without stirring.

With membranes, 20 mM BAEE was passed though the trypsin-modified nylon (2-cm exposed diameter, 1.2 μm pore size) at flow rates ranging from 60 mL/h to 2 mL/h using a syringe pump with a 10-mL syringe. The first 0.15 mL passed through the membrane was discarded to avoid dead-volume effects, and the second 0.15 mL was collected UV/Vis analysis. Based on a membrane thickness of 110 μm and 50% porosity (values provided by Pall for LoProdyne®), these flow rates give residence times of 1.04 to 31.1 s. Because unhydrolyzed BAEE absorbs some light at 253 nm, all the samples were diluted 20-fold with phosphate buffer before measurement against a 1 mM BAEE background. All the experiments were repeated 3 times, and the reported uncertainties are standard deviations.

4.2.4 In-solution and in-membrane protein digestion

For digestion without denaturation, 100 μg of protein was directly dissolved in 1 mL of 10 mM NH_4HCO_3. For digestion with denaturation, proteins were dissolved in 10 mM ammonium bicarbonate buffer containing 6 M urea instead. To digest proteins in solution, 10 μL of freshly made 0.5 mg/mL trypsin in 1 mM HCl was added to 1 mL of 0.1 mg/ml protein solution to achieve a 1:20 ratio of trypsin to substrate protein. After the desired digestion time, the reaction was quenched by addition of 11 μL of acetic acid. For in-membrane digestion, the membrane was cut to fit into a small HPLC disk holder (flangeless fitting system, Upchurch Scientific, A-

424), which was connected to a syringe pump as shown in our previous publication.[20] The holder exposes an external membrane area of 0.02 cm^2. Protein solutions were passed through trypsin-modified membrane at flow rates ranging from 0.06 mL/h to 2 mL/h. The resulting digests were dried (Speed Vac) prior to reconstitution in the MS buffer.

4.2.5 Mass spectrometry and data analysis

Digests were analyzed with ESI-MS. Fifty μL of reconstituted protein digest in MS buffer (1% acetic acid, 50% methonal and 49% water) was loaded into a Whatman multichem 96-well plate and sealed with Teflon Ultrathin Sealing Tape. The samples were introduced into the high-resolution accurate mass Thermo LTQ Orbitrap Velos mass spectrometer using an Advion Triversa Nanomate nanoelectrospary ionization (nESI) source. The spray voltage was 1.4 kV, and the gas pressure was 1.0 psi. High-resolution mass spectra were acquired in positive ionization mode using the FT analyzer operating at 100,000 resolving power with relative intensity as the Y-axis. Peptides were identified manually by comparing the experimental data to m/z values for the theoretical peptides generated using the ProteinProspector MS-Product program (v 5.14.1, University of California, San Francisco, CA). Settings for the theoretical peptide generation included: tryptic digestion, a maximum number of missed cleavages of 99, peptide masses from 200 to 30000 Da, a minimum peptide length of 4 and no signal peptides.

4.3 Results and discussion

4.3.1 Electrostatic and covalent immobilization of trypsin in membranes

Electrostatic adsorption is a very simple method for immobilizing trypsin.[10,20] As Scheme 4.1 (a) shows, PSS adsorption through hydrophobic interactions in membrane pores creates an anionic primer layer. At pH 2~3, trypsin (pI of ~10) has a net positive charge and binds to the

polyanionic PSS layer electrostatically. The low deposition pH avoids trypsin autolysis, and

enzyme activity recovers after washing with 10 mM NH_4HCO_3 prior to protein digestion. [9,20]
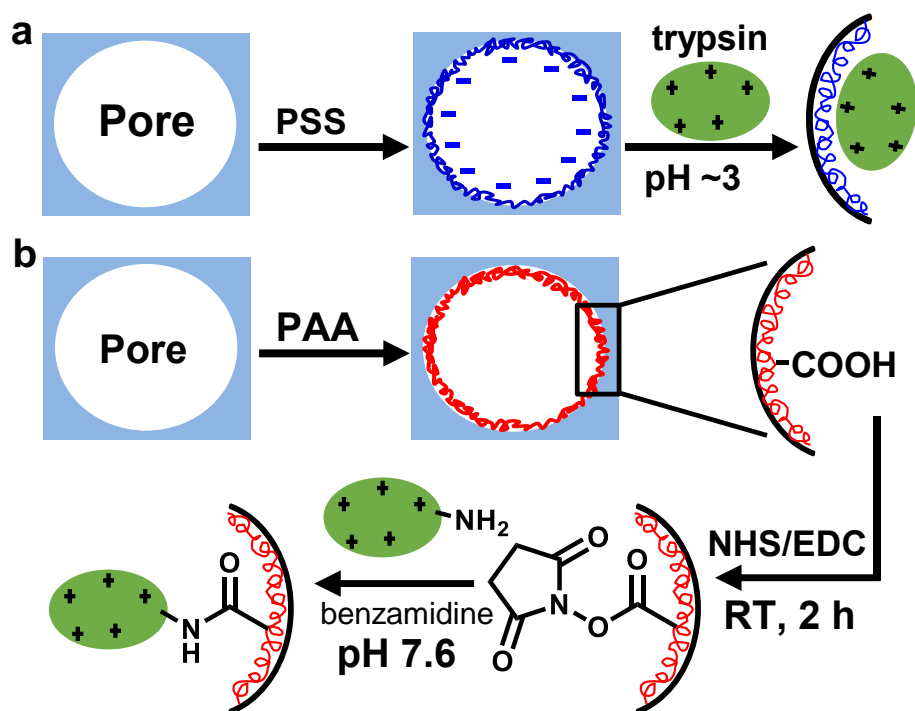
Scheme 4.1. Conceptual drawing of trypsin immobilization in membranes pores via (a)

electrostatic and (b) covalent linkages. In reality, trypsin much smaller than membrane pores.

NHS = N-hydroxysuccinimide; EDC = *N*-(3-dimethylaminopropyl)-*N'*-ethylcarbodiimide

hydrochloride; RT = room temperature.

For covalent immobilization of trypsin, PAA serves as the primer layer to introduce –

COOH groups for coupling with the amines of trypsin. Scheme 4.1 (b) shows the strategy

including adsorption of PAA, activation of –COOH groups with NHS/EDC and covalent

coupling via amide linkages.[35] Several previous studies reported covalent immobilization using

accessible primary amine groups on trypsin,[25,29,36-38] mainly through reaction with epoxy or

aldehyde groups on the solid support. Amide coupling using NHS/EDC is more rapid than

reaction of amine groups with epoxides or aldehydes, and the amide bond is more stable than the imine formed by reaction with aldehydes. At pH 7.6, NHS esters that do not react with amine groups undergo hydrolysis to reform –COOH groups and avoid possible covalent capture of other proteins during digestion with trypsin-containing membranes. To limit trypsin self-digestion during immobilization, we add benzamidine as a competitive inhibitor.[36,37] The benzamidine may also minimize the formation of covalent bonds with amino acids near the active site of trypsin and stabilize the protein tertiary structure.

In principle, hydrolysis of active esters during covalent trypsin anchoring could lead to some immobilization through electrostatic interactions with –COO⁻ groups.[37,39] However, washing of trypsin-modified membranes with buffers containing as much as 1 M NaCl led to no detectable effluent absorbance at 280 nm, demonstrating minimal protein elution under conditions that should disrupt electrostatic interactions. In contrast, trypsin electrostatically adsorbed to PAA (no NHS/EDC activation) or PSS elutes from nylon membranes in 1 M NaCl due to disruption of electrostatic interactions (more than 90% of the trypsin eluted, based on the eluate UV-vis absorbance at 280 nm). These data imply that trypsin capture after EDC/NHC activation occurs via covalent bonds.

Using the decrease in trypsin concentration (determined from the absorbance at 280 nm) in loading solutions circulated through the membrane, we estimated the amount of trypsin immobilized in membranes with different pore sizes. For electrostatic immobilization to PSS the trypsin binding capacity increases from 6 ± 1 to 11 ± 1 mg per mL of membrane when decreasing the nominal membrane pore size from 5 to 1.2 μm, presumably because membranes with a smaller pore size have higher internal surface areas.[30] SEM images of membranes after

trypsin immobilization (Figure 4.1) confirm the differences in pore sizes. The activated PAA

primer layer in membranes with 1.2 µm pores captures 35 ± 2 mg of trypsin per mL of membrane.

Thus, covalent immobilization gives 3-fold more immobilized trypsin than electrostatic capture

in these membranes.
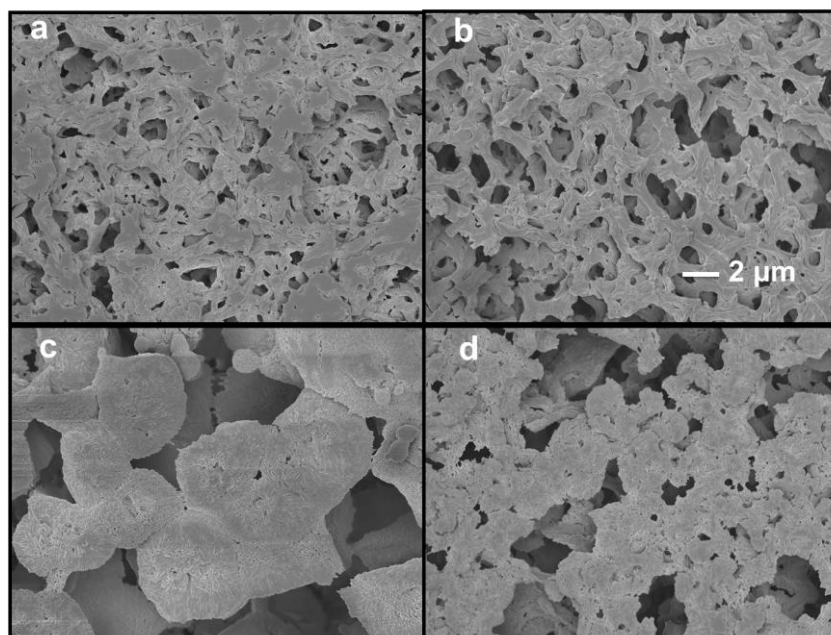
Figure 4.1. SEM images (a-c) of membranes modified with trypsin using electrostatic

adsorption.   Nominal pore sizes prior to modification were (a) 0.45 µm, (b) 1.2 µm, and (c)

5.0 µm.   Image (d) shows a 1.2 µm membrane with covalently immobilized trypsin. The scale

bar is the same for all SEM images.

The higher trypsin binding with covalent rather than electrostatic immobilization may have

two origins. First, the membrane may adsorb more of the weakly acidic PAA than the strongly

acidic PSS. (At its adsorption pH of 3, PAA has a low charge density and thus will be less

extended than the highly charged PSS.[40]) Additionally, the electrostatic trypsin adsorption to

PSS occurs at a lower pH than the covalent adsorption to PAA. At lower pH trypsin will carry

more positive charge, so protein-protein electrostatic repulsion may limit trypsin adsorption.

Nevertheless, SEM images of 1.2 μm membranes after covalent and electrostatic trypsin immobilization are similar because the trypsin does not fill the membrane pores (compare Figures 4.1 (b) and 4.1 (d)). We tried to covalently immobilize trypsin in a membrane with 0.45 μm pores, but the membrane became brittle after adsorption of PAA and further NHS/EDC activation.

4.3.2 Proteolytic activity of trypsin membranes

To examine the effect of immobilization on trypsin activity, we spectrophotometrically monitored the cleavage of the ester group of N_a-benzoyl-L-arginine ethyl ester (BAEE) after passage through membranes (1.2 μm pore sizes) containing covalently and electrostatically immobilized trypsin.[29,37] The absorbance (253 nm) due to the digestion product, N_a-benzoyl-L-arginine (BA), is proportional to the amount of ester cleavage.[41] Trypsin activity typically follows Michaelis-Menten kinetics, where equation (4.1) describes the reaction rate, V,

$$V = -\frac{d[S]}{dt} = V_{max}\frac{[S]}{[s]+K_M} \tag{4.1}$$

in terms of the rate when the enzyme is saturated with substrate, V_{max}, the substrate concentration, $[S]$, and the Michaelis constant, K_m.

Usually a plot of $\frac{1}{V}$ versus $\frac{1}{[S]}$ yields values for V_{max} and K_m. However, for the membrane reactor, the value of $[S]$ varies significantly from the feed to the permeate side of the membrane. At low BAEE feed concentrations, the high trypsin loading in the pores leads to essentially complete BAEE cleavage. Thus, we employ equation (4.2), the integrated Michaelis-Menten equation, to determine kinetic parameters. In this expression

$$t = \frac{K_M}{V_{max}}ln\left(\frac{[S]_0}{[S]}\right) + \frac{[S]_0-[S]}{V_{max}} \tag{4.2}$$

t is the digestion time and $[S]_0$ is the initial substrate concentration. Specifically, for the case

where the membrane behaves as a plug-flow reactor, t is the residence time, t_{res}, of solution in the membrane, $[S]_0$ is the substrate concentration in the feed, and $[S]$ is the substrate concentration in the membrane permeate.   We use equation (4.3) to calculate the residence

$$t_{res} = \frac{Al}{Q\varepsilon} \tag{4.3}$$

time, assuming a porosity, ε, of 0.5; a membrane thickness, l, of 110 μm; and a membrane area, A, of 3.1 cm^2. Variation of the volumetric flow rate, Q, using a syringe pump affords different residence times.

Figure 4.2 shows a plot of t_{res} versus the concentration, $[S]$, of BAEE exiting the membrane. The plot is essentially linear because the $\frac{K_M}{V_{max}} ln\left(\frac{[S]_0}{[S]}\right)$ term is negligible compared to $\frac{[S]_0-[S]}{V_{max}}$, which is consistent with the typical K_M of 0.05 mM[42] for trypsin in solution as well as the small value of $ln\left(\frac{[S]_0}{[S]}\right)$ compared to $[S]_0 - [S]$. Thus, to obtain V_{max}, we employed equation (4.4).

$$t_{res} \cong \frac{[S]_0-[S]}{V_{max}} \tag{4.4}$$

Fitting of the data in Figure 4.2 with equation (4.4) yields V_{max} values of 0.6 ± 0.2 and 1.0 ± 0.3 mM/s for membranes with covalently and electrostatically immobilized trypsin, respectively. We also determined kinetic parameters using in-solution digestion and the same fitting method (see Figure 4.3) and obtained $V_{max} = 0.0027 \pm 0.0001$ mM/s. Thus, the membranes show V_{max} values that are two orders of magnitude higher than V_{max} in solution, and digestion occurs much faster in membranes than in solution because of the high density of enzyme in the membrane. However, after dividing V_{max} by the enzyme "concentration" in membrane pores or solution (3.0 mM for covalently immobilized trypsin, 0.47 mM for electrostatically immobilized enzyme, and 1.4×10^{-4} mM for in-solution digestion), the

normalized values of V_{max} (or the rate constant, k_{cat}, for reaction of the enzyme-substrate complex) become 0.20, 2.1, and 19 s^{-1} for covalently immobilized, electrostatically immobilized, and dissolved enzyme, respectively. The in-solution k_{cat} is similar to literature values[42] and one or two orders of magnitude greater than k_{cat} values for the electrostatically and covalently immobilized trypsin, respectively. Thus, immobilization decreases trypsin activity, and covalent immobilization reduces the trypsin activity more than electrostatic adsorption. Unfortunately, we could not determine K_M with this method, but we expect immobilization to interfere with the binding of trypsin to the substrate so K_M for immobilized trypsin should be higher than K_M for free trypsin.[42,43]
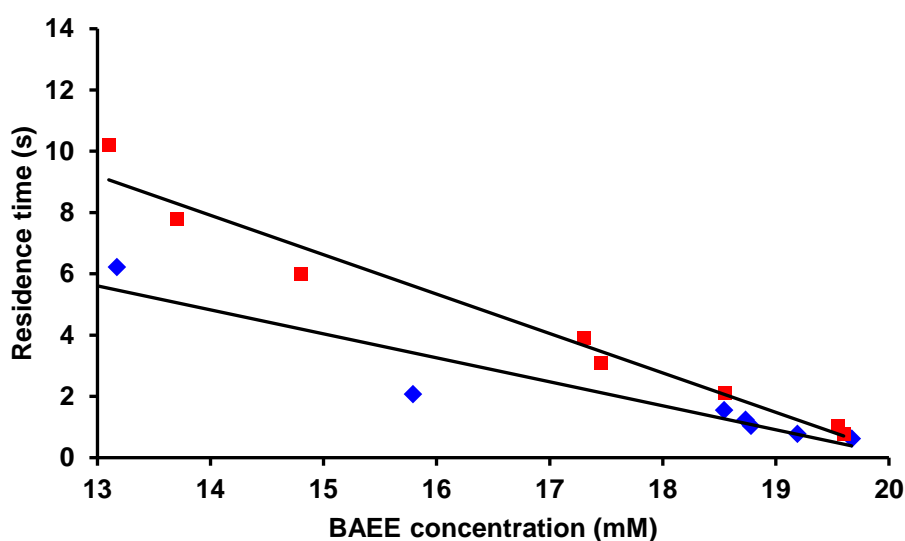
Figure 4.2. Residence time as a function of the permeate BAEE concentration during passage of 20 mM BAEE through a 1.2 μm membrane containing electrostatically (blue diamonds) or covalent immobilized trypsin (red squares). Experiments with two other replicate membranes showed similar results.
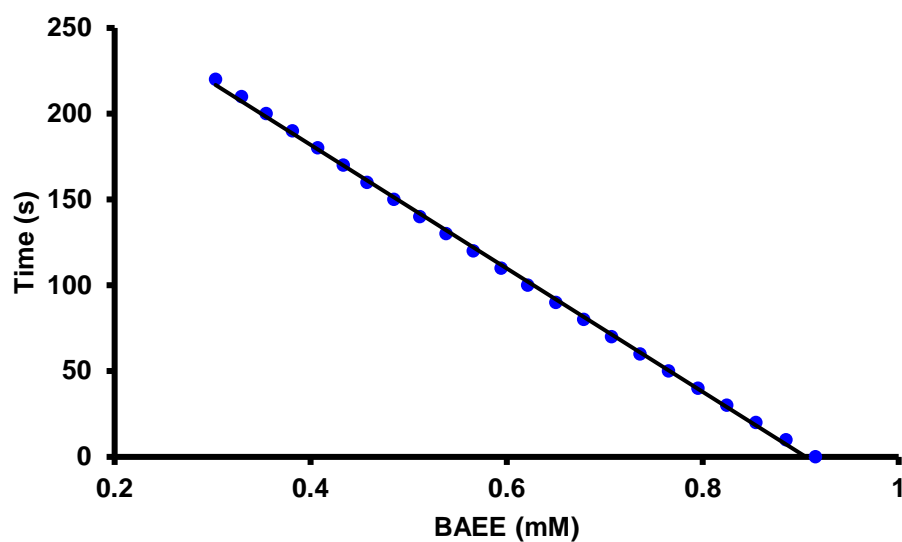
Figure 4.3. In-solution digestion time as a function of the evolving (declining) BAEE concentration. The initial BAEE concentration in the solution was 1 mM, but this value declined during the brief (5 s) mixing period. The curve is the fit to the data using the equation 5.4. Replicate experiments showed a similar trend.

4.3.3 Effect of pore size on in-membrane digestion of a labile protein (electrostatic trypsin immobilization)

No.	AA
1	100-105
2	170-176
3	177-183
4	98-105
5	106-113
6	170-183
7	184-209
8	177-209
9	170-202
10	170-209
11	114-169
12	108-169
13	106-169
14	33-99
15	30-97
16	29-97
17	30-99
18	100-169
19	29-99
20	114-183
21	26-97
22	33-105
23	26-99
24	30-105
25	108-209
26	100-209
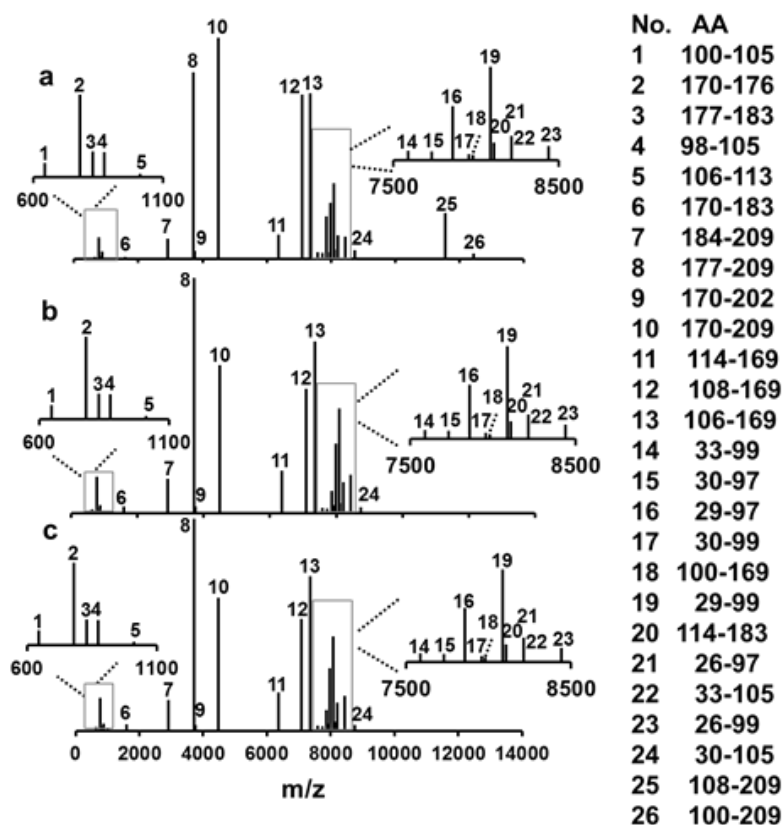
Figure 4.4. Manually deconvoluted ESI-MS spectra of β-casein digested in trypsin-containing (electrostatic adsorption) membranes with (a) 5.0 µm (b) 1.2 µm and (c) 0.45 µm pores. Digestion occurred at a flow rate of 120 mL/h (residence time of 3.3 ms), and signals above 1% of the highest signal were assigned to specific peptides by comparison to theoretical m/z values. The normalized intensities are the sum of signal intensities for all detected charge states of a given peptide, and the spectra show the peptides only at the +1 charge state for the monoisotopic mass. The table lists amino acid sequences corresponding to the numbered peptides.

Using a short (3.3 ms) residence time, we digested the labile protein β-casein in trypsin-containing (electrostatic adsorption) membranes with 5.0 µm, 1.2 µm and 0.45 µm pores. In

this case, digestion in all three membranes generates some detectable peptides with masses of ~8 kDa (see Figure 4.4). However, digestion in 5.0 μm pores yields signals for two peptides with masses of ~12 kDa (amino acids 108-209 and 100-209). Thus, the larger pore size leads to more missed cleavages in some cases. However, besides these two large peptides, the rest of the peptides are similar for digestion with the different membranes. Additionally, gel electrophoresis showed no detectable protein bands (over 10 kDa) after digestion with any of the membranes. Thus, with electrostatic trypsin immobilization, membrane reactors with large pores can generate large peptides when using a residence times of 3.3 ms, but to a limited extent for labile proteins.

4.3.4 Covalent trypsin immobilization enables controlled digestion of labile proteins
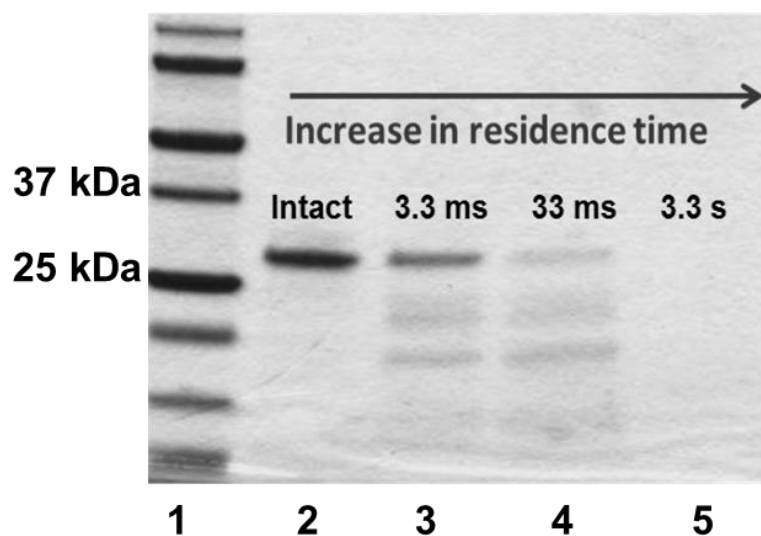
Figure 4.5. SDS-PAGE (Coomassie stain) analysis of intact β-casein (lane 2) and digests of β-casein obtained using different residence times in a 1.2 μm membrane containing covalently immobilized trypsin (lanes 3-5). Lanes 2-5 were loaded with 5 μg of protein or protein digest, and lane 1 shows a protein ladder. Digestion occurred using 0.1mg/mL β-casein in 10 mM NH₄HCO₃.

The BAEE digestion studies described above suggest that covalent immobilization of trypsin in pores reduces the enzyme activity relative to electrostatic adsorption, so membranes containing covalently anchored trypsin may better enable limited digestion of highly labile proteins. Figure 4.5 shows the SDS-PAGE analysis of β-casein digestion products obtained at flow rates of 120, 12 and 0.12 mL/h through a membrane containing covalently immobilized trypsin. These flow rates correspond to residence times of 3.3 ms, 33 ms and 3.3 s, respectively. The gel shows a clear trend toward increased protein digestion at longer residence times. The 3.3 ms residence time yields a significant amount of intact protein along with several proteolytic peptides with masses between 10 and 25 kDa, whereas a 3.3 s residence time leads to no visible large peptides, indicating essentially complete digestion into peptides with masses <10 kDa. The intermediate residence time of 33 ms gives minimal intact protein along with peptides with masses between 10 and 25 kDa.

No.	AA
1	170-176
2	177-183
3	170-183
4	184-209
5	1-29
6	177-209
7	170-202
8	170-209
9	114-169
10	108-169
11	106-169
12	100-169
13	29-105
14	108-209
15	106-209
16	100-209
17	1-107
18	100-105
19	203-209
20	105-113
21	98-105
22	100-107
23	106-113
24	184-202
25	29-88
26	29-97
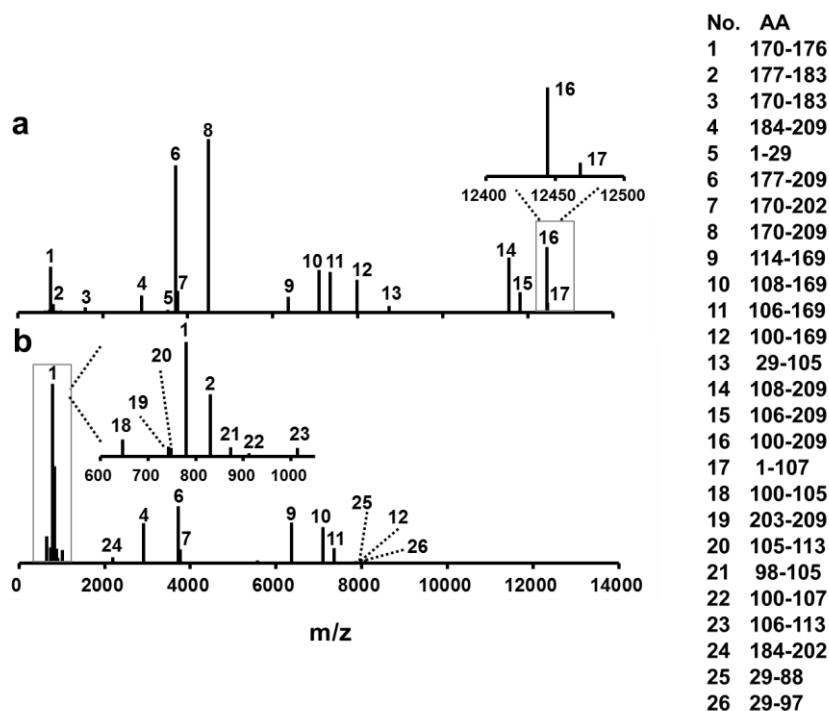
Figure 4.6. Manually deconvoluted ESI mass spectra of β-casein digested in membranes containing covalently immobilized trypsin (pore size: 1.2 µm). The flow rates through the membrane were 12 mL/h (a) and 0.12 mL/h (b) to give residence times of 33 ms and 3.3 s, respectively. Signals above 1% of the highest signal were assigned to specific peptides by comparison to theoretical m/z values. The normalized intensities are the sum of signal intensities for all detected charge states of a given peptide, and the spectra show the peptides only at the +1 charge state for the monoisotopic mass. The table show the amino acid sequences in the identified peptides.

Figure 4.6 compares the deconvoluted ESI-orbitrap mass spectra for β-casein digested with 33 ms and 3.3 s residence times. For the 33 ms digestion (Figure 4.4 (a)), as few as two peptides (i.e. 14 and 17) can cover the entire 209 amino acids in the sequence. In contrast, at the long residence time (3.3 s, Figure 4.7 (b)), all detected peptides have masses less than 8 kDa, which is consistent with the gel electrophoresis (Figure 4.5, lane 5). The long residence times also

lead to relatively high intensities of peptides with masses less than 1000. More missed cleavage occurs at short residence times to decrease the intensities of small peptides. For example, with the 33 ms residence time the strong signal for peptide 8 (170-209) appears while signals for peptides 1 (170-176), 2 (177-183), and 4 (184-209) decrease significantly compared to the MS spectrum of β-casein digested with a 3.3-s residence time. The sequence coverage is also higher for the 33-ms (100%) than the 3.3 ms (86%) residence time.

Comparison of Figures 4.4 and 4.6 shows that changing the immobilization method limits trypsin activity more than variation of pore size and provides better control of digestion of a labile protein. Although V_{max} is similar for BAEE in membranes with covalently and electrostatically immobilized trypsin, β-casein digestion is very different for the two systems. The relatively large protein (compared to BAEE) likely has less access to immobilized enzyme, particularly for the covalent immobilization. Covalent immobilization gives a much higher enzyme loading than electrostatic adsorption, which probably leads to a smaller percentage of protein-accessible enzymes in addition to a lower activity per enzyme.

We also digested urea-denatured BSA in membranes containing covalently immobilized trypsin to examine whether we could control the extent of digestion with a denatured protein. Because of the high urea concentration, we didn't analyze the BSA digests with mass spectrometry. But the SDS-PAGE analysis in Figure 4.7 confirms that the extent of digestion of denatured BSA increases with decreasing flow rate, which corresponds to increasing residence time.
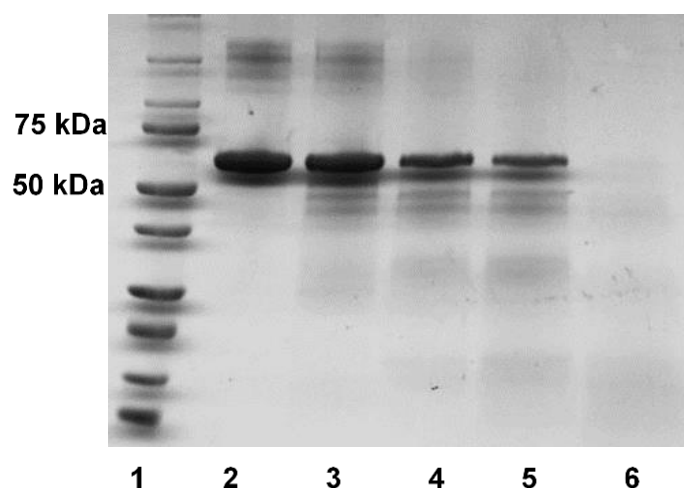
Figure 4.7. SDS-PAGE (Coomassie stain) analysis of native BSA (lane 2) and denatured (6 M urea) BSA before (lane 3) and after digestion in membranes containing covalently immobilized trypsin. Digestion occurred using flow in-membrane residence times of 0.066 s (lane 4), 1.3 s (lane 5), and 6.6 s (lane 6).   The residence times correspond to flow rates of 6, 0.3, and 0.06 mL/h.

4.3.5 Limited proteolysis for the study of native protein structure

In addition to providing high sequence coverage, limited digestion is an attractive tool for locating accessible and flexible regions in a protein.[44] Conventional limited digestion for such studies occurs in solution over minutes to hours and requires partially digested proteins that are relatively stable. Short-time (msec) limited digestion in membranes may overcome issues with the stability of partially digested protein and more reproducibly effect partial digestion.

We first studied apomyoglobin and holomyoglobin as a model system to locate readily digestible sites through limited in-membrane digestion. Myoglobin is a globular protein with eight α-helices.[45] Consistent with prior studies of digestion in solution,[45,46] MS analysis of holomyoglobin passed through trypsin-containing membranes (1.2 μm membranes, electrostatically immobilized trypsin, residence time of 3.3 s) detected only intact protein.

119

Holomyoglobin has a globular structure that resists digestion.
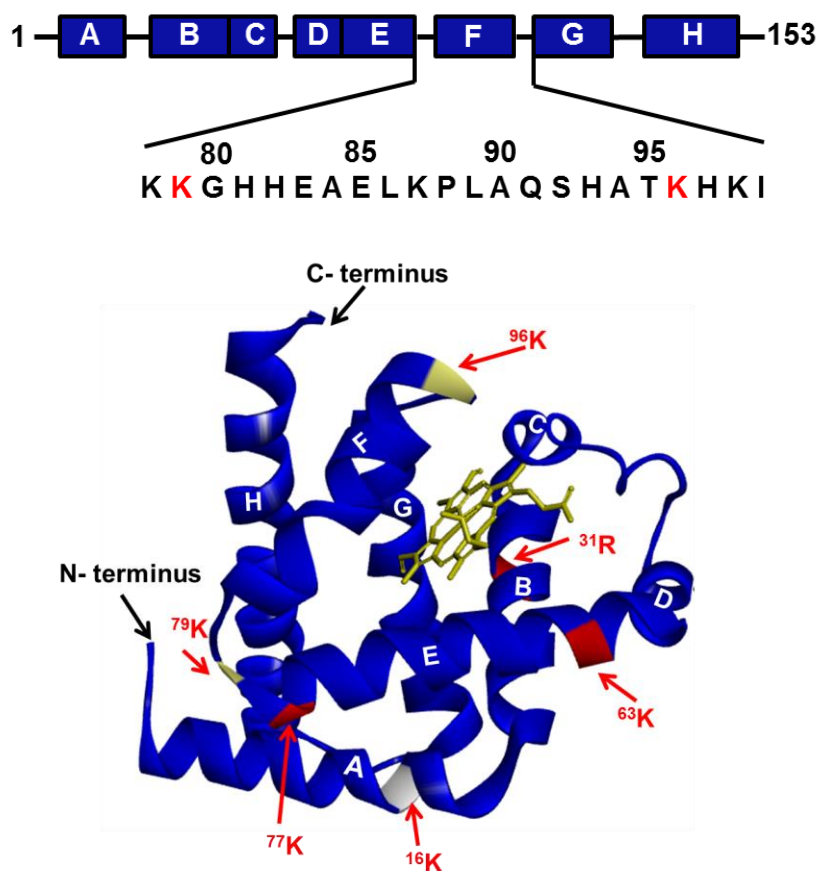
Figure 4.8. 3D structure of myoglobin (1YMB) drawn using Discovery Studio 4.0 Client software.[47]

NMR data suggest that upon dissociation of heme to create apomyoglobin, helix F (amino acids 82-97) and the carboxy terminus of helix H become less ordered while the remainder of the protein retains its structure. Consistent with such a local change in the protein structure, in-membrane digestion of apomyoglobin (1.2 μm membrane, residence time of 33 ms) generated two large peptides: amino acids 1-79 and 80-153 for electrostatically immobilized trypsin and amino acids 1-96 and 97-153 for covalently anchored (original spectra in Figure 4.8 and manually deconvoluted spectra in Figure 4.9). The initial ^{79}K and ^{96}K digestion sites are at both ends of the disordered helix F. The different initial cleavage sites (^{79}K versus) ^{96}K for digestion

in membranes with electrostatically and covalently immobilized trypsin suggest that the immobilization method affects trypsin's access to substrates. The largest peptide signals in Figure 4.9 also indicate cleavage after other amino acids such as [31]R, [63]K and [77]K, (peptides 1-31 and 64-77), but such cleavage could occur after the initial cleavage at [79]K or [96]K. Cleavage after [31]R is consistent with small structural changes in helix B after loss of heme.[45,46] Unfortunately, other small peptides also appear (Figure 4.9), but we suspect these are secondary digestion sites after the initial proteolysis .
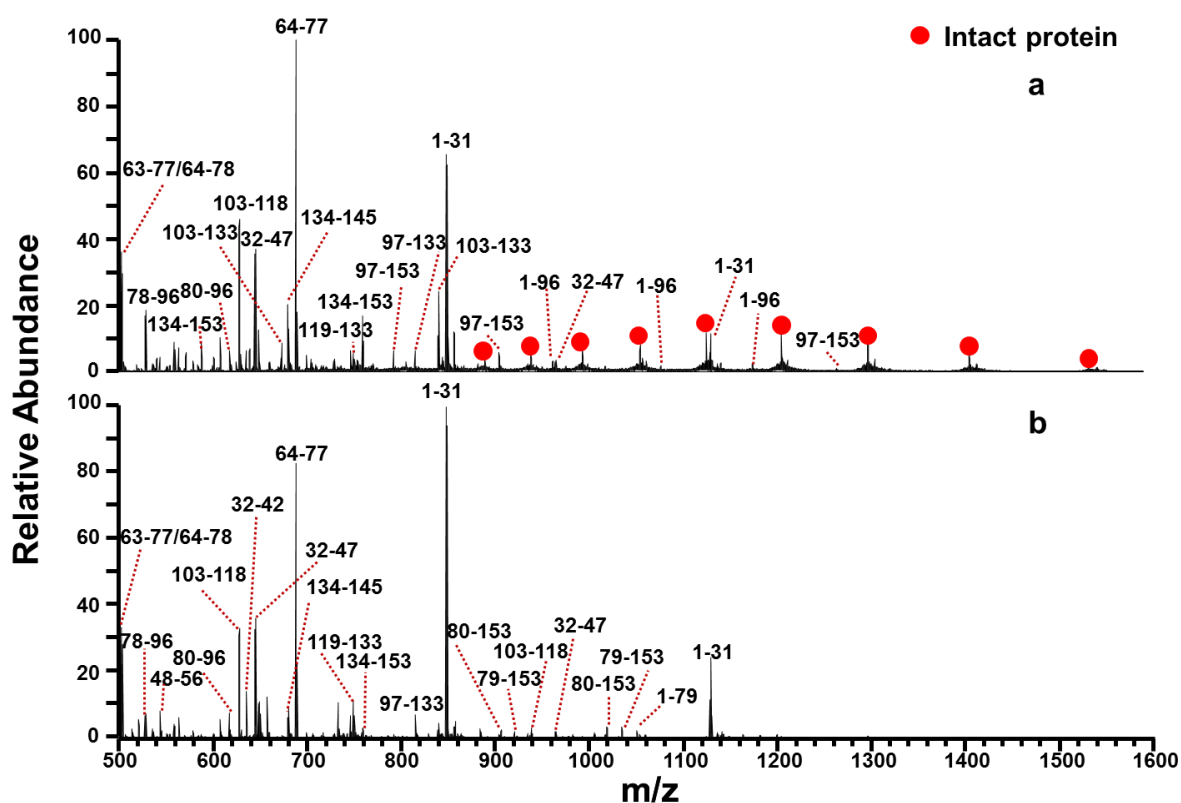
Figure 4.9. ESI-Orbitrap mass spectra of apomyoglobin digested in membranes containing (a) covalently immobilized trypsin and (b) electrostatically immobilized trypsin. The flow rate through the membranes was 12 mL/h (residence time around 33 ms).
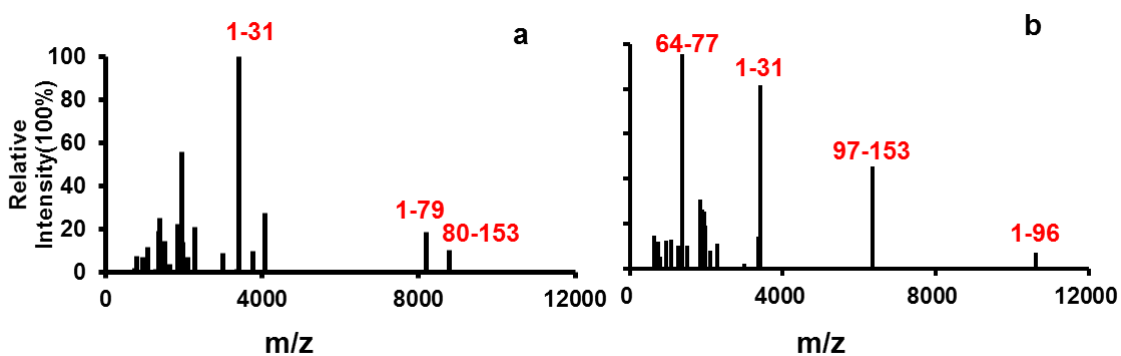
Figure 4.10. Manually deconvoluted ESI-orbitrap mass spectra of apomyoglobin digested in membranes containing (a) electrostatically anchored trypsin and (b) covalently immobilized trypsin. Figure 4.8 shows the original spectra.

We also examined limited apomyoglobin digestion in solution for 15 and 30 min (original spectra in Figure 4.11, manually deconvoluted spectra in Figure 4.12). Under these conditions, signals from intact apomyoglobin dominate the mass spectra, so shorter digestion times are not applicable to generate limited digestion for structural information. A peptide with amino acids 1-16 (cleavage at ^{16}K) only appears after in-solution digestion. The ^{16}K residue resides in helix A, and rapid in-membrane digestion apparently does not significantly cleave the protein after this amino acid. Among the 18 lysine and 2 arginine residues in apomyoglobin, we did not detect any peptides indicative of cleavage at ^{45}K, ^{50}K and ^{98}K for either in-solution or in-membrane digestion. We probably did not identify cleavage after these amino acids because cleavage at both ^{42}K and ^{45}K, ^{47}K and ^{50}K, and ^{96}K and ^{98}K would generate peptides 43-45, 48-50 and 97-98, which have m/z values below the limit we specified. Overall, compared to in-membrane digestion, limited in-solution proteolysis gives one more cleavage site despite strong signals from intact protein. These data suggest that in-membrane digestion is more appropriate for limiting digestion and identifying the most labile digestion sites.
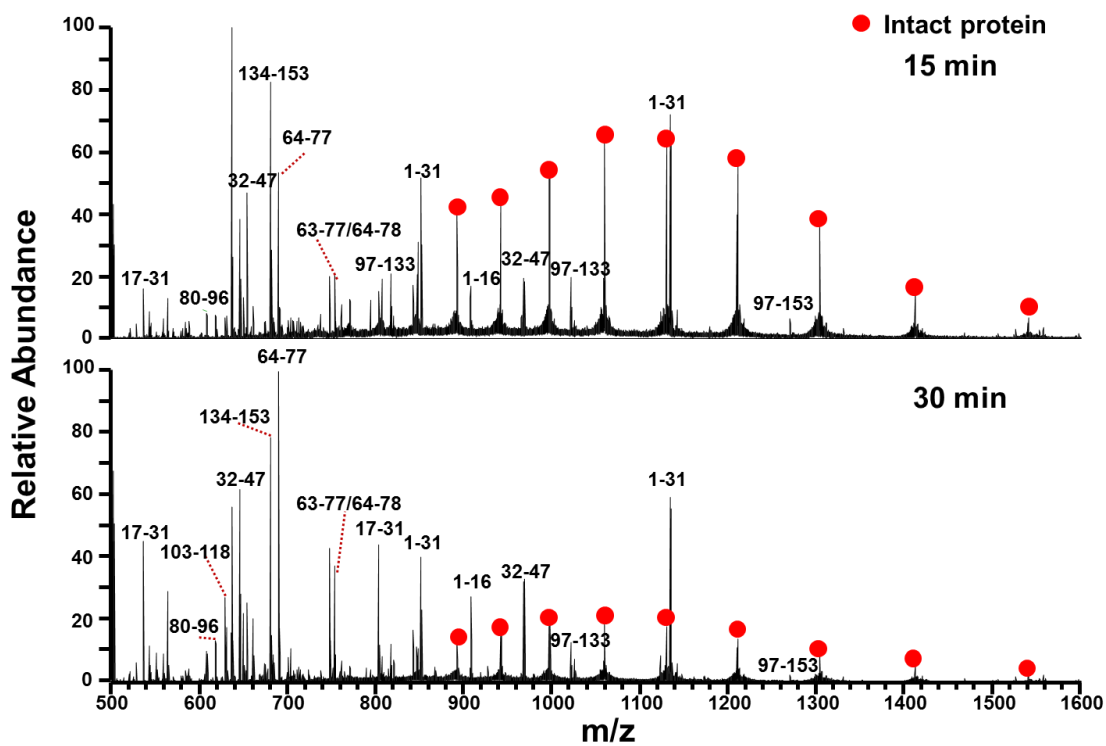
Figure 4.11. ESI-Orbitrap mass spectra of apomyoglobin digested in solution for 15 min or 30 min with a trypsin to apomyoglobin ration as 1:20. Intense intact apomyoglobin peaks appear with both digests.
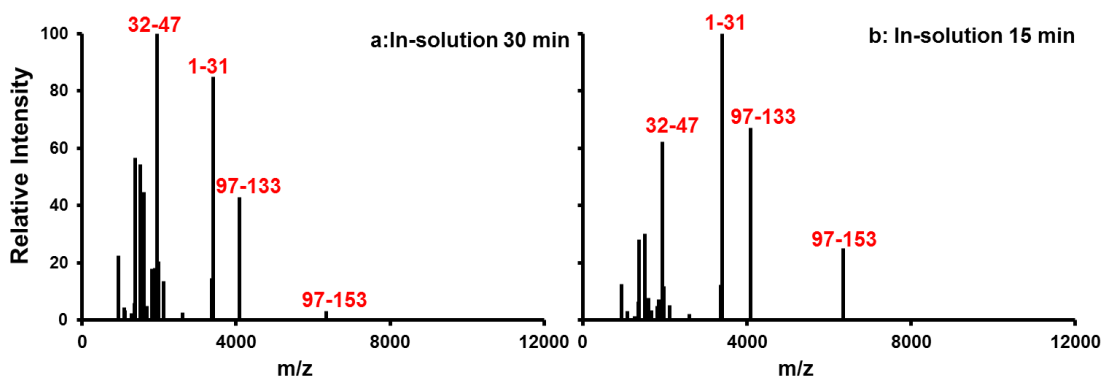
Figure 4.12. Manually deconvoluted mass spectra of in-solution trypsin digestion of apomyoglobin for (a) 30 min and (b) 15 min with trypsin to protein ratio as 1:20. The signal for the intact protein would appear at a higher m/z value.

Cytochrome c, which contains a covalently linked heme,[48,49] is another protein that resists digestion. A membrane (1.2 μm pores) with covalently immobilized trypsin did not digest cytochrome c in a residence time of 33 ms, whereas under the same conditions a membrane containing electrostatically immobilized trypsin generated two peptides 1-79 and 80-104 that cover the whole protein sequence. Figure 4.13 shows the deconvoluted spectrum of in-membrane digested cytochrome c and suggests that amino acid ^{79}K is the most accessible cleavage site. Based on the cytochrome c crystal structure (Figure 4.14), ^{79}K lies in a flexible region (amino acids 75-88) between two helices. Other cleavage sites in this flexible region include ^{86}K, ^{87}K, ^{88}K, but we only identified peptide 80-86. The absence of peptides 80-87 and 80-88 could result from rapid cleavage of terminal lysine residues from these peptides. Meanwhile, the digestion can also occur after ^{39}K and ^{53}K, as we observed peptides 1-39 and 1-53. These peptides could result from further digestion of peptide 1-79, especially for ^{53}K, which resides within a helix in the crystal structure. Overall, cyctochrome c resists trypsin proteolysis more than apomyoglobin and yields fewer small peptides (compare Figure 4.10 and Figure 4.13). The identification of dominant cleavage sites in both apomyoglobin and cytochrome c suggests that in-membrane digestion can enhance identification of disordered protein regions and possible changes in structure.
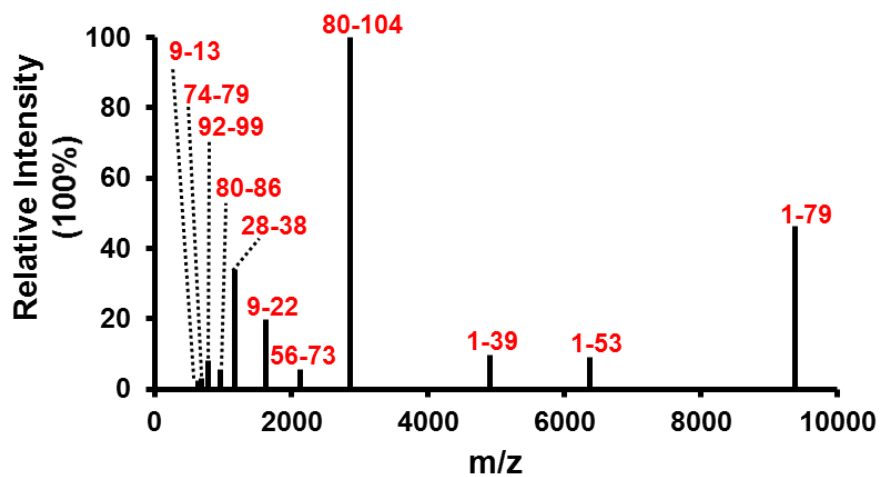
Figure 4.13. Manually deconvoluted ESI-Orbitrap mass spectrum of cytochrome c digested in a membrane containing electrostatically immobilized trypsin. The membrane pore size was 1.2 μm, and the residence time was 33 ms.
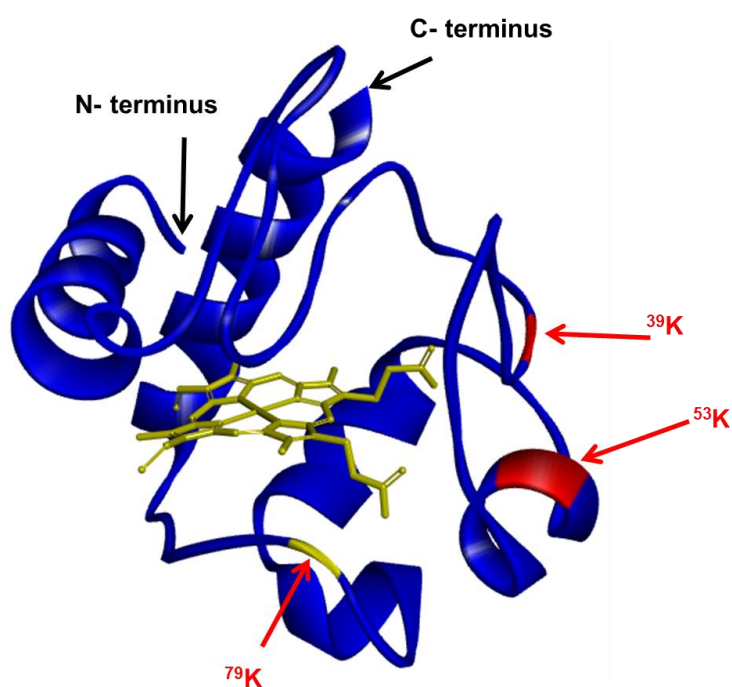
Figure 4.14. 3D structure of cytochrome c (2B4Z) drawn using Discovery Studio 4.0 Client software.[47]

4.4 Conclusion

Rapid passage of protein solutions through enzyme-containing membranes results in limited digestion to peptides containing missed cleavage sites. The extent of digestion decreases for membranes with larger pores, and covalently anchored trypsin is less active than electrostatically immobilized trypsin. For highly labile proteins such as β-casein, controlled digestion is more effective with the less active, covalently immobilized trypsin. In contrast, for proteins such as cytochrome c, even limited digestion requires the electrostatically immobilized enzyme. Limited digestion of cytochrome c suggests that the most accessible cleavage site is ^{79}K, which is consistent with the location of this residue in a flexible, non-helix region. Digestion of apomyoglobin yields a more complicated mass spectrum, but still suggest that peptides ^{79}K or ^{96}K are highly accessible tryptic sites. Short-time in-solution digestion leads to more abundant small peptides, despite significant intact protein remaining in the digest. Thus, in-membrane digestion will likely prove superior to in-solution digestion for mapping accessible and flexible sites in proteins.

REFERENCES

REFERENCES

(1) Pastwa, E.; Somiari, S. B.; Czyz, M.; Somiari, R. I., Proteomics in Human Cancer Research, *Proteom. Clin. Appl.* **2007**, *1*, 4-17.

(2) Um, J. W.; Nygaard, H. B.; Heiss, J. K.; Kostylev, M. A.; Stagi, M.; Vortmeyer, A.; Wisniewski, T.; Gunther, E. C.; Strittmatter, S. M., Alzheimer Amyloid-Beta Oligomer Bound to Postsynaptic Prion Protein Activates Fyn to Impair Neurons, *Nat. Neurosci.* **2012**, *15*, 1227-U1285.

(3) Yates, J. R.; Ruse, C. I.; Nakorchevsky, A. *Annu. Rev. Biomed. Eng.* **2009**; *11*, 49-79.

(4) Xian, F.; Hendrickson, C. L.; Marshall, A. G., High Resolution Mass Spectrometry, *Anal. Chem.* **2012**, *84*, 708-719.

(5) McLafferty, F. W.; Breuker, K.; Jin, M.; Han, X. M.; Infusini, G.; Jiang, H.; Kong, X. L.; Begley, T. P., Top-Down MS, A Powerful Complement to the High Capabilities of Proteolysis Proteomics, *Febs J.* **2007**, *274*, 6256-6268.

(6) Kelleher, N. L.; Lin, H. Y.; Valaskovic, G. A.; Aaserud, D. J.; Fridriksson, E. K.; McLafferty, F. W., Top Down Versus Bottom Up Protein Characterization by Tandem High-Resolution Mass Spectrometry, *J. Am. Chem. Soc.* **1999**, *121*, 806-812.

(7) Han, X. M.; Aslanian, A.; Yates, J. R., Mass Spectrometry for Proteomics, *Curr. Opin. Chem. Biol.* **2008**, *12*, 483-490.

(8) Somiari, R. I.; Renganathan, K.; Russell, S.; Wolfe, S.; Mayko, F.; Somiari, S. B., A Colorimetric Method for Monitoring Tryptic Digestion Prior to Shotgun Proteomics, *Int. J. Proteomics* **2014**, *2014*, 125482-125482.

(9) Tan, Y. J.; Wang, W. H.; Zheng, Y.; Dong, J. L.; Stefano, G.; Brandizzi, F.; Garavito, R. M.; Reid, G. E.; Bruening, M. L., Limited Proteolysis via Millisecond Digestions in Protease-Modified Membranes, *Anal. Chem.* **2012**, *84*, 8357-8363.

(10) Appel, W., Chymotrypsin - Molecular and Catalytic Properties, *Clinical Biochemistry* **1986**, *19*, 317-322.

(11) Lee, T. D.; Shively, J. E., Enzymatic and Chemical Digestion of Proteins for Mass-Spectrometry, *Method Enzymol.* **1990**, *193*, 361-374.

(12) Raijmakers, R.; Neerincx, P.; Mohammed, S.; Heck, A. J. R., Cleavage Specificities of the Brother and Sister Proteases Lys-C and Lys-N, *Chem. Commun.* **2010**, *46*, 8827-8829.

(13) Drapeau, G. R., Substrate-Specificity of A Proteolytic-Enzyme Isolated from A Mutant of Pseudomonas-Fragi, *J. Biol. Chem.* **1980**, *255*, 839-840.

(14) Olsen, J. V.; Ong, S. E.; Mann, M., Trypsin Cleaves Exclusively C-Terminal to Arginine and Lysine Residues, *Mol. Cell. Proteomics* **2004**, *3*, 608-614.

(15) Ma, J.; Hou, C.; Sun, L.; Tao, D.; Zhang, Y.; Shan, Y.; Liang, Z.; Zhang, L.; Yang, L.; Zhang, Y., Coupling Formic Acid Assisted Solubilization and Online Immobilized Pepsin Digestion with Strong Cation Exchange and Microflow Reversed-Phase Liquid Chromatography with Electrospray Ionization Tandem Mass Spectrometry for Integral Membrane Proteome Analysis, *Anal. Chem.* **2010**, *82*, 9622-9625.

(16) Ma, J. F.; Zhang, L. H.; Liang, Z.; Shan, Y. C.; Zhang, Y. K., Immobilized Enzyme Reactors in Proteomics, *Trac-Trends Anal. Chem.* **2011**, *30*, 691-702.

(17) Kim, J.; Kim, B. C.; Lopez-Ferrer, D.; Petritis, K.; Smith, R. D., Nanobiocatalysis for Protein Digestion in Proteomic Analysis, *Proteomics* **2010**, *10*, 687-699.

(18)SHIMADZU, Perfinity iDP (Integrated Protein Digestion HPLC), http://www.shimadzu.com/an/hplc/perfinity/perfinity-2.html, 08/06/2016.

(19)Promega, Immobilized Trypsin, https://www.promega.com/products/mass-spectrometry/proteases-and-surfactants/trypsin-for-protein-characterization/trypsin-reagents/immobilized-trypsin/, 08/06/2016.

(20) Xu, F.; Wang, W. H.; Tan, Y. J.; Bruening, M. L., Facile Trypsin Immobilization in Polymeric Membranes for Rapid, Efficient Protein Digestion, *Anal. Chem.* **2010**, *82*, 10045-10051.

(21) Xu, G. B.; Chen, X. Y.; Hu, J. H.; Yang, P. Y.; Yang, D.; Wei, L. M., Immobilization of Trypsin on Graphene Oxide for Microwave-Assisted on-Plate Proteolysis Combined with MALDI-MS Analysis, *Analyst* **2012**, *137*, 2757-2761.

(22) Zhang, S.; Yuan, H. M.; Zhao, B. F.; Zhou, Y.; Jiang, H.; Zhang, L. H.; Liang, Z.; Zhang, Y. K., Integrated Platform with A Combination of Online digestion and O-18 Labeling for Proteome Quantification via An Immobilized Trypsin Microreactor, *Analyst* **2015**, *140*, 5227-5234.

(23) Yamada, K.; Nakasone, T.; Nagano, R.; Hirata, M., Retention and Reusability of Trypsin Activity by Covalent Immobilization onto Grafted Polyethylene Plates, *J. Appl. Polym. Sci.* **2003**, *89*, 3574-3581.

(24) Cooper, J. W.; Chen, J. Z.; Li, Y.; Lee, C. S., Membrane-Based Nanoscale Proteolytic Reactor Enabling Protein Digestion, Peptide Separation, and Protein Identification Using Mass

Spectrometry, *Anal. Chem.* **2003**, *75*, 1067-1074.

(25) Krenkova, J.; Lacher, N. A.; Svec, F., Highly Efficient Enzyme Reactors Containing Trypsin and Endoproteinase LysC Immobilized on Porous Polymer Monolith Coupled to MS Suitable for Analysis of Antibodies, *Anal. Chem.* **2009**, *81*, 2004-2012.

(26) Liuni, P.; Rob, T.; Wilson, D. J., A Microfluidic Reactor for Rapid, Low-Pressure Proteolysis with on-Chip Electrospray Ionization, *Rapid Commun. Mass Spectrom.* **2010**, *24*, 315-320.

(27) Bayramoglu, G.; Celikbicak, O.; Arica, M. Y.; Salih, B., Trypsin Immobilized on Magnetic Beads via Click Chemistry: Fast Proteolysis of Proteins in a Microbioreactor for MALDI-TOF-MS Peptide Analysis, *Ind. Eng. Chem. Res.* **2014**, *53*, 4554-4564.

(28) Hu, Z. Y.; Zhao, L.; Zhang, H. Y.; Zhang, Y.; Wu, R. A.; Zou, H. F., The on-Bead Digestion of Protein Corona on Nanoparticles by Trypsin Immobilized on The Magnetic Nanoparticle, *J. Chromatogr. A* **2014**, *1334*, 55-63.

(29) Dulay, M. T.; Baca, Q. J.; Zare, R. N., Enhanced Proteolytic Activity Enzymes in Photopolymerized of Covalently Bound Sol Gel, *Anal. Chem.* **2005**, *77*, 4604-4610.

(30) Ning, W. J. B., M.L. , Rapid Protein Purification and Digestion with Membrane-Containing Pipette Tips, *Anal. Chem.* **2015**, *87*, 11984-11989.

(31) Pang, Y.; Wang, W.-H.; Reid, G. E.; Hunt, D. F.; Bruening, M. L., Pepsin-Containing Membranes for Controlled Monoclonal Antibody Digestion Prior to Mass Spectrometry Analysis, *Anal. Chem.* **2015**, *87*, 10942-10949.

(32) Ahn, J.; Cao, M.-J.; Yu, Y. Q.; Engen, J. R., Accessing the Reproducibility and Specificity of Pepsin and Other Aspartic Proteases, *Biochim. Biophys. Acta, Proteins Proteomics* **2013**, *1834*, 1222-1229.

(33) Jung, K. H.; Choi, Y. C.; Chun, J. Y.; Min, S. G.; Hong, G. P., Effects of Concentration and Reaction Time of Trypsin, Pepsin, and Chymotrypsin on the Hydrolysis Efficiency of Porcine Placenta, *Korean J. Food Sci. Anim. Resour.* **2014**, *34*, 151-157.

(34) Miron, T.; Wilchek, M., A Spectrophotometric Assay for Soluble and Immobilized N-Hydroxysuccinimide Esters, *Anal. Biochem.* **1982**, *126*, 433-435.

(35) Bhattacharjee, S.; Dong, J.; Ma, Y.; Hovde, S.; Geiger, J. H.; Baker, G. L.; Bruening, M. L., Formation of High-Capacity Protein-Adsorbing Membranes through Simple Adsorption of Poly(acrylic acid)-Containing Films at Low pH, *Langmuir* **2012**, *28*, 6885-6892.

(36) Bencina, K.; Podgornik, A.; Strancar, A.; Bencina, M., Enzyme Immobilization on

Epoxy- and 1,1'-carbonyldiimidazole-Activated Methacrylate-Based Monoliths, *J. Sep. Sci.* **2004**, *27*, 811-818.

(37) Yao, C.; Qi, L.; Hu, W.; Wang, F.; Yang, G., Immobilization of Trypsin on Sub-Micron Skeletal Polymer Monolith, *Anal. Chim. Acta* **2011**, *692*, 131-137.

(38) Nicoli, R.; Rudaz, S.; Stella, C.; Veuthey, J. L., Trypsin Immobilization on An Ethylenediamine-Based Monolithic Minidisk For Rapid on-Line Peptide Mass Fingerprinting Studies, *J. Chromatogr. A* **2009**, *1216*, 2695-2699.

(39) Buch, I.; Giorgino, T.; De Fabritiis, G., Complete Reconstruction of An Enzyme-Inhibitor Binding Process by Molecular Dynamics Simulations, *Proc. Natl. Acad. Sci. USA* **2011**, *108*, 10184-10189.

(40) Choi, J.; Rubner, M. F., Influence of the Degree of Ionization on Weak Polyelectrolyte Multilayer Assembly, *Macromolecules* **2005**, *38*, 116-124.

(41) Schwert, G. W.; Takenaka, Y., A Spectrophotometric Determination of Trypsin and Chymotrypsin, *Biochim. Biophys. Acta* **1955**, *16*, 570-575.

(42) Sears, P. S.; Clark, D. S., Comparison of Soluble and Immobilized Trypsin Kinetics - Implications for Peptide-Synthesis, *Biotechnol. Bioeng.* **1993**, *42*, 118-124.

(43) Rocha, C.; Goncalves, M. P.; Teixeira, J. A., Immobilization of Trypsin on Spent Grains for Whey Protein Hydrolysis, *Process Biochem.* **2011**, *46*, 505-511.

(44) Feng, Y. H.; De Franceschi, G.; Kahraman, A.; Soste, M.; Melnik, A.; Boersema, P. J.; de Laureto, P. P.; Nikolaev, Y.; Oliveira, A. P.; Picotti, P., Global Analysis of Protein Structural Changes in Complex Proteomes, *Nat. Biotechnol.* **2014**, *32*, 1036-1044.

(45) Fontana, A.; Zambonin, M.; deLaureto, P. P.; DeFilippis, V.; Clementi, A.; Scaramella, E., Probing the Conformational State of Apomyoglobin by Limited Proteolysis, *J. Mol. Biol.* **1997**, *266*, 223-230.

(46) Fontana, A.; de Laureto, P. P.; Spolaore, B.; Frare, E.; Picotti, P.; Zambonin, M., Probing Protein Structure by Limited Proteolysis, *Acta Biochim. Pol.* **2004**, *51*, 299-321.

(47) D. S. M. E. Dassault Systèmes BIOVIA, Release 2017, San Diego: Dassault Systèmes, 2016.

(48) Mirkin, N.; Jaconcic, J.; Stojanoff, V.; Moreno, A., High Resolution X-Ray Crystallographic Structure of Bovine Heart Cytochrome C and Its Application to the Design of An Electron Transfer Biosensor, *Proteins* **2008**, *70*, 83-92.

(49) Nakashim.T; Higa, H.; Matsubar.H; Benson, A. M.; Yasunobu, K. T., Amino acid Sequence of Bovine Heart Cytochrome C, *J. Biol. Chem.* **1966**, *241*, 1166-1177.

Chapter 5. Rapid Protein Digestion and Purification with Membranes Attached to Pipette Tips

This chapter is adapted from our published paper in *Analytical Chemistry* (Ning, W., and Bruening, M. L. *Anal. Chem.* **2015**, *87* (24), 11984–11989.).

The previous chapters described the development of membranes for purification of His-tagged protein and controlled proteolysis. This chapter develops these membranes into a potential high-throughput platform by attaching them to the ends of pipette tips (Scheme 5.1). When combined with automatic pipets, this platform enables proteolysis within 30 s and protein isolation within 2 minutes.
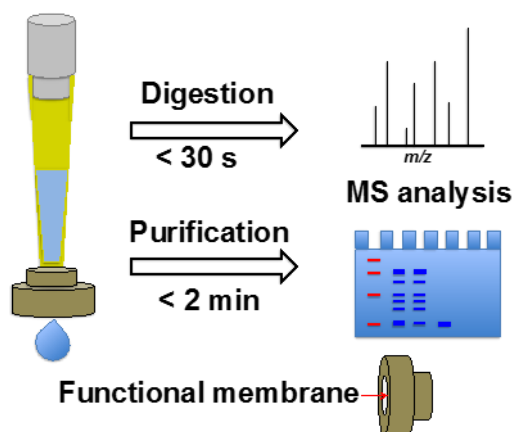
Scheme 5.1. Attaching functional membranes to the end of pipette tips for fast proteolysis and protein purification.

5.1 Introduction

Protein isolation and digestion are often vital steps in mass spectrometry (MS) studies of protein structures, interactions and posttranslational modifications.[1-4] Conventional in-solution digestion with a low protease-to-protein ratio usually takes hours, but immobilization of proteases at high concentrations on solid supports can greatly reduce digestion time.[5,6] Isolation

of specific tagged proteins from complex mixtures such as cell lysates also typically requires 30 min or more, in part because slow diffusion into affinity beads limits the rate of protein capture and elution.[7,8] Porous membranes present an attractive alternative to beads because convective flow can rapidly transport proteins or reagents to functional sites.[9,10]

Using simple layer-by-layer adsorption, the Bruening group functionalized a series of membranes for enrichment of phosphorylated peptides,[11] purification of polyhistidine-tagged (His-tagged) proteins,[12,13] and tryptic or peptic protein digestion.[14,15] As we discussed in chapters 2 and 3, purification of tagged proteins exploited a peristaltic pump and a 20-mL cell,[13] whereas proteolysis occurred using a syringe pump and a membrane with an exposed area of 0.02 cm^2 to enable digestion of low-volume solutions.[14] However, these apparatuses are impractical for high-throughput digestion or purification.

This paper describes membrane-based devices that connect directly to pipette tips to enable convenient proteolysis or protein purification that could potentially couple to robotic systems. Comparable devices employ resin-containing pipette tips.[16-19] For example, Monotip^{TM} (GL Science) and DigestTip^{TM} (ProteoGen Bio) pipette tips contain monoliths or resins for protease immobilization, and PureSpeed Affinity Resin tips (Mettler Toledo) allow purification of His-tagged protein and antibodies. Compared to resins, flow through membrane pores should enhance digestion, washing, and elution. Moreover, membrane functionalization through layer-by-layer adsorption is simple and convenient.

To interface membranes and pipettes, we employ a commercial flangeless ferrule[20] as a membrane holder that fits on the end of a 200-μL pipette tip. Using a mechanical pipette, passage of 100 μL of protein-containing solution through a functionalized membrane takes less

than 30 s, and proteolysis of myoglobin is more complete than in-solution digestion for 30 min and comparable to digestion in MonoTip^{TM} trypsin pipette tips with 20 cycles of aspiration and dispensing followed by 20 min of soaking the tip in the solution. Digestion of the monoclonal antibody Herceptin in membranes attached to pipette tips also requires less than 30 s and, thus, avoids the need for protein alkylation prior to tryptic digestion. Finally, we show that a membrane modified with Ni^{2+} complexes enables purification of His-tagged small ubiquitin modifier (His-SUMO) protein in two minutes when using pipette tips for fluid flow.

5.2 Experimental section

5.2.1 Materials

Trypsin from bovine pancreas (type I, 12200 units/mg solid), pepsin from porcine gastric mucosa, poly (acrylic acid) (PAA, average molecular weight ~100,000 Da, 35% aqueous solution), polyethylenimine (PEI, branched, $M_w = 25\ 000$ Da), poly(sodium 4-styrenesufonate) (PSS,$M_w \approx 70\ 000$ Da), N-(3-dimethylaminopropyl)-N'-ethylcarbodiimide hydrochloride (EDC), N-hydroxysuccinimide (NHS), aminobutyl nitrilotriacetate (NTA), tris(2-carboxyethyl)phosphine (TCEP), apomyoglobin (protein sequencing grade from horse skeletal muscle, salt-free lyophilized powder) and angiotensin II were purchased from Sigma-Aldrich. MonoTip^{TM} trypsin pipette tips were obtained from GL Science. His-SUMO protein was overexpressed in *BL21DE3* cells, and Herceptin (Genentech) was a gift from Dr. Mohammad Muhsin Chisti of Michigan State University. Buffers were prepared using analytical grade chemicals and deionized water (Milli-Q, 18.2 MΩ cm).

5.2.2 Membrane modifications

Nylon membranes with nominal pore sizes of 1.2 µm (Hydroxylated, LoProdyne® LP, Pall, 1.2 µm pore size) and 5.0 µm (Sterlitech, NY5025100) served as substrates for immobilization of proteases or metal-ion complexes. Electrostatic immobilization of trypsin and pepsin followed published procedures that comprise sequential adsorption of PSS and protease.[14,15] Membrane modification with PAA/PEI/PAA-NTA-Ni^{2+} films followed a literature protocol and included adsorption of PAA, PEI, and PAA followed by derivatization with aminobutyl NTA and formation of the Ni^{2+} complex.[13]
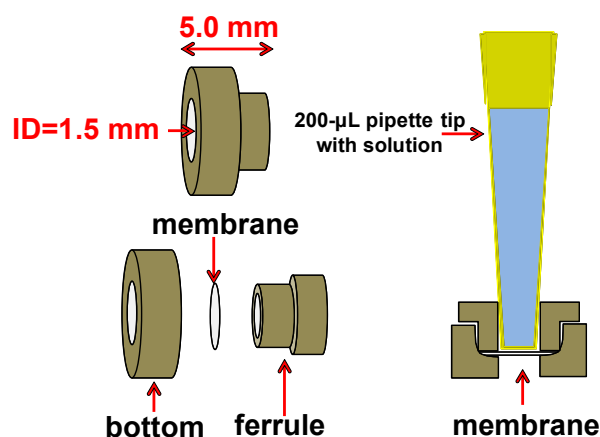
Figure 5.1. Diagram of the membrane holder and attachment of a pipette tip to the holder.

Membranes were cut to fit underneath the ferrule in a PEEK Super flangeless ferrule module (IDEX, Catalogue number: P-260) (Figure 5.1). A 200-µL pipette tip (Denville Scientific) fits into the ferrule to enable flow, and the holder exposes a membrane diameter of 1.5 mm, which is equivalent to an external surface area of 0.02 cm^2.

5.2.3 Protein digestions in protease-modified membranes, in MonoTip[TM] trypsin pipette tips and in solution

Apomyoglobin (0.1 mg/mL) was dissolved in 5% formic acid (pH 2) or 10 mM ammonium bicarbonate (pH 7) for digestion with pepsin or trypsin, respectively. Herceptin (50 µg) was dissolved in 20 µL of HCl (pH 2.5), and after adding 1 µL of TCEP (0.5 M), the mixture was incubated at 56 ºC for 30 min to reduce disulfide bonds. Finally, 479 µL of 5% formic acid or 10 mM ammonium bicarbonate was added to make the Herceptin concentration 0.1 mg/mL for pepsin and trypsin digestion, respectively. Using adjustable volume pipettes (VWR Ergonomic High-Performance), pepsin- and trypsin-modified membranes were rinsed with 100 µL of 5% formic acid (pepsin) or 10 mM ammonium bicarbonate (trypsin, pH 7) prior to passage of 100 µL of protein solution through a membrane. Samples were collected in eppendorf tubes and immediately dried with a SpeedVac.

Apomyoglobin digestion in MonoTip[TM] trypsin pipette tips was performed following the manufacturer's protocol: aspirating and dispensing 100 µL of protein solution for 20 cycles (2-3 min) using the pipette and then soaking the pipette tip in the protein solution for 20 min.[21] One cycle of aspiration and dispensing of apomyoglobin solution in the MonoTip trypsin pipette tip was also performed for comparison to digestion during a single pass of a 100-µL protein solution through a membrane.

For in-solution apomyoglobin digestion, 100 µL of 0.1 mg/mL protein in ammonium bicarbonate was mixed with 1 µL of a 0.5 mg/mL trypsin solution to initiate proteolysis with a protease to protein weight ratio of 1:20. The proteolysis was stopped at the desired time by adding 1 µL of acetic acid.

For in-membrane peptic digestion of cell lysate, 100 µg of Hela cell lysate in 20 µL of HCl (pH~2.5, 1 mM) was mixed with 1 µL of 0.5 M TCEP and heated at 56 ºC for 30 min. The lysate was diluted with 79 µL of 5% formic acid to give a protein concentration of 1 mg/mL. For in-membrane trypsin digestion, 100 µg of Hela cell lysate in 20 µL of 10 mM NH_4HCO_3 containing 6 M urea (pH~8) was mixed with 1 µL of 0.5 M TCEP. After heating at 56 ºC for 30 min, 79 µL of 10 mM NH_4HCO_3 and 1 µL of 2.5 M NaOH were added to dilute and neutralize the cell lysate and give a protein concentration of 1 mg/mL. For digestion, 100 µL of reduced, denatured Hela cell lysate solution was passed through pepsin- or trypsin-modified membranes one or three times. Solutions containing 30 µg of the Hela cell lysate or 30 µg of digested Hela cell lysate were loaded on a 4-20% gradient polyacrylamide gel.

5.2.4 Mass spectrometry and data analysis

Digests were analyzed with electrospray ionization (ESI)-MS. A protein digest reconstituted in 50 µL of MS buffer (1% acetic acid, 50% methanol and 49% water) was loaded into a Whatman multichem 96-well plate and sealed with Teflon Ultrathin Sealing Tape. The samples were introduced into the high-resolution accurate mass Thermo LTQ Orbitrap Velos mass spectrometer (San Jose, CA) using an Advion Triversa Nanomate nanoelectrospray ionization source (Advion, Ithaca, NY). The spray voltage was 1.4 kV, and the gas pressure was 1.3 psi. High-resolution mass spectra were acquired in positive ionization mode using the FT analyzer operating at 100,000 resolving power with relative intensity as the Y-axis. Peptides were identified manually by comparing the experimental data to m/z values for the theoretical peptides generated using the ProteinProspector MS-Product program (v 5.14.1 University of California, San Francisco). Peaks with relative intensities above 1% were analyzed. Settings

for the theoretical peptide generation included: tryptic digestion or peptic digestion, a maximum number of 99 missed cleavages, peptide masses from 300 to 50,000 Da, a minimum peptide length of 2 and oxidation as a variable modification. Although not appropriate for protein identification, these settings ensure that we obtain the total detected peptide coverage of the protein.

5.2.5 His-tagged protein purification from cell lysate

Lysate containing His-SUMO protein was diluted 1:9 in phosphate buffer (20 mM, pH 7.4), and 25 µL of this diluted cell lysate was passed through the membrane holder. A new tip was then used to pass 100 µL of 20 mM phosphate buffer through the holder to wash the membrane. Finally, using a third pipette tip, 25 µL of elution buffer (20 mM phosphate buffer, 0.5 M NaCl, 0.5 M imidazole, pH 7.4) was passed through the membrane to elute the bound His-SUMO protein. The whole process took about 2 minutes. Loading, effluent, and eluate (25 µL each) solutions were mixed with 5 µL of sodium dodecyl sulfate-polyacrylamide gel electrophoresis (SDS-PAGE) loading buffer and loaded on a 4-20% gradient gel.

5.3 Results and discussion

5.3.1 Membrane Selection

When choosing membranes for pipette tips, selection of an appropriate pore size is vital to minimize diffusion limitations without creating a large transmembrane pressure drop. With very small pores, the mechanical pipette is not sufficient to force solution through the membrane. Equation (1) approximately describes the pressure drop, ΔP, across a porous membrane.

$$\Delta P = \frac{8\mu LQ}{\varepsilon Ar^2} \qquad\qquad (5.1)$$

In this equation μ is dynamic viscosity ($\sim 10^{-3}$ Pa s for water); L is membrane thickness ($\sim$100 µm); Q is the volumetric flow rate through the membrane; ε is the membrane porosity ($\sim$0.5); A is the membrane surface area (0.02 cm^2); and r is the radii of membrane pores. This expression assumes cylindrical pores with a tortuosity of 1, and thus likely underestimates ΔP. Based on equation (1), passage of a 100-µL solution through a membrane in 30 s requires 430 and 7400 Pa of pressure for membranes with pore diameters of 5 and 1.2 µm, respectively. A mechanical pipette can provide these pressures, which are <0.1 atm. Notably, however, our mechanical pipette could not force solutions through a membrane (Millipore HNWP 02500) with nominal 0.45 µm pores.

The solution residence time in a membrane will determine the extent of digestion in a protease-containing membrane and whether the kinetics of protein sorption are fast enough for efficient protein isolation in an affinity membrane. Equation (2) describes the residence time, t_r, which for passage of 100 µL of solution through a 100 µm-thick membrane in 30 s is only 30 ms.

$$t_r = \frac{\varepsilon LA}{Q} \qquad\qquad (5.2)$$

Although this residence time is short, rapid mass transport in small membrane pores should allow either protein digestion or affinity capture in this period.[15,22] If needed stacking of membranes can increase residence times, but it will also increase pressure drop.

As pore size increases, the internal membrane surface area decreases, which reduces the protease-immobilization capacity. Table 5.1 lists the amounts of pepsin and trypsin adsorbed in PSS-modified nylon membranes with 5.0 µm and 1.2 µm nominal pore diameters using.

(We detected the adsorption by comparing the UV-Vis spectrum of the loading solution before and after circulating through the membrane). As expected, smaller pore diameters lead to larger protein loading. Interestingly, membranes captured more pepsin than trypsin. Both proteases were deposited in PSS-modified membranes at pH 2, but trypsin has a higher isoelectric point (~10)[23] than pepsin (2-3).[24] Thus, electrostatic adsorption at pH 2 likely requires less trypsin than pepsin to compensate the negative charges of PSS.

Table 5.1. Trypsin and pepsin-adsorption capacities (mg per mL of membrane) in PSS-modified nylon membranes with 5.0 µm and 1.2 µm nominal pores. The uncertainty is the difference between two trials.

Protein Binding		
Enzyme	5.0 µm	1.2 µm
Trypsin	6±1 mg/mL	11±1 mg/mL
Pepsin	32±6 mg/mL	48±5 mg/mL

5.3.2 Apomyoglobin digestion in pipette tips

We chose to initially examine in-membrane proteolysis of apomyoglobin because this protein contains no disulfide bonds, and complete tryptic digestion without denaturation is challenging at neutral pH.[25] As Figure 5.2 (a) shows, passage of apomyoglobin through a 5.0 µm, trypsin-modified membrane (residence time of 30 ms) leads to large MS signals from undigested, intact protein. In contrast, in a 1.2 µm trypsin-modified membrane (Figure 5.2 (b)) the same flow rate leads to minimal protein signals, and the detected proteolytic peptides cover 100% of the protein sequence. The more complete digestion in the small pores stems from both higher local trypsin concentrations and shorter diffusion distances. For digestion in 5.0 µm trypsin-modified membranes, passing the same solution through the membrane 4 times leads

to larger peptide signals and smaller detectable protein signals (Figure 5.2 (c)) due to a 4-fold

increase in residence time.
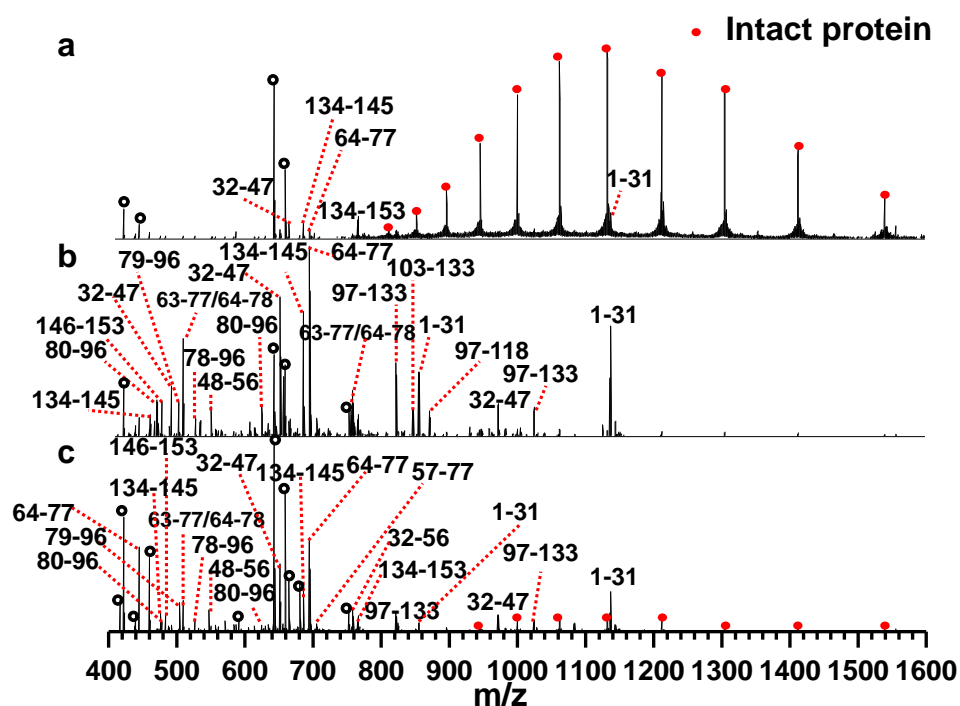
Figure 5.2. Mass spectra (m/z from 400-1600) of apomyoglobin digested using pipette tips

attached to trypsin-modified membranes. Digestion employed passage of 100-μL solutions (a)

one time through a membrane with 5.0 μm pores; (b) one time through a membrane with 1.2

μm pores; or (c) four times through a membrane with 5.0 μm pores. Signals labeled with red

dots stem from undigested protein, and black numbers represent amino acid sequences assigned

to the 20 identified peptide signals with the highest intensities. Black circles denote signals

from singly charged impurities.

As a comparison, we performed apomyoglobin digestion in a MonoTip™ trypsin pipette

tip. One cycle of aspirating and dispensing an apomyoglobin solution through this pipette tip

yields large ESI-MS signals from residual protein (Figure 5.3 (a)), and the identified peptides

cover 94% of the protein sequence. Digestion in the MonoTip™ trypsin pipette tip following

the manufacturer's protocol eliminates most of the intact protein (Figure 5.3 (b)) and provides 100% peptide coverage, but this process requires 20 cycles of aspirating and dispensing followed by soaking the tip in the protein solution for 20 min.
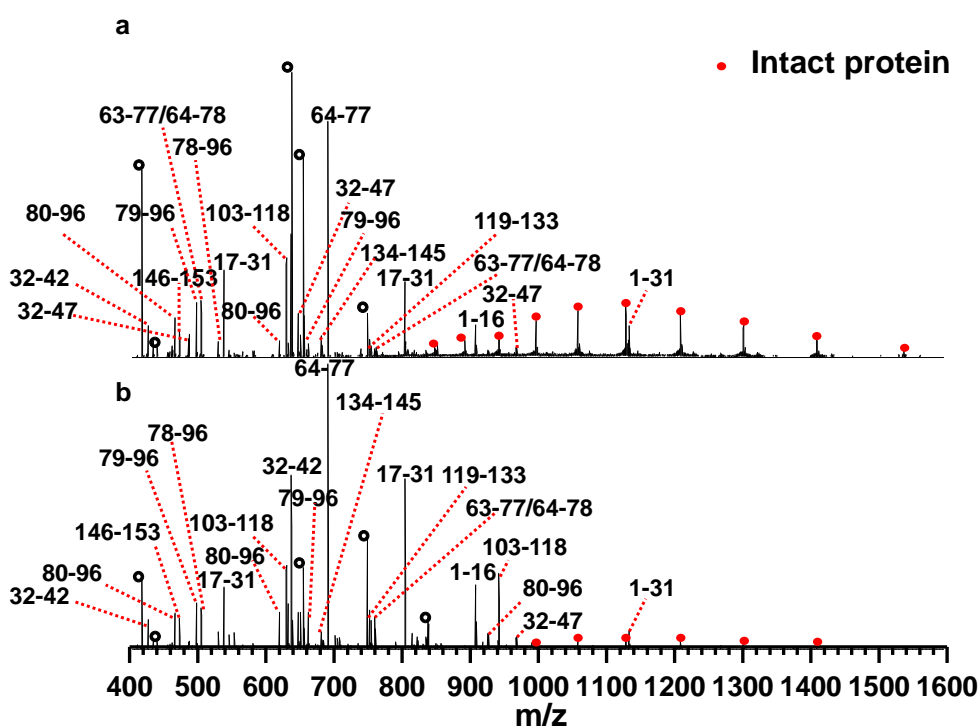
Figure 5.3. Mass spectra (m/z from 400-1600) of apomyoglobin digested in a MonoTip[TM] trypsin pipette tip using one cycle of aspirating and dispensing (a) and 20 cycles of aspirating and dispensing followed by incubation of the tip in the solution for 20 min (b). Signals labeled with red dots stem from undigested protein, and black numbers represent amino acid sequences assigned to the 20 identified peptide signals with the highest intensities. Black circles denote signals from singly charged impurities.

We also performed in-solution tryptic digestion of apomyoglobin. With a protease to protein ratio of 1:20, 30-min digestion still gives strong signals for intact proteins (Figure 5.4), whereas in-membrane (1.2 μm pores) digestion using pipette tips requires <30 s to nearly

eliminate signals from intact protein. Thus, combining trypsin-modified membranes with 1.2

μm pores and pipette tips allows more convenient and rapid proteolysis compared to both the

MonoTip^TM trypsin pipette tip and in-solution tryptic digestion. Moreover, Figure 5.5 shows

that digestions give reproducible patterns in peptide signals. We occasionally detected a single

trypsin autolytic peptide (amino acids 73-92, m/z=1082.03, +2 charge state) in all three kinds

of tryptic digests, but its signal intensity was low.

Figure 5.4. Mass spectrum (m/z from 400-1600) of apomyoglobin digested in solution for 30

min using a trypsin to protein ratio of 1: 20. Signals labeled with red dots stem from undigested

protein, and black numbers represent amino acid sequences assigned to the 20 identified

peptides with the highest signal intensities. Black circles denote signals from singly charged

impurities.

No.	Amino acids	m/z	z
1	134-145	424.56	3
2	80-96	464.24	4
3	146-153	471.24	2
4	32-47	485.01	4
5	79-96	496.27	4
6	63-77/64-78	502.98	3
7	78-96	528.29	4
8	48-56	543.78	2
9	80-96	618.66	6
10	32-47	646.34	3
11	97-118	651.13	4
12	64-77	689.92	2
13	63-77/64-78	753.97	2
14	97-133	817.83	5
15	103-133	842.92	4
16	1-31	851.69	4
17	97-118	867.83	3
18	80-96	927.48	2
19	97-133	1022.04	4
20	1-31	1135.58	3

Figure 5.5. Maximum peak intensities (relative to the signal at m/z 689.92 (z=2), blue bar) for the 20 highest peptide signals in three replicate apomyoglobin digests obtained by passing the protein solution through three different trypsin-modified membranes (1.2 μm pores) at the ends of pipette tips. The error bars represent the standard deviation, and the table lists the peptides.

5.3.3 Peptide adsorption in PSS, PSS/pepsin-, PSS/trypsin- modified membranes and MonoTip^{TM} trypsin tips

One concern when performing digestion in membranes or in MonoTip^{TM} trypsin tips is that adsorption to the membrane or tip may decrease the signals of specific peptides. To evaluate how adsorption affects the peptide recovery, we determined the percentages of digested peptides lost after passing through PSS-coated, PSS/pepsin-coated, PSS/trypsin-coated and MonoTip^{TM} trypsin tips.

In-membrane pepsin digestion occurs at pH 2, so most peptic peptides will carry positive charges that might interact electrostatically with PSS in the membrane. To examine adsorption, we completely digested apomyoglobin in solution (1:20 pepsin to protein ratio, ~20 h, 5% formic acid) and passed 100 µL of this digest (0.1 mg of digested protein/mL) through either a PSS-modified membrane or a PSS/pepsin-modified membrane at the end of a pipette tip. We collected the digests in eppendorf tubes containing 100 µL of acetonitrile to stop pepsin activity and added Angiotensin II (molecular weight of 1046.18 Da) as an internal standard in the digests reconstituted in MS buffer. Figures 5.6 (a) and 5.6 (b) show peptide signal intensities (normalized to the Angiotensin II signal) relative to the normalized signal from a digest that did not flow through the membrane. Passage through the PSS-modified membrane yields decreased relative signals for peptides 13, 14 and 15, whereas flow through the PSS/pepsin-modified membrane gives an obviously reduced signal only for peptide 15. Even with peptide 15, the decrease in the peptide signal is only ~40% for the PSS/pepsin-modified membrane. Peptides 13, 14 and 15 contain 7 lysine residues, and at low pH these positively charged resides may adsorb to negatively charged PSS. However, membrane modification with pepsin

decreases peptide adsorption.
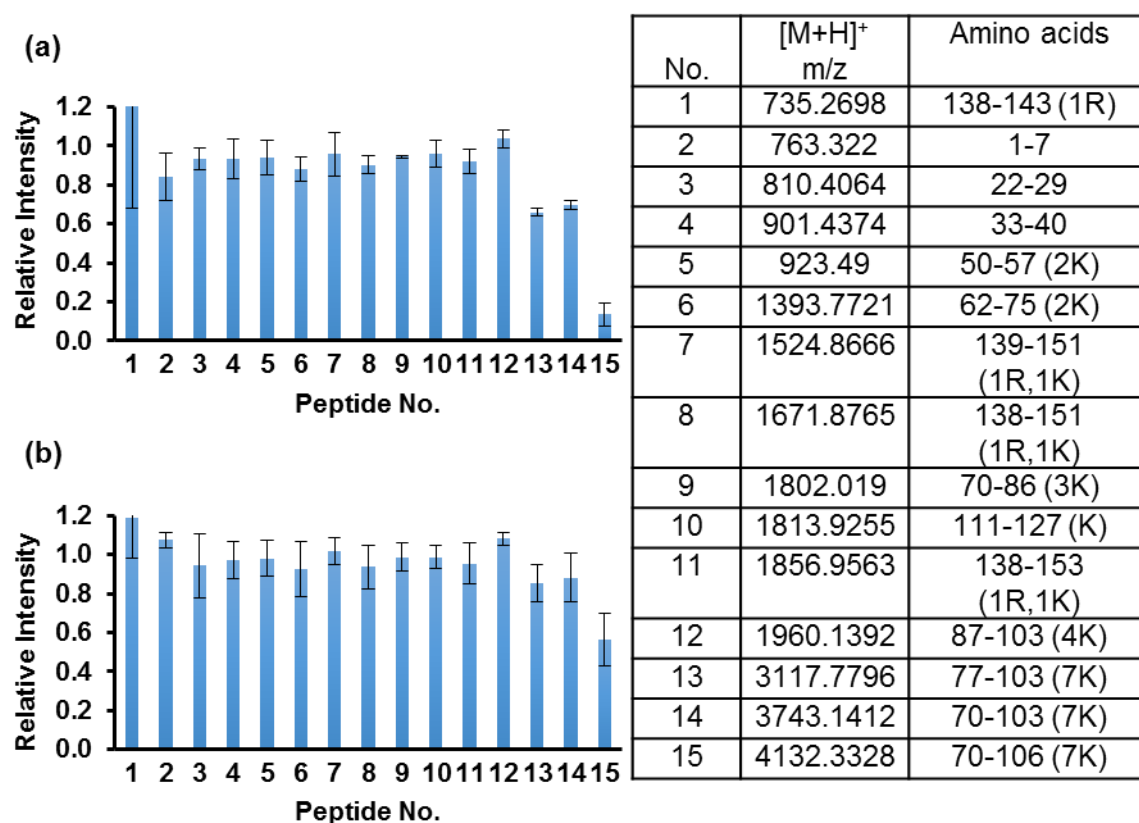
Figure 5.6. Relative peptide MS signal intensities in an in-solution apomyoglobin digest that was passed through (a) a PSS-modified membrane or (b) a PSS/pepsin-modified membrane. The relative intensities are the ratios of signals (normalized by the Angiotensin II signal) after and before passing the digests through the membranes. The table lists the sequences of the peptides, which have the 15 highest peptide signal intensities in the mass spectrum, and the number of basic residues in each peptide. Error bars are differences in two independent experiments.

To examine adsorption of tryptic peptides, we first completely digested apomyoglobin in solution (1:20 trypsin to protein ratio, ~20 h, 10 mM NH_4HCO_3). Trypsin-modified membranes and MonoTip™ trypsin pipette tips were washed twice with 200 μL of 20 mM Benzamidine hydrochloride (Sigma Aldrich) in 10 mM NH_4HCO_3 to inhibit trypsin activity. Subsequently,

we passed 100 µL of the in-solution digest (0.1 mg of apomyoglobin/mL) through either a

trypsin-modified membrane or a MonoTip[TM] trypsin pipette tip and collected the effluent in

eppendorf tubes containing 1 µL of 5% formic acid. Angiotensin II (Molecular weight: 1046.18

Da) added to the reconstituted digests served as an internal standard. Figures 5.7 (a) and 5.7 (b)

show peptide signal intensities (normalized to the Angiotensin II signal) relative to the

normalized signal from a digest that did not flow through the membrane or tip. As Figure 5.7

shows, no peptide signals decrease by more than 40% for both the membrane and MonoTip[TM]

platforms. Part of the average decrease in peptide signals could result from a small amount of

dead volume in the systems.

| No.	[M+H]+ m/z	Amino acids
1	409.2082	43-45
2	470.33	99-102
3	631.3385	140-145
4	662.3355	57-62
5	684.3687	43-47
6	748.432	134-139
7	790.4274	57-63
8	941.4685	146-153
9	1271.6576	32-42
10	1378.8354	64-77
11	1502.6629	119-133
12	1606.8476	17-31
13	1815.8951	1-16
14	1853.954	80-96
15	1885.0145	103-118
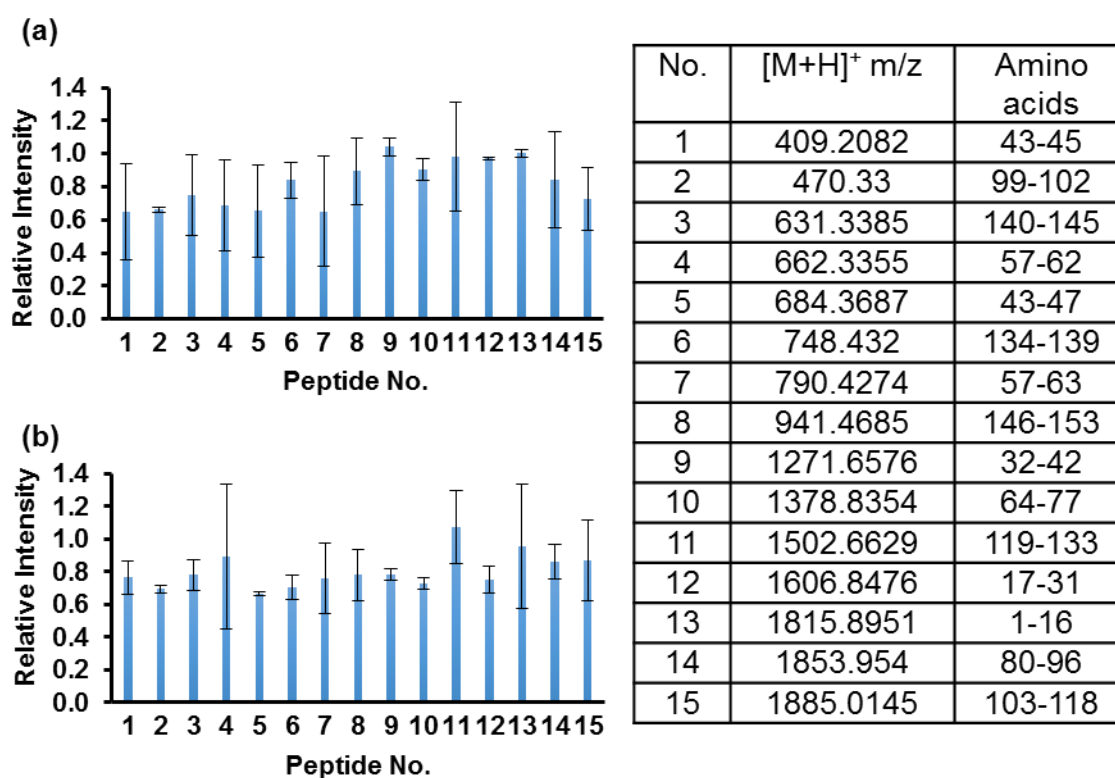
Figure 5.7. Relative peptide signal intensities in an in-solution digest that was passed through

(a) a trypsin-modified membrane or (b) a MonoTip[TM] trypsin tip.   The relative intensities are

the ratios of signals (normalized by the Angiotensin II signal) after and before passing through

Figure 5.7 (cont'd) the membrane or pipette tip. The table lists the sequences of these peptides, which have the 15 highest peptide signal intensities in the mass spectrum. Error bars are differences in two independent experiments.

Overall. we saw minimal peptide adsorption when passing fully digested apomyoglobin through pepsin-modified membranes (14 out of 15 peptides showed a signal decrease of <20% after passing the digest through the membrane, and one peptide with 7 lysine residues showed a decrease of ~40%, Figure 5.6). For peptides from in-solution tryptic digestion, treatment with either MonoTip[TM] trypsin pipette tips or trypsin-containing membranes decreased peptide intensities <40% (Figure 5.7), indicating minimal adsorption.

5.3.4 Herceptin digestion in trypsin- or pepsin-modified membranes attached to pipette tips

Conventional in-solution tryptic digestion employs high concentrations of urea or guanidine hydrochloride to denature the protein at neutral pH, so subsequent MS analysis requires removal of these denaturing agents. In contrast, with in-membrane digestion of antibodies, we can denature and reduce proteins in pH-2.5 TCEP solutions at 56 ℃ for 30 min (without subsequent alkylation) and neutralize the protein solution with ammonium bicarbonate buffer immediately before in-membrane tryptic digestion. Because digestion at the end of a pipette tip requires <30 s, proteolysis and drying of the digest can occur before disulfide bonds fully reform. In contrast to trypsin, digestion with pepsin naturally occurs at low pH and, thus, is attractive for studies of H/D exchange[26,27] as well as digestion of proteins with acid denaturation and no alkylation.[28] Here we digest Herceptin, a monoclonal antibody for breast-cancer treatment,[29,30] using pipette tips coupled to either trypsin or pepsin-modified

membranes. In a recent paper, we described controlled, in-membrane peptic digestion of antibodies,[31] but this work demonstrates the convenience of pipette tips as well as tryptic digestion.
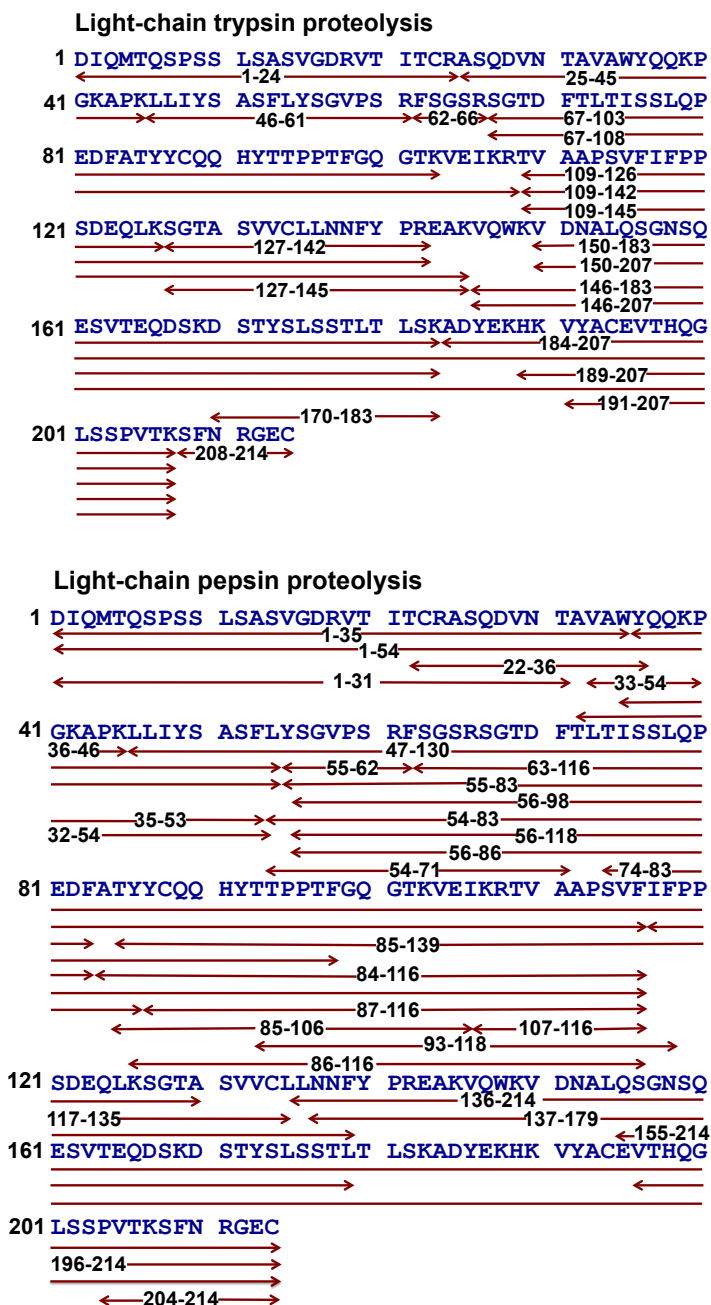
Figure 5.8. Map of the light-chain peptides detected from ESI-MS analysis of tryptic (top) and peptic (bottom) digests of Herceptin. Digestion occurred in ~30 s in protease-modified membranes at the ends of pipette tips.

Figure 5.8 shows the light-chain peptides identified from ESI-MS analysis of tryptic and peptic digests, and Figures 5.9 and 5.10 provides corresponding plots for the heavy chain. Passage of 100 µL of 0.1 mg/mL Herceptin through the membrane in 30 s and ESI-MS analysis result in peptide coverages of 100% for the light chain and 98% for the heavy chain for tryptic digestion and 100% for both the light and heavy chain for peptic digestion. The absence of desalting and alkylation steps may make this digestion procedure especially attractive for MS-based antibody sequencing and protein characterization studies.
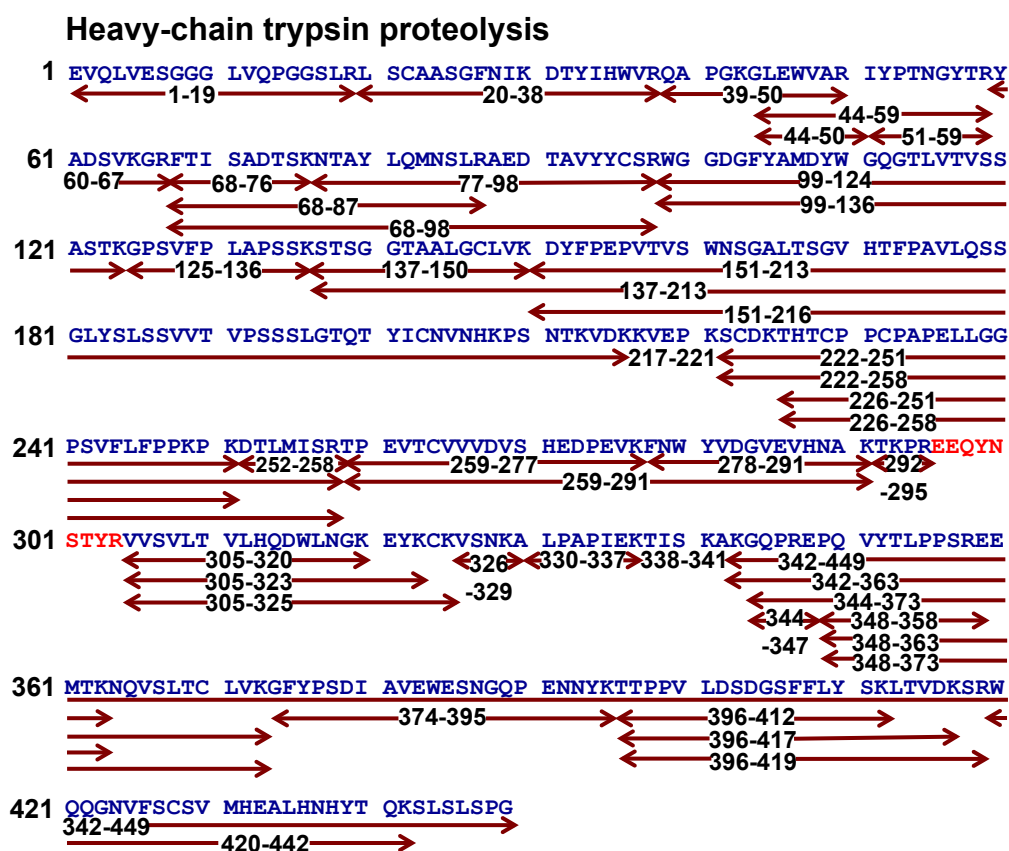
Figure 5.9. Peptide map of the Herceptin heavy chain after digestion during a single pass through a trypsin-modified membrane at the end of a pipette tip. The peptide coverage of the heavy chain is 98%. The absence of peptide EEQYNSTYR may be due to its low ionization efficiency in the positive ion mode.

151

Heavy-chain pepsin proteolysis

1 EVQLVESGGG LVQPGGSLRL SCAASGFNIK DTYIHWVRQA PGKGLEWVAR IYPTNGYTRY

1-27
1-23
1-72
28-80
34-60
21-80
41-94
48-104
35-60

61 ADSVKGRFTI SADTSKNTAY LQMNSLRAED TAVYYCSRWG GDGFYAMDYW GQGTLVTVSS

82-95 81-145
96-105
95-105
106-173
111-129
107-173
69-131
69-88

121 ASTKGPSVFP LAPSSKSTSG GTAALGCLVK DYFPEPVTVS WNSGALTSGV HTFPAVLQSS

154-177
145-202
116-148
149-177
116-177
132-153
144-152

181 GLYSLSSVVT VPSSSLGTQT YICNVNHKPS NTKVDKKVEP KSCDKTHTCP PCPAPELLGG

183-237
183-244
183-255

241 PSVFLFPPKP KDTLMISRTP EVTCVVVDVS HEDPEVKFNW YVDGVEVHNA KTKPREEQYN

239-256
246-256
265-280
265-309
235-254
255-264
256-264
244-255 256-265
245-264

301 STYRVVSVLT VLHQDWLNGK EYKCKVSNKA LPAPIEKTIS KAKGQPREPQ VYTLPPSREE

310-368
310-371
310-335
317-322
343-401

361 MTKNQVSLTC LVKGFYPSDI AVEWESNGQP ENNYKTTPPV LDSDGSFFLY SKLTVDKSRW

372-434
385-420
408-413
380-401
408-426
353-415
408-449

421 QQGNVFSCSV MHEALHNHYT QKSLSLSPG

427-449

410-444
410-449
414-449

Figure 5.10. Peptide map of the Herceptin heavy chain after digestion during a single pass through a pepsin-modified membrane at the end of a pipette tip. The peptide coverage of the heavy chain is 100%.

5.3.5 Digestion of a cell lysate

To investigate digestion of a more complex mixture, we passed Hela cell lysate (provided by Dr. Benita Sjogren from the Department of Pharmacology and Toxicology, Michigan State University) through trypsin- or pepsin-modified membranes at the ends of pipette tips. As Figure 5.11 shows, both trypsin- and pepsin-modified membranes digest the proteins in the lysate to give species with dominant molecular weights <10 kDa. Increasing the number of

passes through the membranes leads to more complete digestion, particularly for membranes containing trypsin.
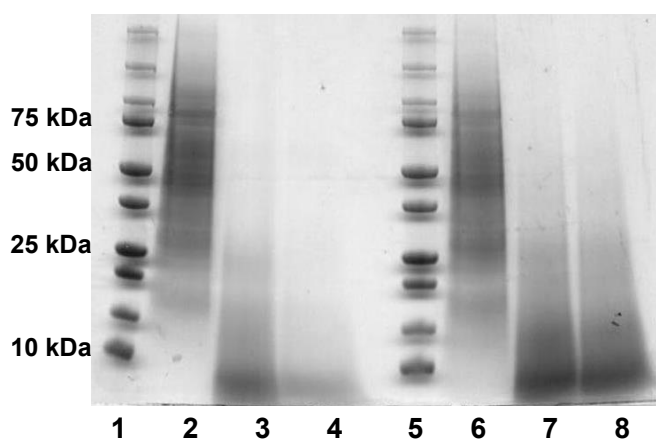
Figure 5.11. Gel electrophoresis (SDS-PAGE) analysis of Hela cell lysates before and after digestion in trypsin- or pepsin-modified membranes at the ends of pipette tips; Lanes 1 and 5: molecular weight markers; Lanes 2 and 6: 30 µg of TCEP-reduced Hela cell lysate; Lanes 3 and 4: 30 µg of Hela cell lysate digested in one (Lane 3) and three (Lane 4) passes through trypsin-modified membranes at the ends of pipette tips; Lanes 7 and 8: 30 µg of Hela cell lysate digested in one (Lane 7) and three (Lane 8) passes through pepsin-modified membranes at the ends of pipette tips.

5.3.6 Purification of His-tagged protein

Membranes are also attractive platforms for protein purification. Specifically, nylon membranes (1.2 µm pore size) modified with PAA/PEI/PAA-NTA-Ni^{2+} films selectively capture His-tagged Ubiquitin with a binding capacity of ~90 mg/mL, which is about 1.5-times the capacity of commercial Ni-NTA beads.[13,32,33] Coupling of these functionalized membranes to pipette tips enables protein purification within 2 min and is very convenient for isolation of microscale samples. To demonstrate His-tagged protein purification with membranes and pipette tips, we used a PAA/PEI/PAA-NTA-Ni^{2+}-modified membrane (1.2 µm pore size) to

purify His-SUMO protein from a diluted *E. coli* extract. Figure 5.12 shows the SDS-PAGE

analysis of the diluted cell extract before (lane 2) and after (lane 3) passing through a

PAA/PEI/PAA-NTA-Ni^{2+}-modified membrane attached to a pipette tip. Lane 3 has a greatly

reduced intensity at the position for His-SUMO protein, which means most of this protein was

captured by the membrane (other proteins with a similar molecular mass or some protein

without a His-tag might contribute to the residual band). Some of the other protein bands in

lane 3 also have a slightly lower intensity compared to lane 2, which might indicate some

dilution due to dead volume in the system or non-specific binding of proteins without His-tags.

However, the eluate shows a dominant His-SUMO band suggesting >95% purity, which shows

that any non-specifically bound proteins were either eluted with washing buffer or not eluted

with imidazole. Specific binding between His-SUMO protein and Ni^{2+}, washing, and selective

elution with imidazole combine to isolate His-tagged protein with high purity.
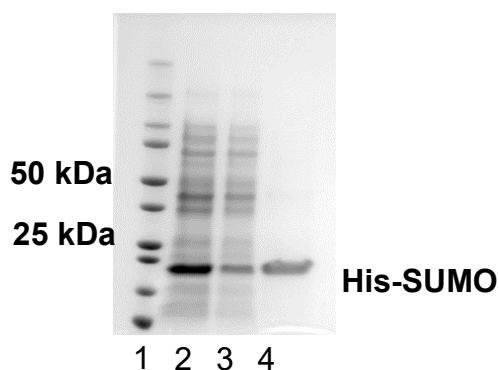
Figure 5.12. SDS-PAGE analysis (Coomassie stain) demonstrating isolation of His-SUMO

protein from a cell lysate. The purification employed a PAA/PEI/PAA-NTA-Ni^{2+}-modified

membrane at the end of a pipette tip. Lane 1: protein ladder, Lane 2: cell lysate containing His-

SUMO protein, Lane 3: cell lysate after passing through the membrane, Lane 4: His SUMO

protein eluted from the membrane with 0.5 M imidazole.

One challenge in these purifications is that the low membrane surface area leads to a relatively low binding capacity. Based on the exposed external surface area of 0.02 cm^2, the membrane volume employed in purification is only 2 x 10^{-4} cm^3. Assuming a binding capacity of ~90 mg/mL, membranes at the end of pipette tips will capture at most 20 μg of protein. Passage of cell lysate through multiple membranes or holders with larger surface area should increase binding capacity.

5.4 Conclusions

Coupling of in-membrane proteolysis to pipette tips yields a convenient method to digest proteins in microscale solutions. In 30 s, trypsin-modified membranes with 1.2 μm pores give more complete proteolysis of apomyoglobin than 30 min of in-solution digestion.   The extent of digestion decreases when using membranes with larger (5.0 μm) pores due to less immobilized protease and longer diffusion distances. Membranes containing pepsin or trypsin also digest the antibody Herceptin to give up to 100 percent peptide coverage in subsequent ESI-MS analysis. Rapid digestion enables denaturation and reduction of the antibody in acidic conditions to avoid alkylation and desalting steps, even for tryptic digestion at neutral pH.

Using PAA/PEI/PAA-NTA-Ni^{2+}-modified membranes at the ends of pipette tips, purification of His-tagged protein from cell lysate can occur in minutes. The binding capacity of one membrane attached to a pipette tip is 20 μg or less, but increasing the exposed area of the membrane holder or stacking membranes should provide higher protein binding capacity if needed. Thus, coupling of functionalized membranes to pipette tips is a promising technique for rapid protein purification and digestion, perhaps for high-throughput studies.

REFERENCES

REFERENCES

(1) Yates, J. R.; Ruse, C. I.; Nakorchevsky, A., Proteomics by Mass Spectrometry: Approaches, Advances, and Applications, *Annu. Rev. Biomed. Eng.* **2009**, *11,* 49-79.

(2) Young, N. L.; Plazas-Mayorca, M. D.; Garcia, B. A., Systems-Wide Proteomic Characterization of Combinatorial Post-Translational Modification Patterns, *Expert Rev. Proteomics* **2010**, *7*, 79-92.

(3) Kalli, A.; Hakansson, K., Electron Capture Dissociation of Highly Charged Proteolytic Peptides from Lys N, Lys C and Glu C Digestion, *Mol. Biosyst.* **2010**, *6*, 1668-1681.

(4) Laskay, U. A.; Lobas, A. A.; Srzentic, K.; Gorshkov, M. V.; Tsybin, Y. O., Proteome Digestion Specificity Analysis for Rational Design of Extended Bottom-up and Middle-down Proteomics Experiments, *J. Proteome Res.* **2013**, *12*, 5558-5569.

(5) Sun, L. L.; Zhu, G. J.; Yan, X. J.; Mou, S.; Dovichi, N. J., Uncovering Immobilized Trypsin Digestion Features from Large-Scale Proteome Data Generated by High-Resolution Mass Spectrometry, *J. Chromatogr. A* **2014**, *1337*, 40-47.

(6) Regnier, F. E.; Kim, J., Accelerating Trypsin Digestion: the Immobilized Enzyme Reactor, *Bioanalysis* **2014**, *6*, 2685-2698.

(7) Kawai, T.; Saito, K.; Lee, W., Protein Binding to Polymer Brush, Based on Ion-Exchange, Hydrophobic, and Affinity Interactions, *J. Chromatogr. B* **2003**, *790*, 131-142.

(8) Bhut, B. V.; Husson, S. M., Dramatic Performance Improvement of Weak Anion-Exchange Membranes for Chromatographic Bioseparations, *J. Memb. Sci.* **2009**, *337*, 215-223.

(9) Wang, J.; Sproul, R. T.; Anderson, L. S.; Husson, S. M., Development of Multimodal Membrane Adsorbers for Antibody Purification Using Atom Transfer Radical Polymerization, *Polymer* **2014**, *55*, 1404-1411.

(10) Yin, D. X.; Ulbricht, M., Antibody-Imprinted Membrane Adsorber via Two-Step Surface Grafting, *Biomacromolecules* **2013**, *14*, 4489-4496.

(11) Tan, Y. J.; Sui, D. X.; Wang, W. H.; Kuo, M. H.; Reid, G. E.; Bruening, M. L., Phosphopeptide Enrichment with TiO_2-Modified Membranes and Investigation of Tau Protein Phosphorylation, *Anal. Chem.* **2013**, *85*, 5699-5706.

(12) Ning, W. J.; Wijeratne, S.; Dong, J. L.; Bruening, M. L., Immobilization of Carboxymethylated Polyethylenimine-Metal-Ion Complexes in Porous Membranes to Selectively Capture His-Tagged Protein, *ACS Appl. Mater. Interfaces* **2015**, *7*, 2575-2584.

(13) Bhattacharjee, S.; Dong, J. L.; Ma, Y. D.; Hovde, S.; Geiger, J. H.; Baker, G. L.; Bruening, M. L., Formation of High-Capacity Protein-Adsorbing Membranes through Simple Adsorption of Poly(acrylic acid)-Containing Films at Low pH, *Langmuir* **2012**, *28*, 6885-6892.

(14) Xu, F.; Wang, W. H.; Tan, Y. J.; Bruening, M. L., Facile Trypsin Immobilization in Polymeric Membranes for Rapid, Efficient Protein Digestion, *Anal. Chem.* **2010**, *82*, 10045-10051.

(15) Tan, Y. J.; Wang, W. H.; Zheng, Y.; Dong, J. L.; Stefano, G.; Brandizzi, F.; Garavito, R. M.; Reid, G. E.; Bruening, M. L., Limited Proteolysis via Millisecond Digestions in Protease-Modified Membranes, *Anal. Chem.* **2012**, *84*, 8357-8363.

(16) Ota, S.; Miyazaki, S.; Matsuoka, H.; Morisato, K.; Shintani, Y.; Nakanishi, K., High-Throughput Protein Digestion by Trypsin-Immobilized Monolithic Silica with Pipette-Tip Formula, *J. Biochem. Bioph. Methods* **2007**, *70*, 57-62.

(17) Thingholm, T. E.; Jorgensen, T. J. D.; Jensen, O. N.; Larsen, M. R., Highly Selective Enrichment of Phosphorylated Peptides Using Titanium Dioxide, *Nat. Protoc.* **2006**, *1*, 1929-1935.

(18) Rappsilber, J.; Mann, M.; Ishihama, Y., Protocol for Micro-Purification, Enrichment, Pre-Fractionation and Storage of Peptides for Proteomics Using Stagetips, *Nat. Protoc.* **2007**, *2*, 1896-1906.

(19) Hahn, H. W.; Rainer, M.; Ringer, T.; Huck, C. W.; Bonn, G. K., Ultrafast Microwave-Assisted in-Tip Digestion of Proteins, *J. Proteome Res.* **2009**, *8*, 4225-4230.

(20) Health&Science, I., Super Flangeless™ Ferrule PEEK, 1/4-28 Flat-Bottom, 1/16"OD - Natural, https://www.idex-hs.com/super-flangelesstm-ferrule-peek-1-4-28-flat-bottom-1-16-od-natural.html, 08/06/2016.

(21) Sciences, G., MonoTip™ Trypsin (Product Features), http://www.glsciences.com/c-product/sample/proteins/monotip-trypsin-product-features/, 08/06/2016.

(22) Anuraj, N.; Bhattacharjee, S.; Geiger, J. H.; Baker, G. L.; Bruening, M. L., An All-Aqueous Route to Polymer Brush-Modified Membranes with Remarkable Permeabilites and Protein Capture Rates, *J. Memb. Sci.* **2012**, *389*, 117-125.

(23) Cunningham, L. W., Molecular-Kinetic Properties of Crystalline Diisopropyl Phosphoryl Trypsin, *J. Biol. Chem.* **1954**, *211*, 13-19.

(24) Jonsson, M., Isoelectric Spectra of Native and Base Denatured Crystallized Swine Pepsin, *Acta Chem. Scand.* **1972**, *26*, 3435-3440.

(25) Fontana, A.; Zambonin, M.; deLaureto, P. P.; DeFilippis, V.; Clementi, A.; Scaramella, E., Probing the Conformational State of Apomyoglobin by Limited Proteolysis, *J. Mol. Biol.* **1997**, *266*, 223-230.

(26) Majumdar, R.; Manikwar, P.; Hickey, J. M.; Arora, J.; Middaugh, C. R.; Volkin, D. B.; Weis, D. D., Minimizing Carry-Over in an Online Pepsin Digestion System Used for the H/D Exchange Mass Spectrometric Analysis of An IgG1 Monoclonal Antibody, *J. Am. Soc. Mass. Spectrom.* **2012**, *23*, 2140-2148.

(27) Hamuro, Y.; Coales, S. J.; Molnar, K. S.; Tuske, S. J.; Morrow, J. A., Specificity of Immobilized Porcine Pepsin in H/D Exchange Compatible Conditions, *Rapid Commun. Mass Spectrom.* **2008**, *22*, 1041-1046.

(28) Vanerp, P. E. J.; Brons, P. P. T.; Boezeman, J. B. M.; Dejongh, G. J.; Bauer, F. W., A Rapid Flow Cytometric Method for Bivariate Bromodeoxyuridine DNA Analysis Using Simultaneous Proteolytic-Enzyme Digestion and Acid Denaturation, *Cytometry* **1988**, *9*, 627-630.

(29) Bryant, J., Herceptin Adjuvant Therapy, U.S. Patent 20060275305, 12/07/2006.

(30) Baselga, J.; Perez, E. A.; Pienkowski, T.; Bell, R., Adjuvant Trastuzumab: A Milestone in the Treatment of HER-2-Positive Early Breast Cancer, *Oncologist* **2006**, *11*, 4-12.

Chapter 6. Summary and future work

6.1 Research summary

In this dissertation, I present my research to develop functionalized membranes for protein purification and proteolysis, as well as development of a prototype membrane holder that attaches functionalized membranes to pipette tips for fast and convenient purification or digestion.

Chapter 2 describes adsorption of polyelectrolytes that chelate metal ions to create functionalized membranes that selectively capture His-tagged proteins. The binding capacities of these membranes are equal to those of high-binding commercial beads, and purification can occur in minutes during flow through the membrane. Adsorption of functional polyelectrolytes is simpler than previous membrane-modification strategies such as growth of polymer brushes or derivatization of adsorbed layers with chelating moieties. Sequential adsorption of protonated poly(allylamine) (PAH) and carboxymethylated branched polyethyleneimine (CMPEI) leads to membranes that bind Ni^{2+} and capture ~60 mg of His-tagged ubiquitin per mL of membrane. Moreover, these membranes enable isolation of His-tagged protein from cell lysates in <15 min. Metal-ion leaching from PAH/CMPEI- and PAH/poly[(N,N-dicarboxymethyl) allylamine] (PDCMAA)-modified membranes is similar to that from GE Hitrap^{TM} FF columns. Eluates with 0.5 M imidazole contain less than 10 ppm Ni^{2+}.

Chapter 3 introduces an enzymatic membrane reactor for removal of His-tagged SUMO tags from fusion proteins. The reactor contains His-tagged SUMO protease electrostatically immobilized in membranes modified with PAA/PEI/PAA polyelectrolyte multilayers. With identical protease to substrate protein weight ratios of 1:100, membrane-immobilized enzymes

show the same activity as enzymes in solution. Moreover, similar tag removal efficiencies occur for in-solution and in-membrane reactions when total digestion times are the same. However, the membrane reactor effectively separates the enzyme from the substrate and is reusable over three digestions.

Chapter 4 explores controlled, limited proteolysis in porous nylon membranes containing immobilized trypsin. Compared to complete digestion, limited proteolysis gives rise to larger peptides that often cover a greater portion of the protein's amino acid sequence. Passage of protein solutions through 100-μm thick membranes enables reaction residence times as short as milliseconds to limit digestion. Additionally, variation of the membrane pore size (5.0, 1.2 or 0.45 μm) and the protease-immobilization method (electrostatic adsorption or covalent anchoring) affords control over the proteolysis rate. Large pores (5.0 μm) and covalent anchoring yield particularly long tryptic peptides and high protein sequence coverages. Limited proteolysis followed by mass spectrometry can also help identify flexible regions in a protein. With both cytochrome c and apomyoglobin, in-membrane trypsinolysis cleaves the protein after lysine residues in highly flexible regions to generate two large peptides that cover the entire sequence of the protein.

Chapter 5 presents my efforts to integrate rapid in-membrane protein-purification and proteolysis with pipette tips. Pushing a protein-containing solution through a protease-modified membrane at the end of a pipette tip digests proteins in 30 s or less, and the short proteolysis time avoids reformation of disulfide bonds to enable tryptic digestion without alkylation of cysteine residues. Moreover, proteolysis is more complete than with 30 min of in-solution digestion. Digestion of the antibody Trastuzumab (Herceptin) at the end of a pipette tip leads

to 100% peptide coverage in MS analyses. Similarly, when membranes contain Ni^{2+} complexes, pipetting aqueous His-tagged protein through the membrane and subsequent rinsing and elution yield purified His-tagged protein in 2 min. These applications demonstrate the potential of combinations of functional membranes and pipette tips for rapid sample purification and pretreatment.

6.2 Future work – membrane modification with peptide ligands that capture antibodies

Chapter 2 shows that direct adsorption of relatively inexpensive polyelectrolytes containing chelating groups effectively modifies membranes to bind metal ions and capture His-tagged protein. In addition to purification of His-tagged protein, isolation and quantification of monoclonal antibodies are critical for developing new antibody therapies and performing pharmacodynamics studies. However, separation of a single monoclonal antibody from human serum, which contains large amounts of other antibodies and proteins, is challenging. Conventional antibody purification employs affinity adsorption chromatographic columns with immobilized protein A or protein G. While protein A and protein G affinity adsorption columns are effective, they do suffer from limitations such as high cost and lack of specificity among antibodies.[1,2] Therefore, recent research focused on enhancing the purification of monoclonal antibodies using small-molecule affinity chromatography,[3] non-protein A multi-step purifications,[4] biomimetic triazine ligands[3] and peptide mimotopes.[4]

Peptide mimotopes mimic the epitope of a specific antibody and bind to the Fab (fragment, antigen-binding) antigen-binding site, so they may prove useful for monoclonal antibody purification. For example, Jiang, *et al.* isolated the peptide QLGPYELWELSH via phage display as a HER2 epitope mimotope.[4]   Shang, *et al.* subsequently added seven amino-

terminal residues to this mimotope and immobilized it on a gold substrate to specifically bind

Trastuzumab (Herceptin) for detection in blood serum.[5] We recently began considering

immobilization of this peptide in membrane pores to create materials that selectively capture

Trastuzumab. Because of convective flow and short radial diffusion distances, such membrane

may enable rapid Herceptin isolation.[6-8] This is similar to our development of membranes for

capture of His-tagged proteins (see chapter 2 for example),[9-11] but mimotope immobilization

will expand the range of analytes we can isolate in functional membranes.   Specifically, in

preliminary work we immobilized the peptide KGSGSGSQLGPYELWELSH (K19) in porous

membranes to examine the possibility of Herceptin isolation in membranes (Scheme 6.1).
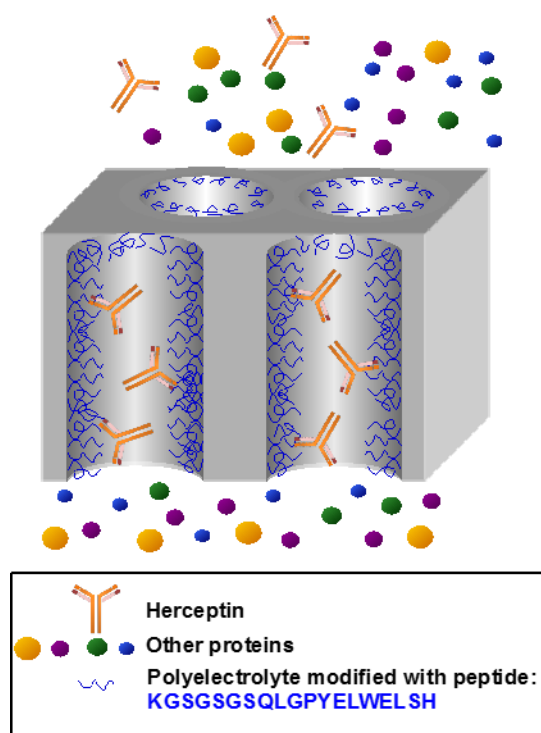
Scheme 6.1. Scheme of selective Herceptin capture during flow though membranes containing

the peptide KGSGSGSQLGPYELWELSH (K19) anchored to adsorbed polyelectrolytes.

6.2.1 Immobilization of K19 in porous nylon membrane

After membrane exposure to UV/O$_3$ for 15 min, 20 mL of 0.1 M PAA (0.5 M NaCl, pH 3)

was circulated through the membrane for 40 min, followed by passage of 20 mL of water. Subsequently, 20 mL of 2 mg/mL branched PEI (pH 3) was circulated through the membrane for 40 min, and after again rinsing with 20 mL of water, another layer of PAA was deposited on top of the branched PEI using the same procedure as for the first PAA layer. Then immobilization of peptide K19 occurred following a literature procedure.[11] First, 5 mL of 0.1 M NHS, 0.1 M EDC was circulated through (PAA/PEI/PAA)-modified membranes for 1 h, followed by passage of 10 mL of water through the membrane. Then a 1 mg/mL K19 solution (pH adjusted to 8-9 using 0.1 M NaOH) was circulated through membranes for 1 h, followed by passage of 20 mL of deionized water through the membrane.

6.2.2 Quantification of K19 binding in porous nylon membranes

The amount of K19 immobilized in PAA/PEI/PAA-modified nylon membranes was determined by comparing the florescence intensity of the K19 loading solution before and after circulating through the membrane. All the samples were diluted 1/24 in deionized water to obtain K19 concentrations ranging from 0 to 20 μM. The calibration curve of florescence intensity at 355 nm versus K19 concentration (Figure 6.1) demonstrates the requisite linearity for the analysis. Figure 6.2 shows the fluorescence spectra of the K19 loading solution before and after circulating through the membrane. Based on the large decrease in the fluorescence intensity of the solution after circulating through the membrane, PAA/PEI/PAA-modified nylon membranes (area: 3.14 cm^2) capture almost all of the K19 peptides. The calculated K19 binding is 24.7 ± 3.8 mg per mL of PAA/PEI/PAA-modified membrane. Even assuming that only 1 in 10 K19 molecules capture an antibody, this extent of K19 immobilization would give a Herceptin binding capacity of 1.8 g per mL of membrane, due to the high molecular weight

(~150 kDa) of antibodies. (Quantitation of K19 capture in membranes was completed with help

from Austin Bennett.)
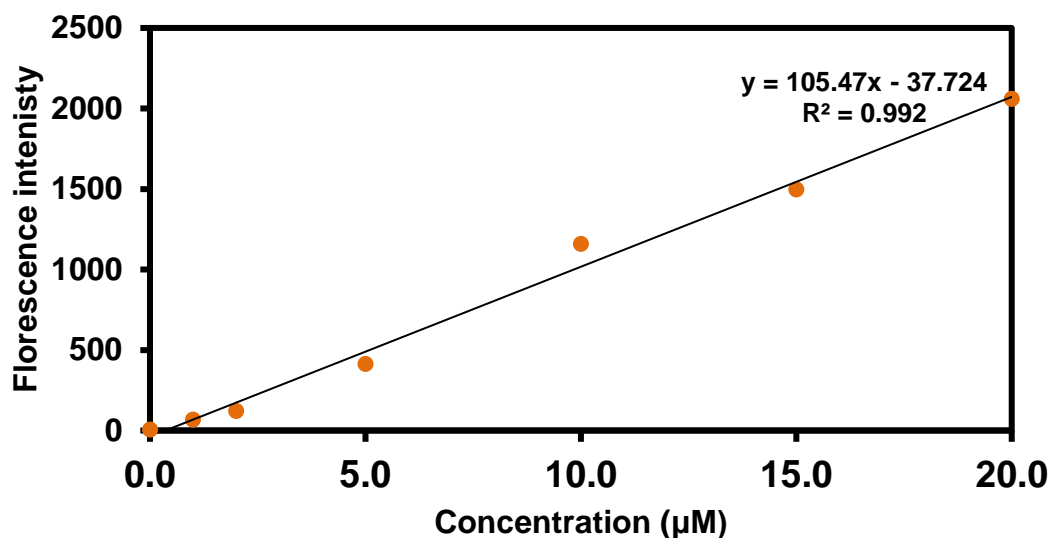

Figure 6.1. Calibration curve of florescence intensity (355 nm) versus the concentration of

K19 peptide in water. The excitation wavelength was 280 nm.
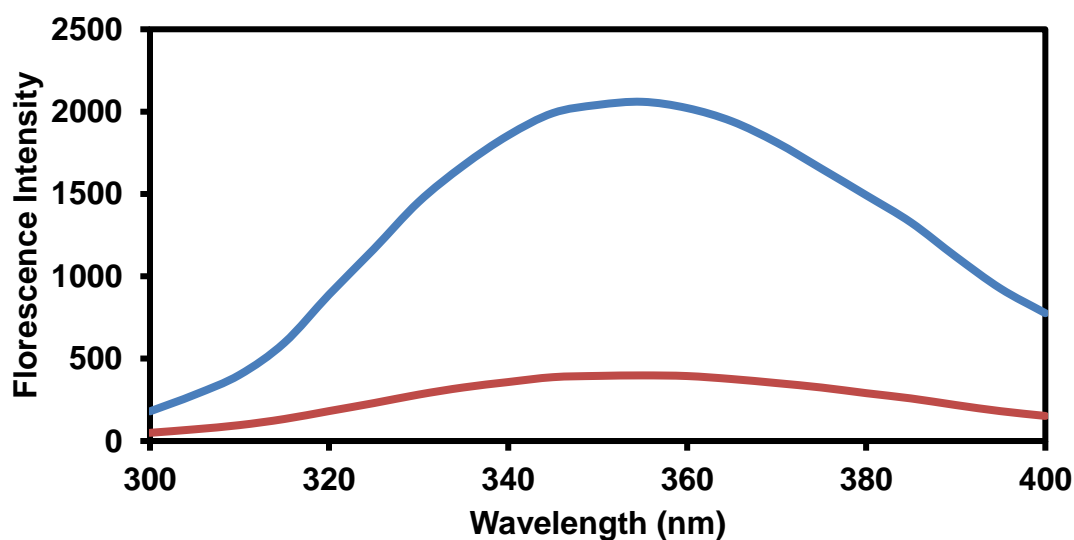

Figure 6.2. Fluorescence emission spectra (excitation wavelength of 280 nm) of a K19

(KGSGSGSQLGPYELWELSH) loading solution before (blue line) and after (red line)

circulating through a PAA/PEI/PAA-modified membrane for 1 h.

6.2.3 Adsorption of Herceptin and Avastin in K19-modified nylon membranes

Figure 6.3. Breakthrough curve obtained during passage of a 1 mg/mL Herceptin solution through a membrane containing KGSGSGSQLGPYELWELSH (K19) immobilized to a PAA/PEI/PAA film. The flow rate through the membrane (area of 3.14 cm^2) was 0.2 mL/h.

After determining the amount of K19 immobilized in the membrane, we examine Herceptin binding in membranes modified with (PAA/PEI/PAA)-K19 using breakthrough curves such as that in Figure 6.3. Based on the integral of the difference between the feed concentration and the effluent concentration in the breakthrough curve, the membrane captured 15 mg/mL of Herceptin. This number is much smaller than the theoretical one calculated with K19 binding capacity. This huge difference may be due to the steric hindrance caused by large size of Herceptin. However, this is already 10 times of beads for monoclonal antibodies purification.[12,13] As a comparison, the Avastin breaks through the membrane immediately (Figure 6.4) and shows a binding capacity of only 2 mg/mL. Thus, the non-specific binding in the K-19 modified membranes is small.
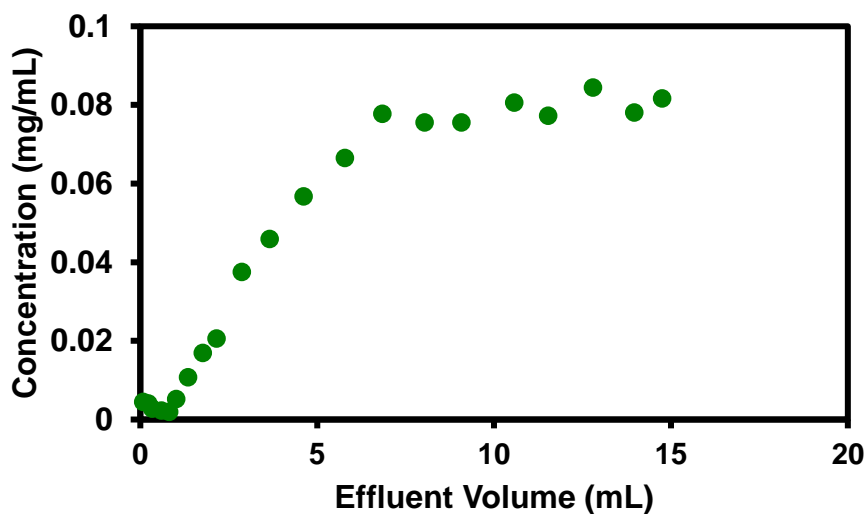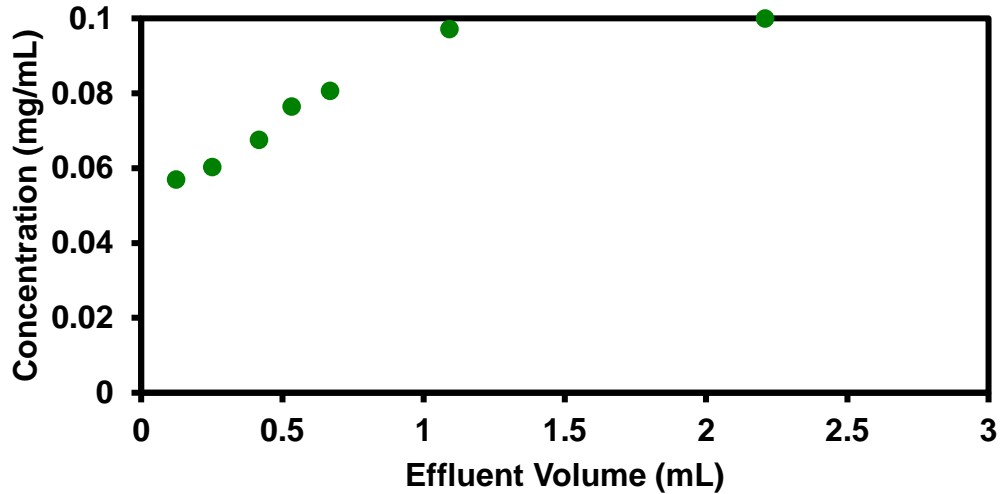
Figure 6.4. Breakthrough curve obtained during passage of a 1 mg/mL Herceptin solution through a membrane containing KGSGSGSQLGPYELWELSH (K19) immobilized to a PAA/PEI/PAA film. The flow rate through the membrane (area of 3.14 cm^2) was 0.2 mL/h.

6.2.4 Purification of Herceptin from human serum

Figure 6.5. SDS-PAGE analysis of the purification of Herceptin from human serum using PAA/PEI/PAA-K19-modified membranes. Lane 1: Molecular weight marker; Lane 2: Human serum with Herceptin; Lane 3: Effluent of human serum containing Herceptin after passing through a K19-modified membrane; Lane 4: Herceptin eluted with 2% SDS, in 20 mM Tris

Figure 6.5 (cont'd) buffer; Lane 5: Effluent of human serum without Herceptin after passing through a K19-modified membrane; Lane 6: Eluate (2% SDS in 20 mM Tris buffer) from a K19-modified membrane after loading with human serum without Herceptin.
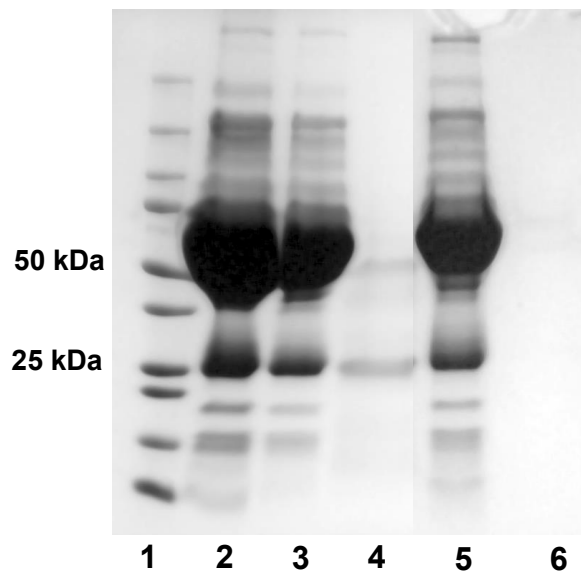
To further demonstrate that membranes can isolate Herceptin directly from complex matrices, we used PAA/PEI/PAA-K19-modified membranes to isolate Herceptin spiked in human serum. Human serum was diluted 1:3 in phosphate buffer and spiked with the Herceptin to achieve a concentration of 100 μg/mL. The diluted human serum (1 mL) containing Herceptin was circulated through the K19-containing membrane for 30 min, followed by washing twice with 2 mL of phosphate buffer containing 137 mM NaCl, once with phosphate buffer containing 500 mM NaCl, and then eluting with 150 μL of 2% SDS. Aliquots containing 50 μL of loading, effluent, and eluate solutions were first concentrated to around 20 μL with a Speed Vac and mixed with 5 μL of SDS-PAGE sample buffer. After immersion in boiling water for 3 min, samples were loaded on the 4-20% gradient SDS-PAGE gel.

Figure 6.5 shows the SDS-PAGE analysis of human serum that contained Herceptin (lane 2), the same serum solution after passing through a PAA/PEI/PAA-K19-modified membrane (lane 3), and the eluate (lane 4) from the membrane loaded with this serum. Notably, the only detectable band from the eluate stems from the heavy chain and light chain of Herceptin. To show that these bands do not result from another antibody, we also loaded the K19-containing membrane with human serum that was not spiked with Herceptin. As lane 6 in Figure 6.2.5 shows, SDS-PAGE shows no detectable bands in the eluate. Thus the membranes are selective for Herceptin. This is a distinct advantage over non-selective affinity chromatographic methods, e.g. binding to columns with immobilized protein A, that bind non-discriminately to the Fc

region of all IgG antibodies.[14,15]

6.2.5 Conclusions

Covalent linking of KGSGSGSQLGPYELWELSH (K19) to PAA/PEI/PAA multilayers in porous nylon membranes allows immobilization of 25 mg of peptide per mL of membrane. Moreover, these K19-modified membranes bind 15 mg of Herceptin per mL, which is higher than the binding capacity of most commercial beads that capture monoclonal antibodies. SDS-PAGE analysis shows that the modified membranes also successfully isolate Herceptin from human serum. The membranes do not capture other antibodies in serum. These preliminary results show the potential of applying ligand-modified membranes for antibody purification. However, elution of the Herceptin from the membrane requires SDS, which will interfere with MS analysis. Thus, future work will focus on developing easy and convenient way to elute or analyze Herceptin captured in membranes. The possible methods for analyzing bound Herceptin include (1) screening elution buffers for higher antibody recovery and compatibility with mass spectrometry;[16,17] (2) development of optical analysis methods that are compatible with SDS;[18] (3) modifying the peptide sequence or spacer length to adjust the binding affinity between the peptide ligand and antibody for easy elution;[19,20] (4) in-membrane digestion of Herceptin or other antibodies followed by quantitation with surrogate peptides using MRM (multiple reaction monitor)[21,22] or PRM (parallel reaction monitoring).[23] With such improvements, we think that mimotope-containing membranes may readily enable analysis of therapeutic antibodies in patient sera.

REFERENCES

REFERENCES

(1) Low, D.; O'Leary, R.; Pujar, N. S., Future of Antibody Purification, *J. Chromatogr. B* **2007**, *848*, 48-63.

(2) Sadana, A.; Beelaram, A. M., Efficiency and Economics of Bioseparation: Some Case Studies, *Bioseparation* **1994**, *4*, 221-235.

(3) Barroso, T.; Lourenco, A.; Araujo, M.; Bonifacio, V. D. B.; Roque, A. C. A.; Aguiar-Ricardo, A., A Green Approach Toward Antibody Purification: A Sustainable Biomimetic Ligand for Direct Immobilization on (Bio)polymeric Supports, *J. Mol. Recognit.* **2013**, *26*, 662-671.

(4) Jiang, B. H.; Liu, W. B.; Qu, H.; Meng, L.; Song, S. M.; Tao, O. Y.; Shou, C. C., A Novel Peptide Isolated from A Phage Display Peptide Library with Trastuzumab Can Mimic Antigen Epitope of HER-2, *J. Biol. Chem.* **2005**, *280*, 4656-4662.

(5) Shang, Y. Q.; Singh, P. R.; Chisti, M. M.; Mernaugh, R.; Zeng, X. Q., Immobilization of a Human Epidermal Growth Factor Receptor 2 Mimotope-Derived Synthetic Peptide on Au and Its Potential Application for Detection of Herceptin in Human Serum by Quartz Crystal Microbalance, *Anal. Chem.* **2011**, *83*, 8928-8936.

(6) Thommes, J.; Etzel, M., Alternatives to Chromatographic Separations, *Biotechnol. Prog.* **2007**, *23*, 42-45.

(7) Orr, V.; Zhong, L. Y.; Moo-Young, M.; Chou, C. P., Recent Advances in Bioprocessing Application of Membrane Chromatography, *Biotechnol. Adv.* **2013**, *31*, 450-465.

(8) Ghosh, R., Protein Separation Using Membrane Chromatography: Opportunities and Challenges, *J. Chromatogr. A* **2002**, *952*, 13-27.

(9) Ning, W. J.; Wijeratne, S.; Dong, J. L.; Bruening, M. L., Immobilization of Carboxymethylated Polyethylenimine-Metal-Ion Complexes in Porous Membranes to Selectively Capture His-Tagged Protein, *ACS Appl. Mater. Interfaces* **2015**, *7*, 2575-2584.

(10) Jain, P.; Sun, L.; Dai, J. H.; Baker, G. L.; Bruening, M. L., High-Capacity Purification of His-Tagged Proteins by Affinity Membranes Containing Functionalized Polymer Brushes, *Biomacromolecules* **2007**, *8*, 3102-3107.

(11) Bhattacharjee, S.; Dong, J. L.; Ma, Y. D.; Hovde, S.; Geiger, J. H.; Baker, G. L.; Bruening, M. L., Formation of High-Capacity Protein-Adsorbing Membranes through Simple Adsorption of Poly(acrylic acid)-Containing Films at Low pH, *Langmuir* **2012**, *28*, 6885-6892.

(12) Zandian, M.; Jungbauer, A., An Immunoaffinity Column with A Monoclonal Antibody as Ligand for Human Follicle Stimulating Hormone, *J. Sep. Sci.* **2009**, *32*, 1585-1591.

(13) Monoclonal antibody against C-terminus presented AviTag, https://www.avidity.com/technologies/monoclonal-antibody-against-c-terminus-presented-avitag, 08/30/2016.

(14) Yang, L.; Biswas, M. E.; Chen, P., Study of Binding Between Protein A and Immunoglobulin G Using A Surface Tension Probe, *Biophys. J.* **2003**, *84*, 509-522.

(15) Hober, S.; Nord, K.; Linhult, M., Protein A Chromatography for Antibody Purification, *J. Chromatogra. B Analyt. Technol. Biomed. Life Sci.* **2007**, *848*, 40-47.

(16) Shukla, A. A.; Hubbard, B.; Tressel, T.; Guhan, S.; Low, D., Downstream Processing of Monoclonal Antibodies—Application of Platform Approaches, *J. Chromatogr. B* **2007**, *848*, 28-39.

(17) Ejima, D.; Yumioka, R.; Tsumoto, K.; Arakawa, T., Effective Elution of Antibodies by Arginine and Arginine Derivatives in Affinity Column Chromatography, *Anal. Biochem.* **2005**, *345*, 250-257.

(18) Brown, R. E.; Jarvis, K. L.; Hyland, K. J., Protein Measurement Using Bicinchoninic Acid - Elimination of Interfering Substances, *Anal. Biochem.* **1989**, *180*, 136-139.

(19) Shang, Y.; Singh, P. R.; Chisti, M. M.; Mernaugh, R.; Zeng, X., Immobilization of a Human Epidermal Growth Factor Receptor 2 Mimotope-Derived Synthetic Peptide on Au and Its Potential Application for Detection of Herceptin in Human Serum by Quartz Crystal Microbalance, *Anal. Chem.* **2011**, *83*, 8928-8936.

(20) Gabius, H.-J., Influence of Type of Linkage and Spacer on the Interaction of B-Galactoside-Binding Proteins with Immobilized Affinity Ligands, *Anal. Biochem.* **1990**, *189*, 91-94.

(21) Picotti, P.; Aebersold, R., Selected Reaction Monitoring-Based Proteomics: Workflows, Potential, Pitfalls and Future Directions, *Nat. Methods* **2012**, *9*, 555-566.

(22) Picotti, P.; Rinner, O.; Stallmach, R.; Dautel, F.; Farrah, T.; Domon, B.; Wenschuh, H.; Aebersold, R., High-Throughput Generation of Selected Reaction-Monitoring Assays for Proteins and Proteomes, *Nat. Methods* **2010**, *7*, 43-46.

(23) Anderson, L.; Hunter, C. L., Quantitative Mass Spectrometric Multiple Reaction Monitoring Assays for Major Plasma Proteins, *Mol. Cell. Proteomics.* **2006**, *5*, 573-588.